ALPHA FOUNDATION FOR THE IMPROVEMENT OF MINE SAFETY AND HEALTH

Final Technical Report

Project Title: Analysis of the Influence of Macro Fractures on Underground Coal Mine Ventilation Seals.

Grant Number: AFCRFP20-131

Organization: University of Kentucky - Mining and Minerals Resources, Lexington, KY

Principle Investigator: DR. JHON SILVA (PI)

Contact Information: Mining and Minerals Resources Building, Lexington, KY
859-257-1173 (office)
859-323-1962 (fax)
JHON.SILVA@UKY.EDU;

Period of Performance: 09/30/2020 - 10/31/2021

Acknowledgement / Disclaimer:

"This study was sponsored by the Alpha Foundation for the Improvement of Mine Safety and Health, Inc. (ALPHA FOUNDATION). The views, opinions, and recommendations expressed herein are solely those of the authors and do not imply any endorsement by the ALPHA FOUNDATION, its Directors and staff."

1 Executive Summary

The final rule on mine seals from The Mine Safety and Health Administration, (MSHA) dictates several considerations of design, requirements, and maintenance of these structures. Some of the MSHA approved mine seal designs are based on the use of cementitious materials. To date, questions remain regarding the likelihood of macro-fractures generation during the curing process of the cementitious materials and its effects on the integrity and structural behavior of the mine seals when subject to dynamic solicitations (explosions). This project was proposed to accomplish three objectives, coinciding with three consecutive stages. The objectives (and stages) initially proposed were:

Objective I – Mine seals inventory and macro-fracture generation assessment
Objective II – Structural and integrity assessment of the effects of macro-fractures on mine seals
Objective III – Proposal for alternative materials solutions

The project was proposed and planned so that the results from a previous objective were used to decide on the continuation of the project. After analyzing the results from objective, I, where no macro-fractures were detected, it was determined to end the project. This document is the compilation of the results and analysis of objective I and the conclusions that determined the non-continuation of the project. Objective I and all its respective tasks are included next:

Objective I – Mine seals inventory and macro-fracture generation assessment. This objective was divided into several tasks:

- **Task 1:** To inventory and analyze, according to the MSHA database and other available data, the different mine seal designs approved and in use in industry,
- **Task 2:** To construct representative samples of mine seals to collect information relevant to macro-fracture generation during the curing process (heat, strains) combined with available MSHA results,
- **Task 3:** To identify and assess the characteristics and properties of the macro fractures generated during the curing process (location, geometry).

For Task 1, it was expected that MSHA has a database with all the seals installed on underground coal mines in the USA. However, and after contacting different offices from MSHA, it was determined that such information is not readily available. This project team was able to develop some statistics based on proprietary information from the companies that provide the materials and installation of those structures in underground coal mines. For Task 2, the project team poured fifteen (15) different representative samples using materials and procedures from two companies that provide the materials and installation services of seals in the USA. This task collected information relevant to macro-fracture generation during the curing process, such as heat, strains, and other parameters. For Task 3, Ground Penetrating Radar (GPR), Tracer Gases, and Acoustic Emission analyses were used with the aim of identifying and assessing the characteristics and properties of the macro-fractures, if any, generated during the curing process (location and geometry).

The following framework was used for the interpretation of the results, and the justification about the non-continuation of the project:

Macro-fractures – are defined as apertures in the material with a distance similar to or greater than the thickness of a piece of paper (>0.07 mm).

Seal sample – is defined as a cube with dimensions 4 x 4 x 4 ft. poured (a) following the standards (materials proportions and casting procedures) recommended by the provider of the materials for the construction of the seals (b) following a procedure to develop out of spec seals again based on a recommendation by the provider of the materials.

The curing process – is defined as the process for the cementitious material to attain its final strength. The mine seal material providers have recommendations regarding the environmental conditions to cure their products successfully.

The conclusions after the completion of Objective I of this project are listed below:

- This project team did not observe macro-fractures during the curing stage for seal samples constructed, after properly following the proportions and standard procedures developed by two companies (approved by MSHA) that provide materials for the construction of mine seals.
- The importance of the constructability and quality control during the initial pouring and curing behavior of mine seals were demonstrated by observing the different behaviors in strength, temperature, and strains for similar and different mixtures, as well as similar and different construction methods. This is highlighted as a significant factor that may affect the integrity and performance of these seals at the early stages and their life cycle when in use.
- After using visual inspection, Tracer Gases, GPR, and Acoustic Emission systems, it was concluded that the adequately constructed and cured seal samples for this project did not exhibit any visually or otherwise detected macro-fractures.

As the project team did not find macro-fractures in any of the samples, the project was terminated after completion of Objective I.

Some of the analyses in this report to assess the likelihood of macro fractures generation during the curing process were based on parameters, variables, and theories developed on the research of the hydration process of traditional cement and concrete. However, it should be noted that the rigorous study of the hydration process of materials used for mine seals is a research topic that was beyond the scope of this project. Because of this, the analysis of the strength behavior and the stresses calculated for the samples should be taken with caution and may not reflect the actual behavior of the seals.

TABLE OF CONTENTS

2 Problem Statement and Objectives

The Mine Safety and Health Administration's, (MSHA), final rule on mine seals dictates several considerations of design, requirements, and maintenance of these structures. However, questions remain regarding the likelihood of the generation of macro-fractures during the curing process and its effects on the integrity and structural behavior of the mine seals. The proposed research addressed those questions through testing and parametric analysis. This final report is the compilation of all reports and includes all the work and information regarding Objective I of the respective tasks.

Objective I – Mine seals inventory and fracture generation assessment. This objective was divided into several tasks listed below:

- ***Task 1:*** Inventory and analyze, according to the MSHA database and other available data, the different mine seal designs approved and in use in industry,
- ***Task 2:*** Construct representative samples of mine seals to collect information relevant to fracture generation during the curing process (heat, strains, and other parameters) combined with available MSHA results,
- ***Task 3:*** Identify and assess the characteristics and properties of the macro-fractures generated during the curing process (location, geometry).

3 Research Approach

3.1 Task 1.1- MSHA database compilation and analysis

In this task of the proposal, the intent was to collect and review all informational data from the MSHA database. The idea was to collect information focusing on the type of mine seal, materials, analyses, and construction procedures. Other aspects like quality control during the implementation of the seals and any other available information of the operation after the construction and relative to the project were to be documented. This task was expected to establish the statistics of the type of mine seals (plug design and flexural, others). Other relevant information to the project, such as heating data, macro-fracture generation, chemical reaction properties, etc., were to be collected in this task.

Development of Task 1.1

The project team attempted to reach MSHA in order to acquire the data. Discussions with MSHA representatives indicated that MSHA does not keep an accessible inventory or database of installed seals. MSHA does, however, keep on file seal approvals for each mine, yet the file information cannot be easily manipulated to obtain quantity and type of seals. MSHA representatives provided a link to available seal approval information on the MSHA webpage. The link to the current MSHA webpage containing approved seal information is shown below:

https://arlweb.msha.gov/Seals/SealsSingleSource2007.asp

The following is a list of the information available through the above link.

a) MSHA Mine Seal Requirements,
b) MSHA Guidelines for Completing the Seal Design Approval Application - 30 CFR § 75.335(b),
c) Approved Seals under the Final Rule,
    I. Approved Seals Designed to Withstand an Overpressure of 50 psi
    II. Approved Seals Designed to Withstand an Overpressure of 120 psi
    III. Seals Designed to Withstand an Overpressure > 120 psi,
d) Mine Inerting Information (gases),
e) Regulatory History of the Seals Rule.

It is evident that the above list does not include any information or statistics regarding mine seals such as:

- The number of installed seals and their type (plug, flexural, etc.)
- Construction materials (regular concrete, bricks, resins, etc.)
- Calculations,
- Construction procedures (quality control procedures, heating data)
- Other, i.e., macro fracture generation, chemical reaction properties, etc.

A first attempt to contact MSHA was through the office of Mine Emergency Operations. The following is the response from that MSHA office.

"In response to your inquiry, MSHA Technical Support does not track the number or types of seals installed in U.S. coal mines. I recommend contacting MSHA Headquarters for statistics on seal installations. Calculations relative to seal designs remain the confidential intellectual property of the developer. Construction procedures are contained in the installation guidelines for each seal design. The installation guidelines are on the Seals Single Source page of the MSHA website, which you reference in your message. I hope this information helps."

Following the recommendation in the response quoted above, the team contacted the MSHA Directorate of Technical Support. The response from that office is included below:

"After our call, I talked with multiple people in Technical Support and Enforcement to see if this information was out there anywhere or easy to get. We do not keep the information. A mine operator would file a supplement to the ventilation plan with the District to build seals, but this generally would not remain in the ventilation plan after the mine constructs them. On top of that, if the new seals enclose old seals, then this is not tracked either. The number and type of seals is not information that we keep."

In conclusion, the information expected from MSHA in Task 1.1 regarding the amount and type of mine seals installed in the USA underground coal mines is not readily available.

According to available information by MSHA, six companies provide or have approved seals to withstand 50 and 120 psi overpressure. These companies are:

- Strata Mine Services (SMS),
- Minova (M),
- Micon (Mc),
- JennChem (JC),
- BHP Billiton (BHP) and,
- Precision Mine Repair (PMR).

Figure 3.1 shows the number of approved seals by each company for the two design overpressures after reviewing the available information.

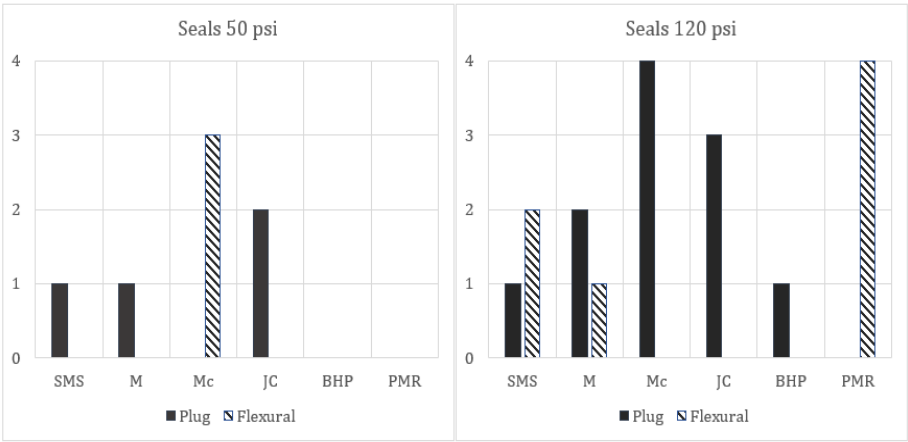

Figure 3.1 The number of approved seals by a company and by design overpressure

As seen in Figure 3.1, the number of approved plug seals is greater than the number of flexural seals. The total number of plug seals is 15 compared to a total of 10 flexural seals. The company with more approved seals designs is Micon, with seven (7) approved seal types. Minova and Strata Mine Services have the same number of approved seals, four (4). Finally, there are 18 approved seals that can withstand 120 psi overpressure and only seven (7) seals that can withstand 50 psi overpressure.

Table 3.1 includes a summary of the material type used by each company and the main components of the mixture.

Table 3.1 Material type and components of the mixture

Manufacturer	Material	Components
BHP Billiton	Portland Cement Concrete	3,000 psi minimum compressive strength Portland cement concrete
JennChem	J-Seal	410 psi avg. product
	1 Day J-Seal	450 psi avg. product
Micon	HybriBond &70	Solid concrete masonry unit blocks (cmu), HybriCrete blocks, #57 stone, Micon 70, & HybriBond polymers.
	HybriBond & SIGNUM	Solid concrete masonry unit blocks (cmu), #57 stone or pea gravel, SIGNUM & HybriBond polymers, untreated wood wedges, fibrous filler chinking material/open cell backer-rod.
	HybriBond & PU37A	Solid concrete masonry unit blocks (cmu), HybriCrete blocks, #57 stone or pea gravel, PU37A, & HybriBond polymers.
Minova	Tekseal®	415 psi minimum compressive strength, product.
Precision Mine Repair	Shotcrete	Portland cement (25%) and sand (75%), deformed steel reinforcement bar, wire mesh.
Strata Mine Services	Medium Strength Stratacrete®	3,000 psi uniaxial compression test product, 115 psi minimum shear strength, plasticizer (Portland, fly ash, water, and sand)
	High Strength Stratacrete®	4,000 psi product, deformed steel reinforcement bar.

The following is a summary of quality control or testing procedures before and/or after seal construction as indicated in the approval documents:

- The site should be prepared, and surrounding strata should be reviewed
- A mix water temperature is recommended in some approval plans
- Material storage is specified in some approval plans
- A test for water compatibility is recommended for some in some approval plans
- A recommendation for collection of samples for uniaxial compressive strength is specified in some approval plans
- Some approval plans recommend following specific standards from the American Society for Testing and Materials (ASTM); standards pertain to concrete, cellular materials and expanded plastics.

Appendix I includes detailed information on each approved seal and the testing included as quality control. It is important to note that none of the approved seals recommend heating or thermal testing as part of the construction procedures.

As mentioned before, MSHA does not record the number or type of installed seals, so approved seals manufacturers have been contacted directly. The information presented in Table 3.2 has been acquired by contacting the respective seals manufacturers (in no specific order).

Table 3.2 Total seals pumped per company as of Jan 2021

Company	**Total Seals**	**Plug Seals**	**Rebar Seals**	**Comments**
JennChem	2,948			This includes all JennChem approved seals (five). According to the information, the number of 50 psi seals is less than 50.
Strata Mine Services	850	500	350	This includes all the Precision Mine Repair seals installed since Strata acquired that company.
BHP Billiton (Westmoreland)	704	704		Total remaining in service 226; Flexural seals: 0
Minova	12,744			Total seals between 50 psi and 120 psi, plug seals.
Micon	5,000			4,000 installed seals for 120 psi overpressure. 1,000 installed seals for 50 psi overpressure.

3.2 Task 1.2 - Mine seal-sample preparation

The project team completed wood forms for casting the seal samples. The selected dimensions for the seal samples are 4 x 4 x 4 ft. Fifteen (15) samples were cast with different ratios and mixtures from two suppliers of these products. Company 1 provides a "Two-Component Pumpable Seal". While Company 2 provides a typical "Portland Cement / Fly-ash / Aggregate / Sand Seal. Table 3.3 summarizes the Seal, Sample Type, Supplier, and Mixture Description, used in the specific mixtures.

Table 3.3 Seal Sample Type – Supplier & Mixture Description

Sample Type	No of Samples	Supplier	Mixture Description (Specification)
Mixture A (Pumpable)	4	Company 1	Standard (Within Spec) Mix Ratio of Supplier (pumped using pump provided by the manufacturer)
Mixture B (Pumpable)	4	Company 1	Out of Specification Mix Ratio of Supplier (pumped using pump provided by the manufacturer)
Mixture C (Concrete)	4	Company 2	Standard (Within Spec) Mix Ratio of Supplier (Concrete Truck)
Mixture A (Pumpable)	1	Company 1	Standard (Within Spec) Mix Ratio of Supplier (poured manually)
Mixture D (Pumpable)	1	Company 1	Out of Specification Mix Ratio of Supplier (poured manually)
Mixture E (Concrete)	1	Company 2	Out of Specification Mix Ratio (Manual Pouring & Aggregates removed)

Figure 3.2 shows a picture of the forms prepared in the Mining Department for casting the seals.

Figure 3.2 Forms for mine seal samples

Various water/powder ratios, not all approved by the MSHA, and not all used in the mine installations were selected. The main idea was to use a standard, specified ratio commonly used by the manufacturer and a non-specified, out-of-specification standard that could increase the likelihood of crack generation.

In all cases where a non-standard specification was used, a higher powder to water ratio was used with the Company 1 samples and in the case of the Company 2 a higher cement content was used, and the aggregates were removed for Mixture E.

The first eight samples were poured in February 2021, and they were built using materials and methods provided by Company 1. These eight samples correspond to two mix designs (four samples per design). Another four samples were poured in April 2021 using materials and methods provided by Company 2; these correspond to one mix design.

Three samples were poured with a non-conventional manual pouring method in June 2021, two based on materials supplied by Company 1 and one based on materials supplied by Company 2. As per Table 3.3, the repeat sample for Mixture A was the only sample out of the three that was within a supplier, specified standard mix.

The three additional samples correspond to one sample with a standard powder/water ratio, one sample with an out-of-specification powder/water ratio from Company 1, (pumpable seal material), and one 4x4x2 ft sample (out of specification in mix and dimensions), compared to other samples of 4x4x4 ft with non-standard material proportions from Company 2. The additional standard sample from Company 1, was constructed because the strain gauge system did not work for the original sample that was cast in early 2021 due to a technical failure; hence the team could not collect strain information for that sample.

The two (2) out-of-specification samples were constructed with the intention to generate macro-fractures during the curing process. A particular consideration for the three final samples is that the pouring was done manually, given that it was not possible to mobilize all the support equipment to pour the samples from Company 1, and the amount of material required for the sample, using material from Company 2, was not commercially available (the concrete companies only sell a minimum one truck of concrete). Seal construction should be tightly controlled in terms of mixture specifications. The change in the specification was not extreme mixes as constructability issues can occur in practice and in a mine and therefore the test to investigate the results of these changes to the mixes. All the mixes and samples still achieved the required strength requirements once tested in the laboratory for uniaxial compression strength.

As mentioned initially, the project team finally cast in total fifteen (15) seal samples: fourteen (14) (4x4x4 ft) and one (1) 4x4x2 ft sample. In total, around thirty-seven (37) cubic yards of material were poured using the products from the two companies supporting the project.

3.3 Task 1.3- Mine seals-data collection during curing

Seal Sample instrumentation was designed for two purposes: a) to record the changes in variables that can be related to the generation of macro-fractures, and b) to assess the likelihood of the presence of macro-fractures in the samples. The description of the instrumentation is included next.

a. Thermocouples

The internal heat in the samples due to the curing process was measured in several locations. The instrumentation used consisted of MadgeTech Software and Hardware as the data acquisition system and TJ180-CASS-18G-6 thermocouple sensors from Omega embedded in the concrete during the pouring of test samples. Figure 3.3 shows the data loggers and the thermocouple sensors used.

a) Data logger (MadgeTech)

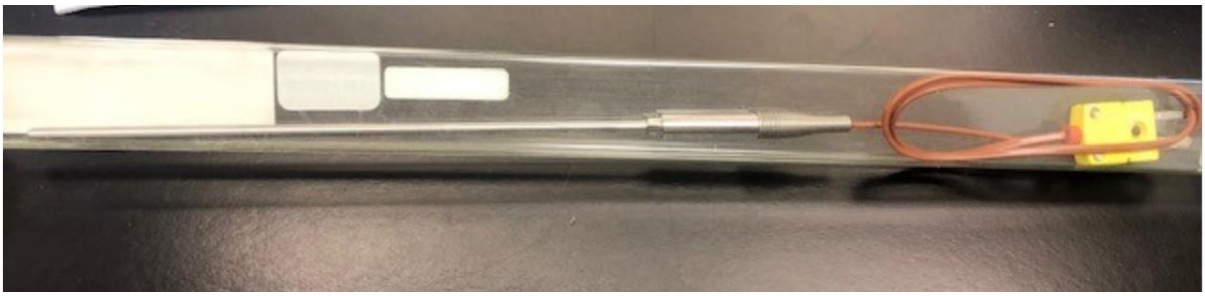

b) Omega thermocouple

Figure 3.3 System to measure the internal heat of the samples during the curing process

The data was collected using a sampling rate of 1 reading every minute.

b. Embedded Strain gauges

The use of concrete-embedded strain gauges is common in civil engineering applications. It allows measuring mainly the expansion and or shrinkage of the concrete during the curing process. The application of this technology in this project aimed to find a relationship between the changes in the internal temperature, the values and rate of strain changes, and the potential presence of micro and especially macro-fractures. With this in mind, the Strain Smart Model 8000 Software, and Hardware from Micro-Measurements was used for data collection. Also, the EGP-5-350 Embedment Gauges from the same company were used as sensors. Figure 3.4 shows the data collector and the sensors used for strain measurements.

a) Unit – Model 8000-8-SM b) EGP 5-350 gauge

Figure 3.4 System to measure strains of the samples during the curing process

Model 8000-8-SM (Figure 3.4a) is a versatile, precision data acquisition instrument intended for static and dynamic test and measurement applications. Model 8000-8-SM has eight (8) channels of data acquisition. Each channel was configured, via software, to input signals from the seven (7) off strain gauges per box. The strain gauge channels accepted full, half, or quarter-bridge configurations, and for this specific application, 350-ohm bridges were used. Model 8000-8-SM communicated with a pre-installed personal computer (laptop) via an Ethernet connection.

The data was collected using a sampling rate of 5 readings every minute for both Mixture A, Mixture B, Mixture D and Mixture E.

The strain data for Mixture C were collected using a sampling rate of 600 readings every minute up to day 5 of curing. After the 5 days, the sampling rate was then reduced to 5 readings every minute.

c. Tracer Gases

Two tracer gases in two passive sources were embedded in each of the three seal samples, Perfluoromethylcyclohexane (PMCH) and Perfluoromethylcyclopentane (PMCP). One source was embedded at the centroid of the samples, and the other centered at a depth of 12 inches from the top surface. The location of each of the sources was recorded as well as the type of gas it contained for each sample (Figure 3.5).

Each source contained 6 ml of either PMCH or PMCP capped with a fluoroelastomer plug and was labeled for identification prior to installation. PMCH is non-toxic, and PMCP is an oral irritant, toxic if swallowed (liquid form). The passive source containment was designed with a protective covering for handling while embedding the sources, and to provide a barrier between the source container and the uncured seal material. The gases are expected to elute even if the seal material directly contacts the fluoroelastomer plug. The elution rates are temperature sensitive, but the underground mine environment was expected to maintain a relatively constant temperature range during the proposed sampling period.

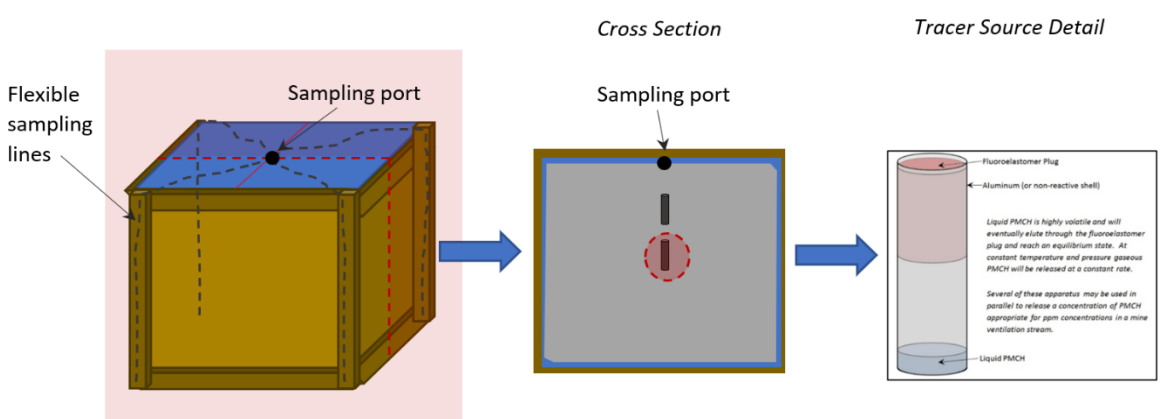

Figure 3.5 Tracer gas collection network and source location in seal material samples

The gas sampling process places a small amount of pressure on the material, but it is not problematic since this differential is far less than expected for in situ seals. Sampling required connecting a vacuum pump to the sampling port extending from the formwork using flexible tubing (equipped with a valve). The discharge/exhaust port on the pump was then connected to a TEDLAR® sample bag also equipped with an isolation valve (Figure 3.6). Sample bags were filled to capacity by the pump, and then the valves on each end of the system were closed.

Each gas sample bag was labeled with the date, seal material sample, and sampling port location and then filled during the prescribed schedule. Some minor dilution from the atmosphere is expected, but just the presence of the tracer and large magnitude changes with time was the focus rather than the ppm level accuracy with each sample.

Figure 3.6 Vacuum pump system, sampling ports, and TEDLAR® gas sample bag

Table 3.4 provides the frequency and schedule of collecting gas samples from each of the seal material samples equipped with the Tracer Gas sampling apparatus.

Table 3.4 Tracer Gas Sampling Schedule

Sample Schedule	Frequency
1	2 days from casting seal material sample
2	Daily samples from day 2 until day 12
3	Weekly samples from day 13 until day 28
4	Monthly samples after day 28

Once the sampling schedule was completed for the first phase of the seal material testing, the gas samples were analyzed using a gas chromatograph (GC). The GC analysis focused on sensing the two different types of tracer gases embedded in the seal material and sudden spikes or upward trends on gas content.

d. Acoustic Emission System

It has been demonstrated in the literature that when materials are cracking, deforming, or suffering damage, the release of energy can produce sound signals. Acoustic Emission detection systems (AE) to capture such sounds can help identify the generation of cracks or fractures. Several events can generate AE:

- The dislocation movement(s) are caused by plastic deformation or yielding.
- The formation and extension of cracks in an object under stress
- Thermal stresses
- Cracking during cooldown
- Stress build-up
- Twinning, a form of crystalline distortion
- Debonding

With the aim of correlating parameters such as generated heating, shrinkage, and the generation of fractures, an Acoustic Emission System (AE) from Mistras Group Inc. was installed on two samples (Mixture C and Mixture D). The data acquisition module is composed of a MicroSHM system Node. This system is a 4-channel Acoustic Emission digital signal conditioner with a full set of AEs hit and time-based features, including waveforms. Through the Ethernet Connector, the system is easily interfaced to a notebook or PC running a Windows operating system (Win7, Win10, etc.). It comes equipped with the AEwin™ software. The MicroSHM has two wireless communication options: 3G wireless or Wi-Fi. In the current application, the ethernet option is being used. The MicroSHM can accept single-ended/differential sensors amplified by an internal low noise preamplifier. Additionally, PK Series low power integral preamp sensors can be used with this system.

Four (4) sensors were used for the test. Two are model PK3I sensors, which are low power sensors, 30 kHz with an integral preamplifier, and an SMA connector. The other two are model Generic 30 sensors, which are low power, 4.5 kHz, 26 dB preamplifier and BNCR connector. Figure 3.7 shows the AE system used in the project.

a) MicroSHM system Node b) Sensors

Figure 3.7 System to collect AE data of the samples during the curing process

Figure 3.8 shows the thermocouples and the embedded strain gauges used on specific samples.

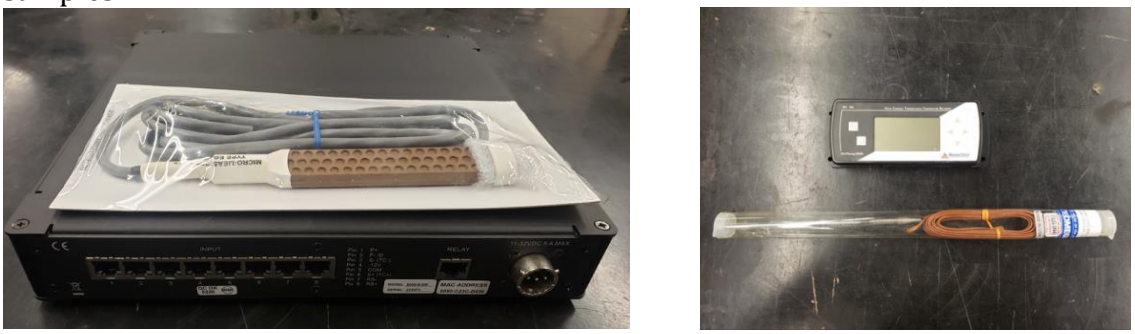

a) Strain gauges b) Thermocouples

Figure 3.8 Instrumentation to collect data during curing

As seen in Table 3.5, various, different types of instrumentation were installed in each sample. The control samples do not have any instrumentation in at all; data from these samples can be used to investigate whether the presence of sensors can create fractures in their proximity.

The aim of pouring samples without any instrumentation (besides the tracer gas capsules) was to measure the instrumentation's influence on possible crack generation using ground-penetrating radar (GPR). Table 3.5 summarizes the instrumentation embedded in the seal samples used for the research.

Table 3.5 Instrumentation Embedded in Seal Samples

Sample Type	Number of Samples	Instrumentation Included & Data Collected
Mixture A	4	Thermocouples, Tracer Gas, Control Sample *2
Mixture B	4	Strain Gauges, Thermocouples, Tracer Gas, Control Sample
Mixture C	4	Strain Gauges, Thermocouples, Tracer Gas, Acoustic Emission
Mixture A (Repeat)	1	Strain Gauges, Thermocouples
Mixture D	1	Strain Gauges, Thermocouples, Acoustic Emission
Mixture E	1	Strain Gauges, Thermocouples

Given that all samples (besides sample 15) have the same dimensions, it was decided to install the instrumentation in the same locations in the representative samples 1 and 2 for specific mixtures. The objective of this distribution was to find any relationship between heat and strain during the curing process. Figure 3.9 shows the locations selected for the installation of the instrumentation.

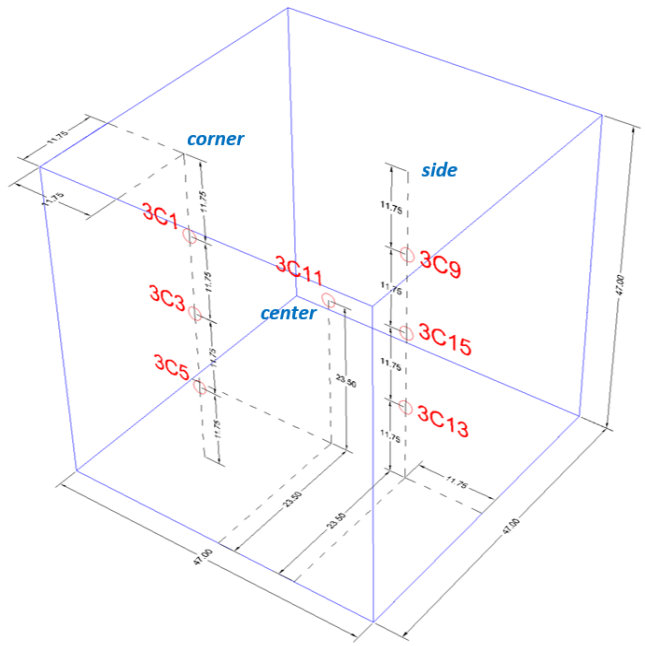

Figure 3.9 Location of the instrumentation in applicable samples

The specific locations (corner, center, and side) were selected to investigate the influence of the number of free faces for heat exchange in the measured parameters of the curing process, such as heat and strains. Figure 3.10 shows the arrangement of strain gauges and thermocouples before pouring the mine seals mixture.

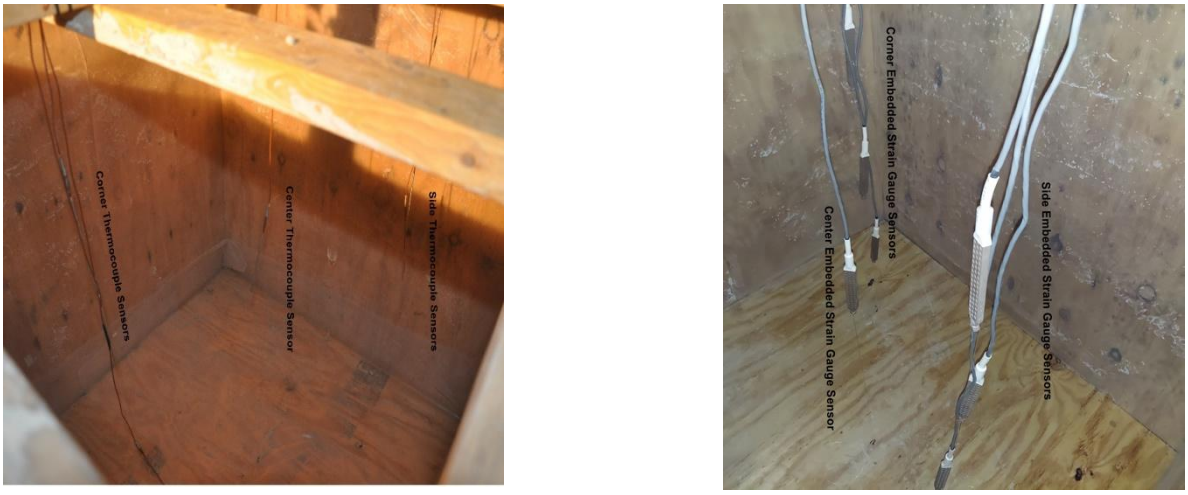

Figure 3.10 Strain gauges and thermocouple sensors before pouring the mine seal mixture

One sample for Mixture A, Mixture B, and Mixture C included tracer gases. Figure 3.11 shows the preparation of the tracer gas collection network prior to pouring the mine seal mixtures.

Figure 3.11 Sample preparation to monitor tracer gases

The Acoustic Emission system was not available since the beginning of the project, and it was installed on the control samples of Mixture C and D poured in June.
Figure 3.12 shows the installation of the AE system in the control sample for Mixture C.

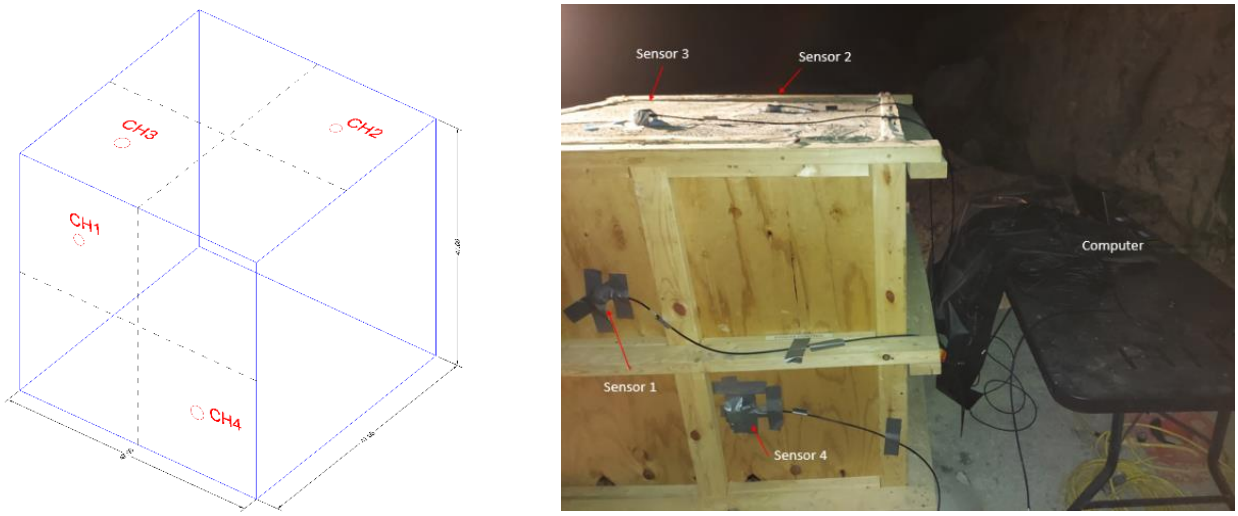

a) Schematic

b) Sensor Location

Figure 3.12 Acoustic Emission system in control sample Mixture C

As mentioned before, three final samples were poured after May. The same instrumentation setup that was presented earlier was used for these samples as well. However, as only two out of spec samples were available, all the instrumentation to collect both temperature and strain was installed in the same sample. This is different compared to the original samples, where each sample featured only one type of instrumentation.

The instrumentation for both temperature and strain were installed together in the same sample. Figure 3.13 and Figure 3.14 show the instrumentation location for the additional samples poured after May.

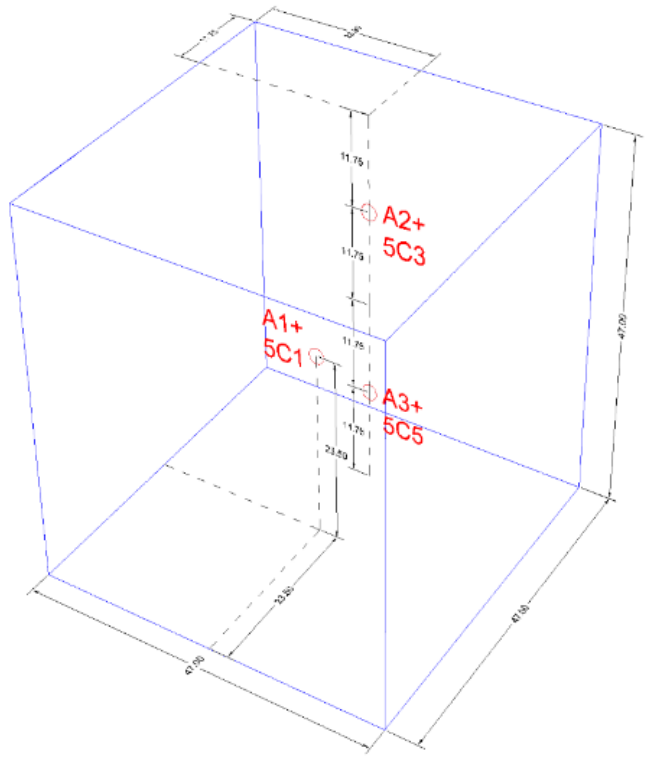

Figure 3.13 Instrumentation location for an additional sample of mixture D (Company 1)

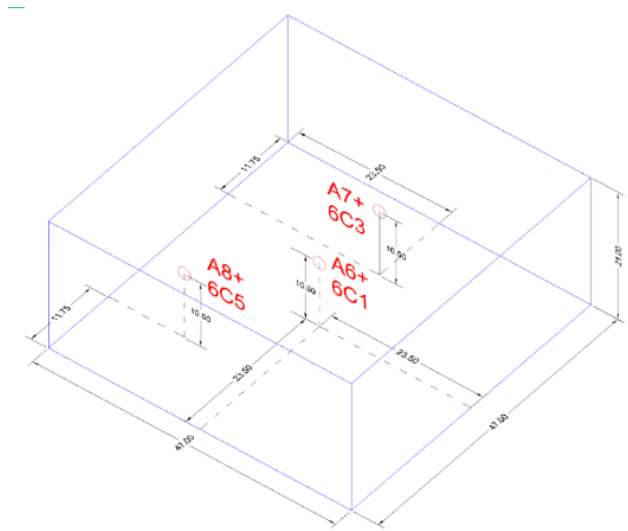

Figure 3.14 Instrumentation location for additional sample of mixture E (Company 2)

The acoustic emission (AE) system was installed on the standard sample from Company 2 (Mixture C) and on the sample out of the specification of Company 1 (Mixture D). With this, the project team collected AE data from both types of materials used in these tests. Figure 3.15 shows the installation of the AE sensors.

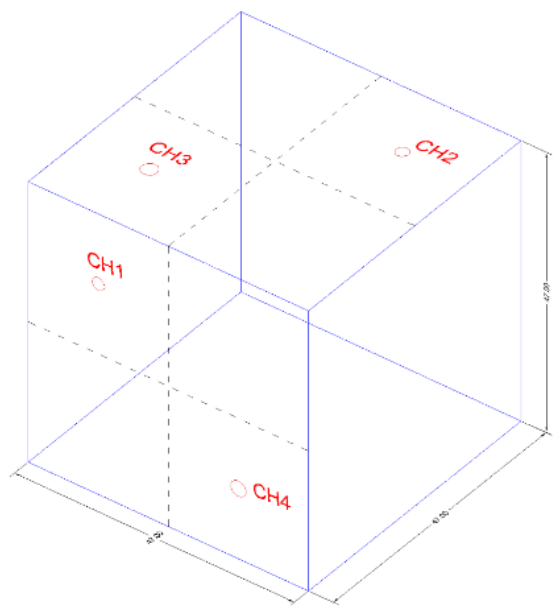

Figure 3.15 AE system installation setup in the samples for both Mixture C (Company 2) and Mixture D (Company 1)

In addition to pouring samples out of specifications to promote macro-fractures, the wooden forms were removed the second day after casting. This was done in order to accelerate the drying process and thus increase the rate of change in temperature in the samples.

3.4 Task 1.3- Mine seals-samples pouring procedures

Five different mixtures were used to cast fifteen (15) samples for this project. The mixtures used were based on materials and methods provided by two companies that commercially provide mine seals for underground coal mines in the US. Between the two companies, there are more than 13,000 mine seals installed. The following sections include a description of the pouring procedures of the different mixtures.

Mixture A and B

Company 1 provided the material for Mixtures A, B and D. One particular consideration was that the mine seals installed by this company included all the mine seal materials, the mixing equipment, supervision, and specific procedures had to be followed for each pour. Additionally, it is essential to keep the moisture of the material once it is poured in the form. The following figures show the different stages in the construction of the samples using Mixtures A and B.

a. Mixture material

The material for the mixtures is in the form of powder in bags. Figure 3.16 shows all the materials used to cast the samples.

Figure 3.16 Bags of material for the preparation of the Mixtures A and B

b. Mixer, Pump, and auxiliary equipment

This mixture requires the use of specific equipment. The following is a list of additional materials and equipment used for the samples:

- A water tank of 2,500 gallons,
- Power generator (480 volt and 250 amp),
- Water heater,
- Mixer and Pump.

Figure 3.17 shows the equipment used during the pouring of the samples.

a) Wooden forms and Bobcat

b) In the back, Water truck, and Power Generator

c) Mixer, Pump, and water heater

Figure 3.17 Equipment used during pouring of mixtures A and B

Once the material was mixed, it was pumped into the forms. As mentioned before, Mixture A followed the regular specifications used by the company, while Mixture B corresponded to an "out of specification" mixture. The mixture developed by Company 1 controls the time to achieve a pre-determined compressive strength based on the powder to water ratio. If mixture A is considered as the standard, Mixture B was done using 1.25 times more powder than mixture A, to the same water ratio. In that case, it was expected for Mixture B to have higher temperatures on the samples, reach the pre-determined compressive strength faster, and most likely generate more cracks (micro and macro) than Mixture A.

Figure 3.18 shows the details during the pouring of the samples.

Figure 3.18 Pouring of Mixtures A and B into the wooden forms

Mixture C

For Mixture C, Company 2 provided their approved seal material additive to be incorporated in an approved conventional mortar mix of the following materials:

- Water,
- Portland cement,
- Fly Ash,
- Aggregate, and
- Sand

For this project, the mortar was provided by a concrete (ready-mix) company close to the facilities. In total, two batches of about five (5) cubic yards per batch, were trucked underground and used for the four (4) samples. Figure 3.19 shows the additive incorporated into the mortar and the concrete truck being ready for pouring.

Figure 3.19 Additive in bags and concrete truck used for Mixture C

The pouring process was to discharge the material directly from the truck to the wooden form for this mixture. Figure 3.20 shows some of the details of this process, including the direct supervision provided by the company.

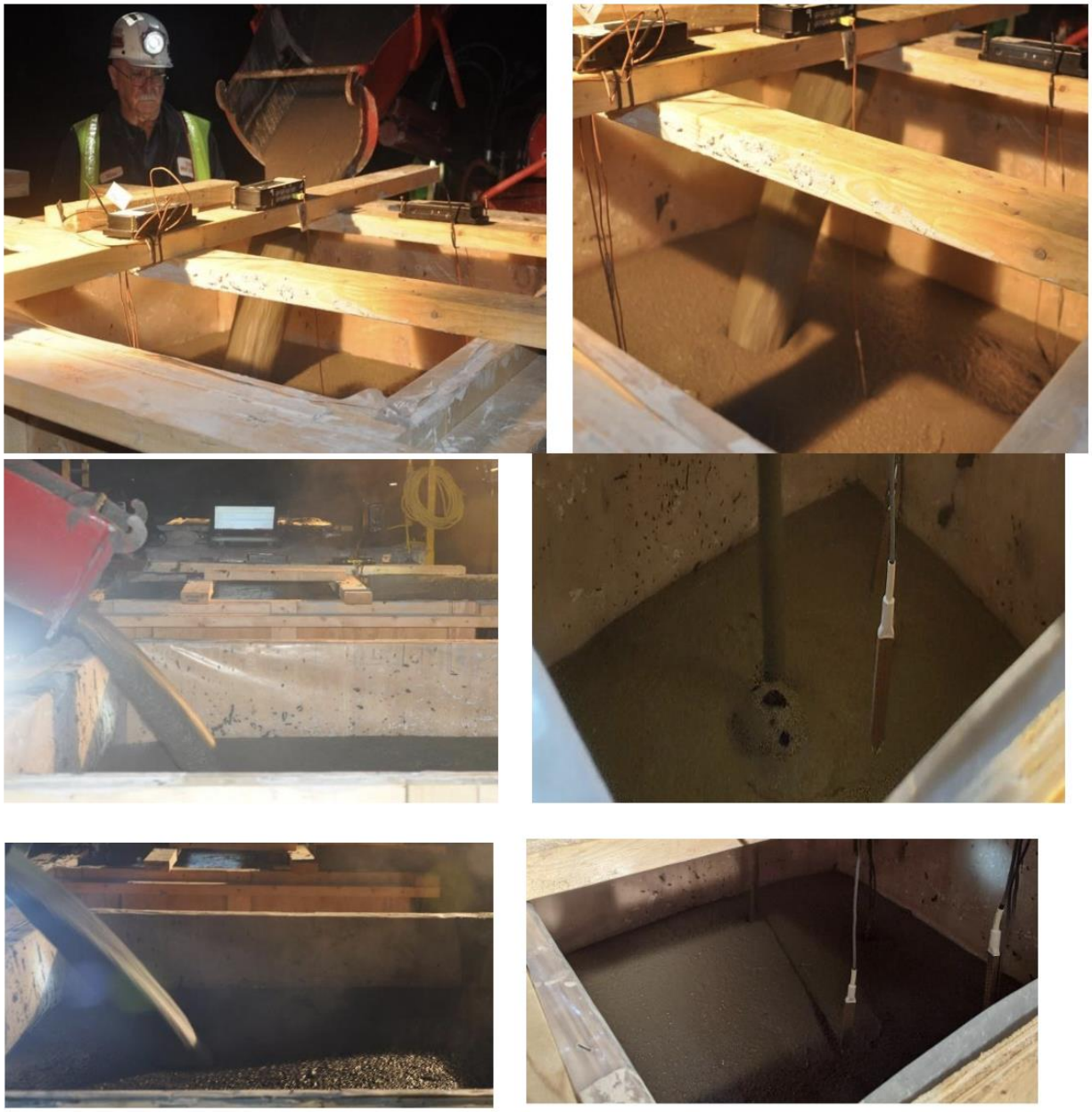

Figure 3.20 Pouring of Mixture C into the wooden forms

Figure 3.21 and Figure 3.22 show the pouring process for the final three additional samples poured manually after May 2021.

Figure 3.21 Manual mixing and pouring for additional sample (Company 1 – Mixture A (Within Spec) & Mixture D (Out of Spec – manual pouring)

Figure 3.22 Manual mixing and pouring for additional sample Mixture E (Company 2 – Out of Spec)

Uniaxial compressive strength data

During the pouring process of all mixtures, samples for uniaxial compressive testing were collected. The samples were tested at 7, 14, and 28 days. All the results are included in the following sections of this report.

Due to various mixing methods applied, test samples were collected at the bottom, mid, and top sectors of the seal samples. In total, forty-two (42) samples were collected and tested for all Mixtures at 7, 14 and 28 days. Figure 3.23 shows the collection of samples during the pouring process.

Figure 3.23 Collection of samples for uniaxial compressive tests

After tasks 1.1, 1.2 and 1.3 were completed additional work was performed to verify or discard the presence of macro-fractures in the mine seals as a result of the curing process. The additional work is listed below:

- The team visited an active underground coal mine with installed seals.
- Casting of the three additional samples, which were poured "manually", using materials provided by the two companies supporting the project. This was significantly different from an actual mine installation, especially for pumped type seal materials, but manual pouring was investigated to determine possible different behavior and results.
- Two GPR scan surveys were performed to calibrate the scanning technique and scan "old" and "new" mine seal samples.
- Data from all 15 samples were collected and compared.

Before presenting the additional work, the data, and the analysis, it is considered necessary to establish the following framework for the interpretation of the results:

Macro-fractures – are defined as apertures in the material with a distance similar to or greater than the thickness of a piece of paper (>0.07 mm).

Seal sample – is defined as a cube with dimensions 4 x 4 x 4 ft. poured (a) following the standards (materials proportions and casting procedures) recommended by the provider of the materials for the construction of the seals (b) following a procedure to develop out of spec seals again based on recommendations by the material providers. The only deviation to the sample size was for Mixture E (Company 2 sample) which was only casted with a dimension of 4 x 4 x 2 ft.

Curing process – is defined as the process for the cementitious material to attain its final strength. The mine seal material providers have recommendations regarding the external conditions to cure their products successfully.

The successful metric for this project stage was to determine if macro-fractures occur during the seal curing process.

3.5 Visit of active mine seals at an underground coal mine operation.

The PI, co-PI, and the two graduate students involved in the project visited the Leer Mine Complex in West Virginia on 05 June 2021. The expectation was to visualize existing seal installations and perhaps discuss the maintenance required or applied (if any) in an active mine. This mine is a longwall coal mine operation with 4 million tons of metallurgical coal yearly. The project team had a meeting with the mine's engineering group, and the objectives and purpose of the visit were presented. Even though this operation doesn't use the materials from the two companies collaborating on the project, several topics for mine seals were discussed. The mine seal material used in this Complex, is essentially the same pumpable, type material tested in this project. Some of the relevant information for this project, discussed during the visit, is listed next:

- At the time of the visit, the mine had already installed 45 mine seals,
- All installed seals have a system of floor to roof support,
- All seals are constructed with a sampling tube established from "inby" the seal,
- Each bank of seals has an individual seal strategically selected for water trap installation,
- In addition to the water trap, a sight gauge is installed to monitor water levels "inby" the seal,
- Seals are visually inspected once per week after construction.

Figure 3.24 and Figure 3.25 include the two types of seals installed in this operation.

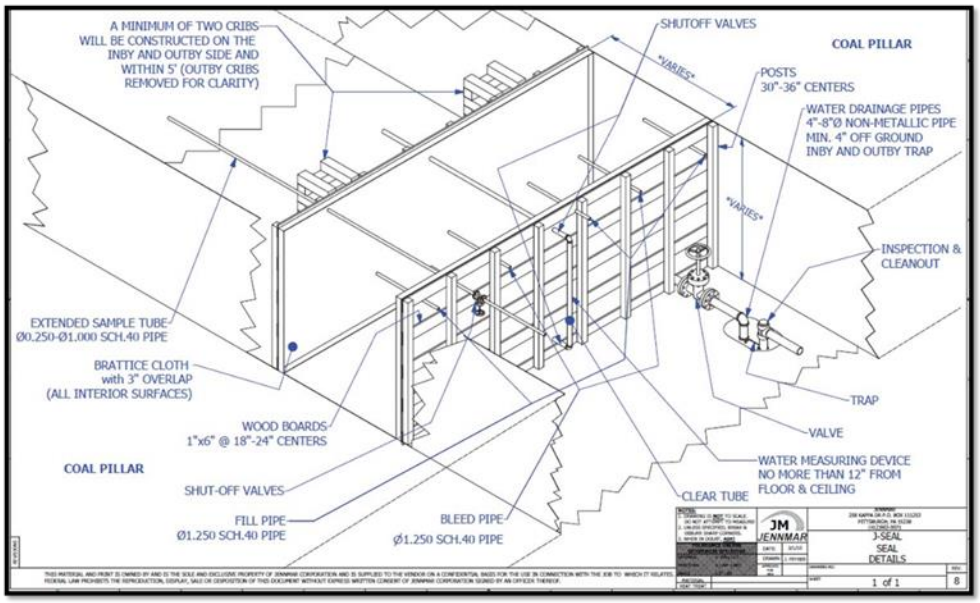

Figure 3.24 Jennchem J-Seal used at the Leer Mine (Source: Leer Mine Presentation)

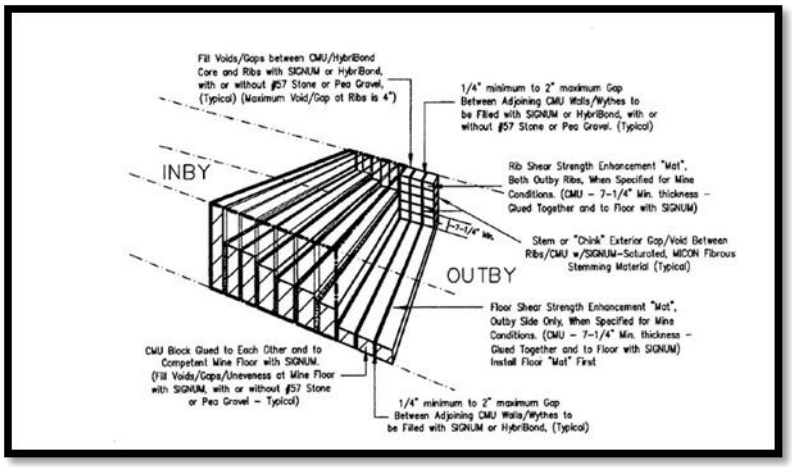

Figure 3.25 Micon Hybrid II-Seal used at the Leer Mine (Source: Leer Mine Presentation)

The mine's engineering team discussed the following specific topics regarding mine seals.

Mine seals construction procedures:
Usually, the mine seals are installed by a contractor with the appropriate skills and know-how. The mine personnel may, in some instances, install the seals on their own, but always following the specifications of the companies that provide the materials.

Data collected during the mine seals construction:
The "only" data collected during construction are samples to perform uniaxial compressive testing at different curing times, usually 7, 14, and 28 days. The mine had never experienced any complications with the samples, and the material consistently achieves the expected strength values.

Mine seals inspection:
The seals are inspected every week by the mine. The inspection is visual, and the focus of the inspection is the water levels and any possible leakage from locations different than the drainage pipes installed in the seals. In this regard, the team was not able to directly see the mine seal material because there is an impermeable membrane wrapping the seal after construction and during the whole life of the structure. What is evident is that no real structural inspections are done on these seals on a regular basis.

Other data related to the seals:
The team visited two places inside the mine with mine seals. In both places, a convergence system is installed to measure the possible movement of the roof and the entry floor. The seals were implemented five (5) years ago, and there are no convergence problems to date.

Unfortunately, due to MSHA regulations, it was not possible to obtain photographic records of the places visited inside the mine. The mine engineering team did not express any concerns about macro-fractures occurring during the curing process when asked. The main concerns were water accumulations and leakages at locations different from the drainage pipes. The visit was beneficial for the team to understand the magnitude of these structures and their importance for the safety of the mine.

3.6 Ground Penetrating Radar information

The Virginia Tech team collected the ground-penetrating radar (GPR) information with the support of UKERT. In total, two surveys were performed at the Georgetown facility.

The purpose of the first visit on 25 May 2021, was to test and calibrate the GPR system and to verify that it was the right tool to detect macro-fractures. Based on the preliminary results, a second visit was done on 11 June 2021. In the second visit, an improved methodology was applied with respect to the collection of information that allowed a better resolution of the scanned images. Figure 3.26 shows some of the procedures during the collection of the GPR information.

Figure 3.26 Collection of the GPR information

The calibration of the system was done using samples from a different project poured more than five (5) years ago. Weathering and other factors facilitated the generation of macro-fractures in those samples. The macro-fractures could easily be identified by visual inspection in the exterior faces of the samples. This was highly relevant purely for the system's calibration and determining if the GPR could identify the visually observed cracks. The cracks in these old seals were not relevant to any part of the seal samples' current investigation, as some were even mechanically introduced.

The description of the data collected, and the analysis and results are included in the next chapter of this document.

4 Research Findings and Accomplishments

4.1 Visual inspection of the samples

All wooden forms of the samples for this project were stripped to allow a visual inspection of the faces. Artificial light was used to improve the quality of the photographs. Figure 4.1 illustrates the appearance of the samples for this project. The left column includes the original picture, and the right, the marked-up delineation of visible changes in the texture of the material in the sample. It should be noted that the changes noted in the texture is a subjective process and does not represent the presence of a macro-fracture or discontinuities. Appendix I includes the analysis of additional photographs.

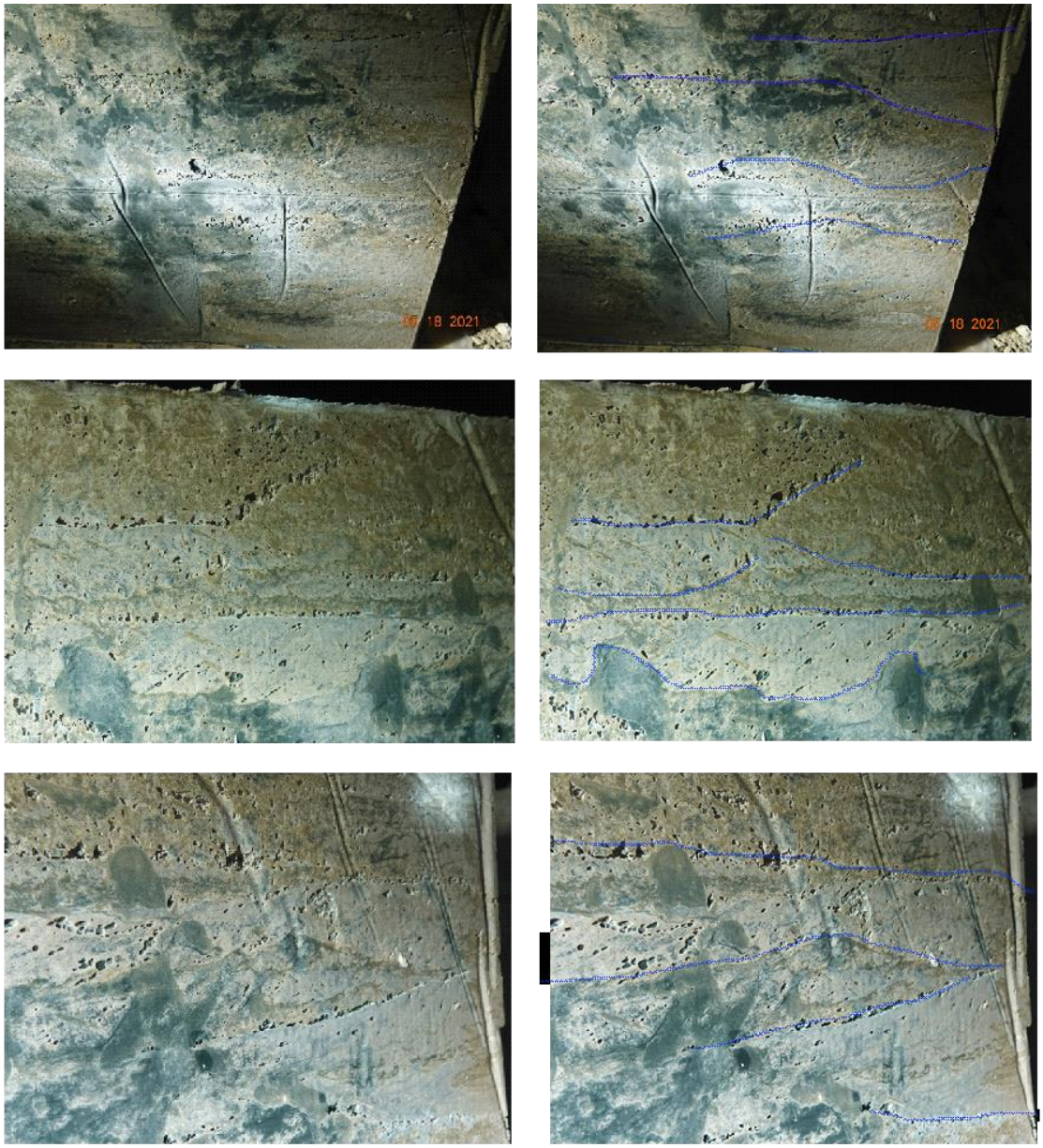

Figure 4.1 Visual inspection of samples for this project

In conclusion, there is no evidence of any macro-fractures formed to all visual inspections of the exterior of the samples.

4.2 Analysis of temperature and strain information

A general overview of the curing process in cementitious materials was done for this project. Appendix II includes all the concepts for interpreting the estimated heat evolution curves included in this chapter.

Heat evolution curves for the mixtures of this project

As described in Appendix II, the study of the heat evolution, the chemical reactions, the thermochemical processes occurring during the curing stages, and all the effects in the final strength, behavior, and the likelihood of cracking for the mixtures are a complex problem beyond the scope of this project. Despite the complexity of the problem, the team attempted to analyze the collected data applying the concepts described in Appendix II.

There are several methodologies and tests to measure the heat evolution of cementitious materials. The most used is a calorimetry test. The calorimetry test can be classified into three types:

- Adiabatic test (no gain or loss through the system),
- Semi-adiabatic (the heat loss through the system is known),
- Isothermal calorimetry (the temperature is constant in the system)

All these tests are used in the concrete industry depending on the concrete's application (dams, bridges, buildings, etc.). There are also many considerations to account for when performing each calorimetric test. This project didn't measure the heat evolution using a calorimetric test but estimated such a curve using the collected temperature information.

Given that temperature information is available at different locations within each sample and that the heat evolution curve represents how fast the heat changes over time, the collected thermocouple information was used to obtain the "pseudo heat evolution curves" for the different mixtures used in the project. Figure 4.2 includes the temperature data collected in all the mixtures used in the project.

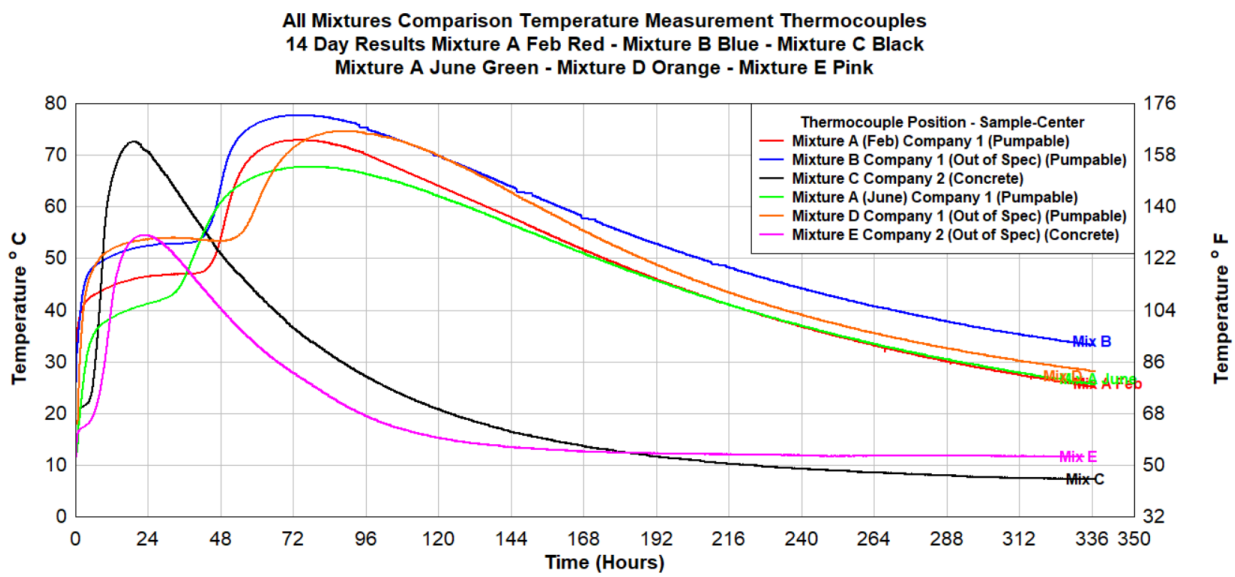

Figure 4.2 Temperature data at the center of the samples for each mixture

As seen in Figure 4.2, the shape of the curve temperature-time is consistent between mixtures of the same company. In other words, despite changing the material proportions and the water/powder ratio, the shapes of the curves are similar in shape. On the other hand, the curves are different when a comparison is made between companies. Figure 4.3 was developed using the information of Figure 4.2.

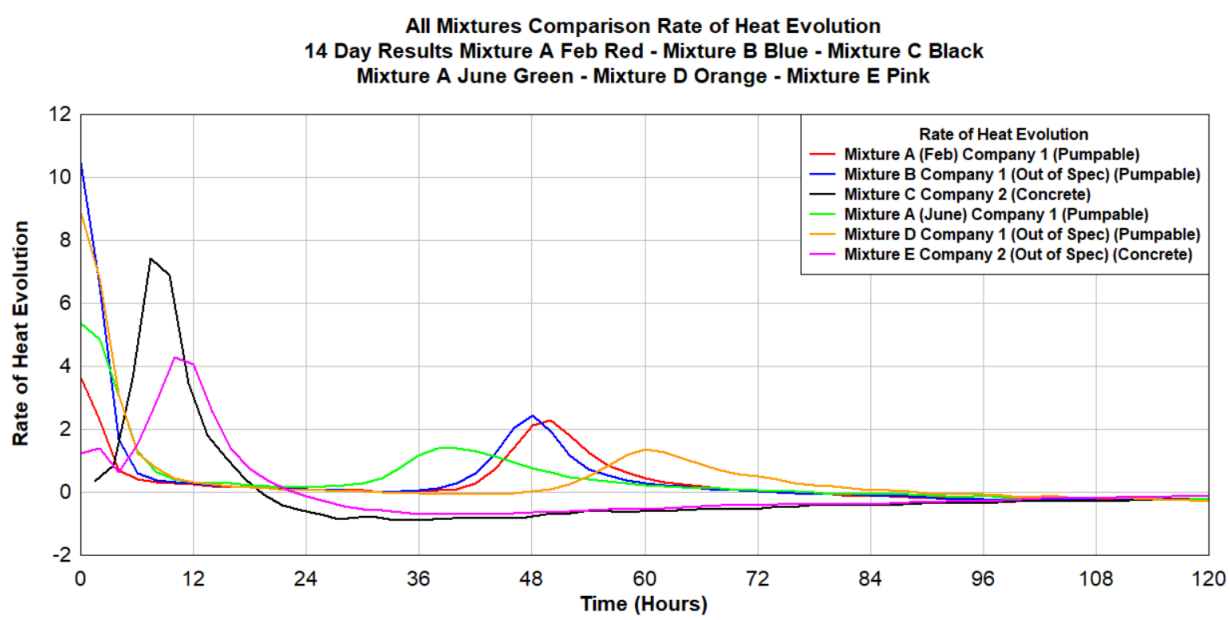

Figure 4.3 Pseudo heat evolution curves for each mixture used in the project

Figure 4.3 shows the pseudo heat evolution curves for the mixtures used in this project. The characteristics of each mixture as illustrated from these curves are explained below. Similar conclusions can be drawn when other parameters such as mixture strength and strain behavior are analyzed.

Temperature Behavior & Analysis for Different standard mine seals Mixtures

Figure 4.4 and Figure 4.5 for Mixture A and Mixture B, respectively, with material from Company 1, clearly demonstrate a rise in temperature for the initial 12 hours, whereafter a decline in temperature for a small period is evident. Following that, the temperature increases again, reaching peak temperatures around 62 hours after the pour, with maximum temperatures being measured in the sample center and followed by the middle of the sample for corner and side positions.

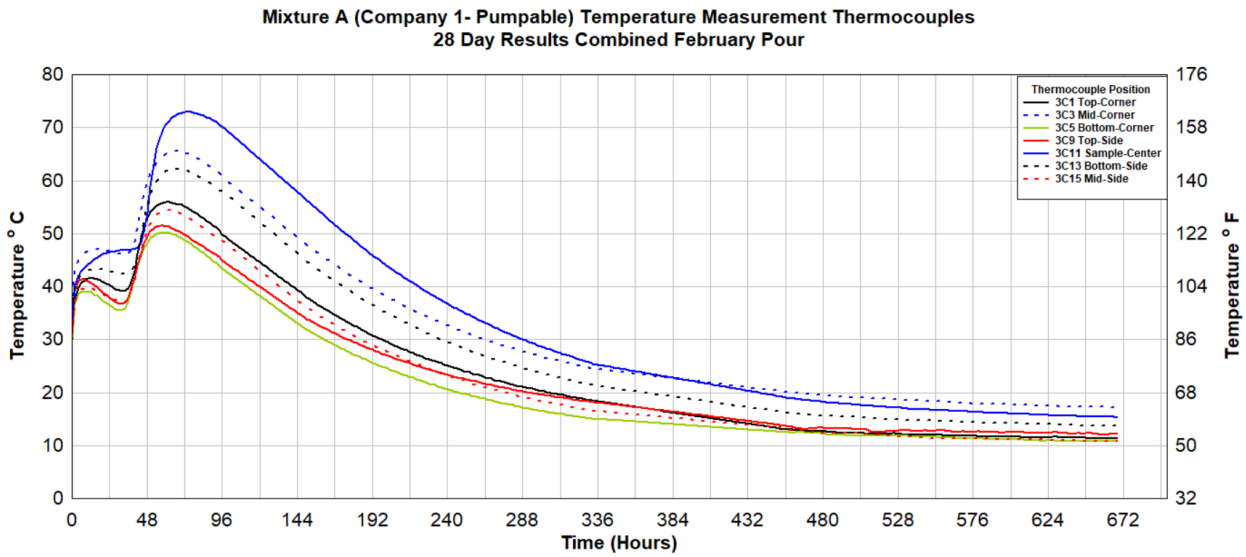

Figure 4.4 Mixture A Temperature Measurement in different locations of samples

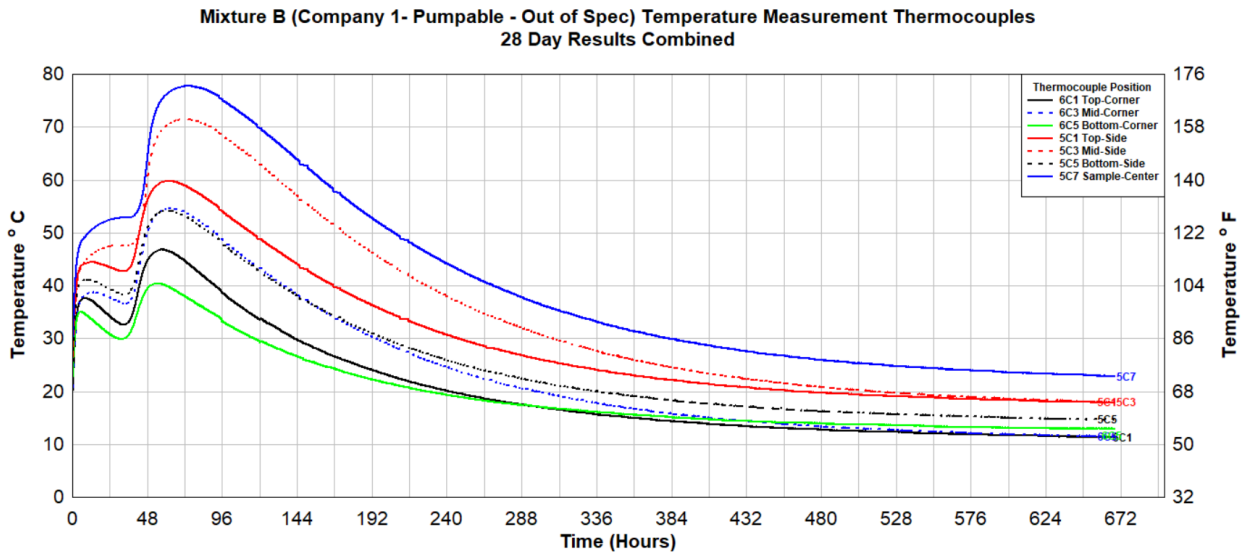

Figure 4.5 Mixture B Temperature Measurement in different locations of samples

Figure 4.6 for Mixture C (Company 2 Material) and consisting of a more conventional concrete mix clearly demonstrate peak temperatures over 90 °C within the first 24 hours of the pour. These high temperatures were recorded for thermocouples positioned at the bottom, on the side of the sample. The sample center still reached a temperature above 70 °C.

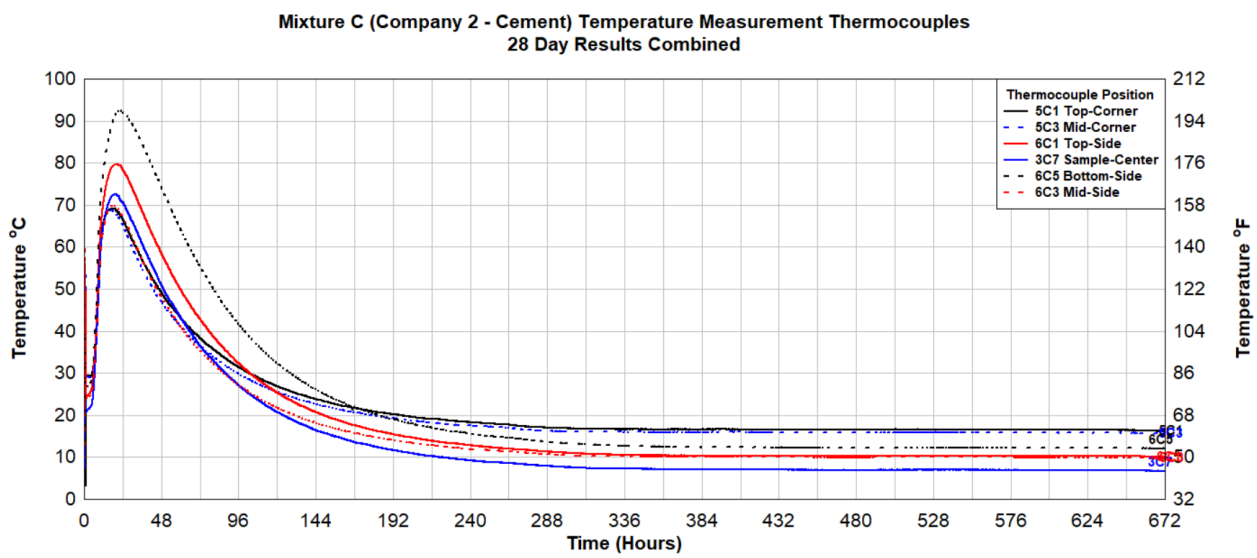

Figure 4.6 Mixture C Temperature Measurement in different locations of samples

The repeated Mixture A (Company 1 – Pumpable – Within Spec) pour was necessary to record strain gauge data not collected from the initial pour in February. Two thermocouples were installed to capture and monitor temperatures. Figure 4.7 demonstrates a similar behavior and temperatures recorded as the sample poured in February. This allowed the strain gauge data to be collected and used in the analysis.

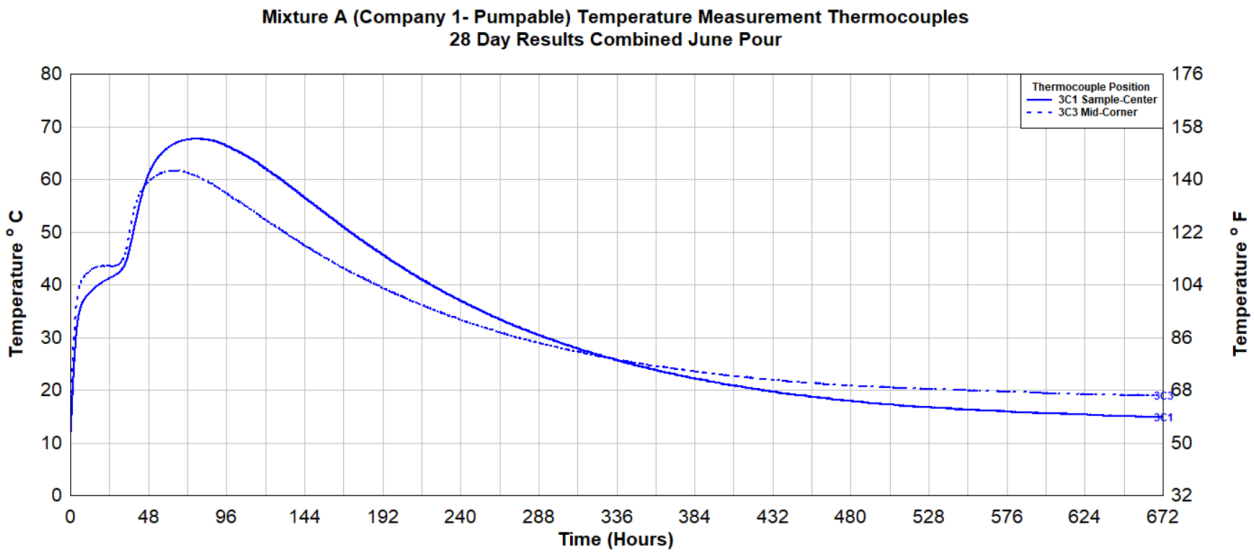

Figure 4.7 Mixture A June Pour, Temperature Measurement in different locations of samples

Mixture D (Company 1 – Pumpable – Out of Spec – Manual Mixing), was a further deviation from the conventional supplier standard but also from Mixture B in an attempt to introduce even more variance to the behavior of strain and temperatures for analysis purposes. Figure 4.8 presents the behavior for the 28-day curing period. Recorded temperatures are slightly lower than temperatures recorded for Mixture B, Figure 4.5. This can be attributable to the difference in mixing methods used, pump versus manual, and water temperature at the mixing stage.

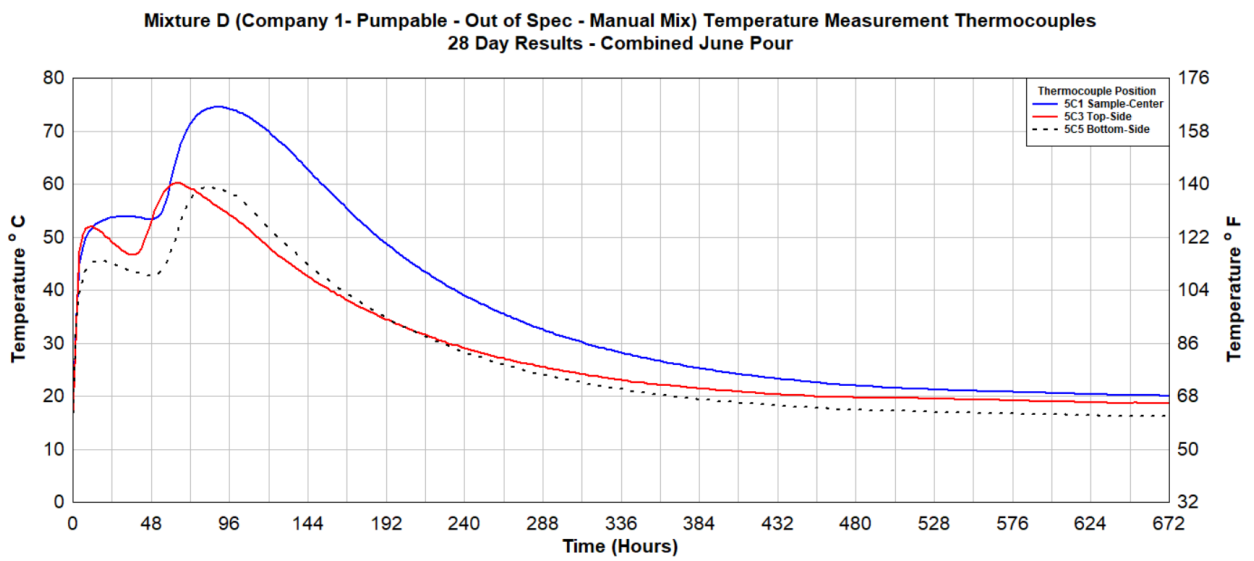

Figure 4.8 Mixture D Temperature Measurement in different locations of samples

Mixture E was a major deviation from the standard mix for Company 2 (Cement). The decision was made to remove all aggregates from the standard mixture and only pour a 4 x 4 x 2 ft sample manually. The data collected over the 28-day curing period, as shown in Figure 4.9, indicate a significant decrease in peak temperatures compared to the standard Mixture C Company 2 (Cement).

Maximum temperatures were still achieved within the first 24 hours, similar to the behavior and data collected for Mixture C, Figure 4.6.

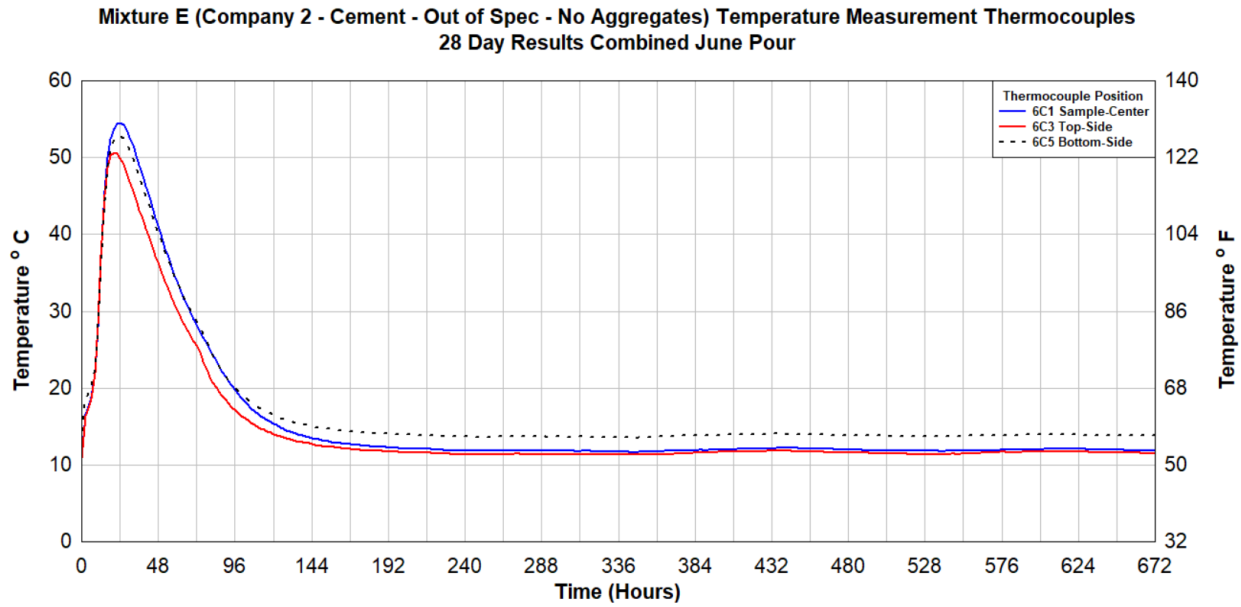

Figure 4.9 Mixture E Temperature Measurement in different locations of samples

Figure 4.10, Figure 4.11, and Figure 4.12 compare temperatures for the initial three Mixtures A, B and C, (Company 1 A, B and Company 2 C) at three different thermocouple positions. The time scale for the graph includes the initial 14 days to increase the detail in the graphs for the period when maximum temperatures were recorded. The more conventional type of concrete, Mixture C for Company 2, reached maximum temperatures within the first 24 hours of curing, and maximum temperatures reached in the seal sample are higher than that for both Company 1, Mixtures A and B. It should be noted that the maximum temperatures are measured in different locations for the different mixtures. This is also discussed later in the report.

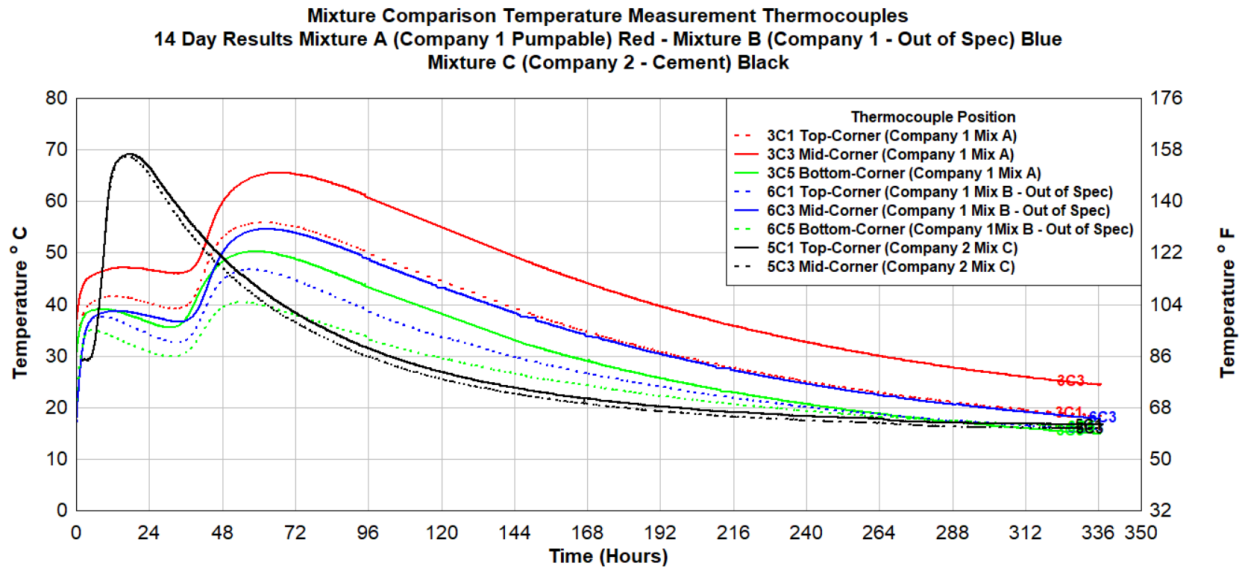

Figure 4.10 Mixture A, B, C Temperature Comparison in corner positions of samples

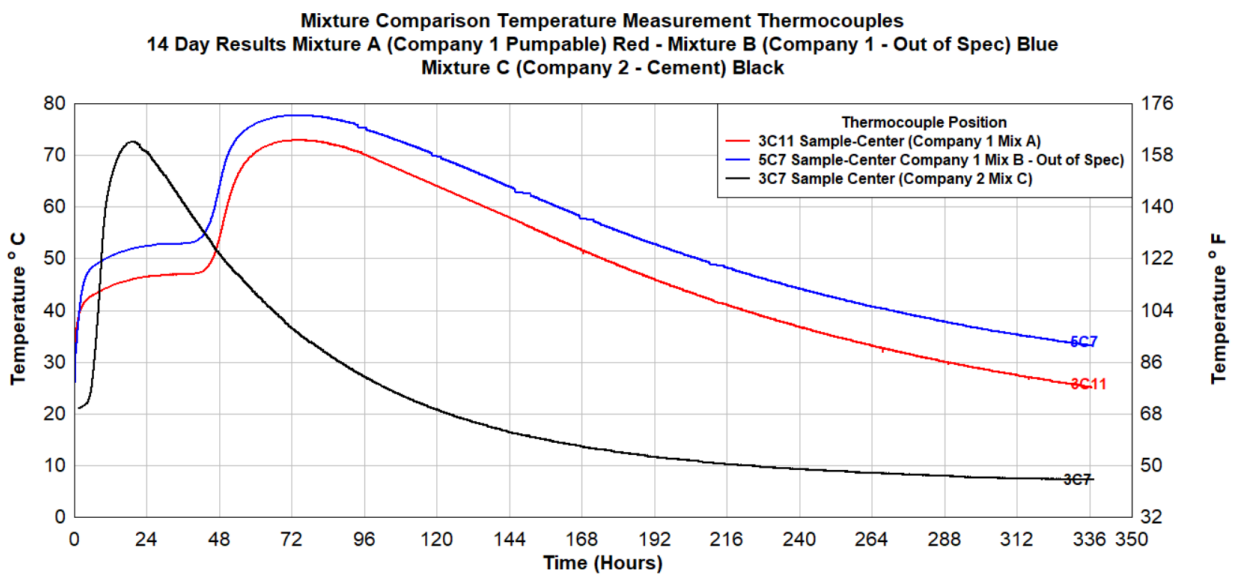

Figure 4.11 Mixture A, B, C Temperature Comparison in sample center positions

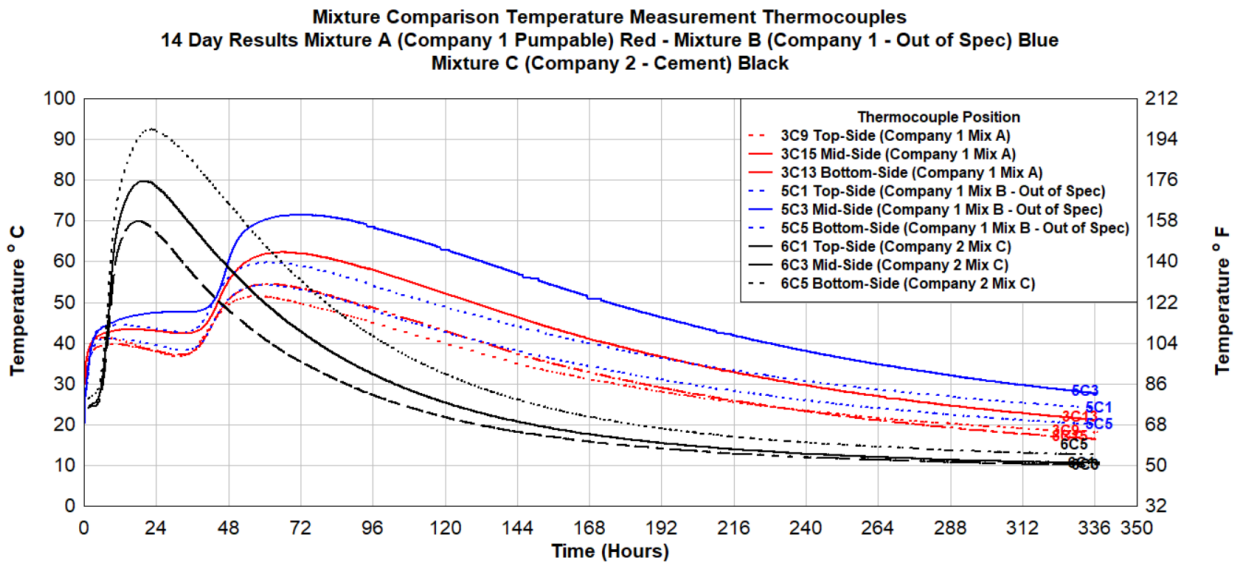

Figure 4.12 Mixture A, B, C Temperature Comparison on side positions of samples

4.2.1.1 *Analysis of the temperature information.*

The concrete industry uses the cracking index concept to assess the likelihood of crack generation during the curing process based on temperature changes within the material. Appendix III includes the theoretical discussion of the cracking index. In this project, it was not possible to use such a concept due to the lack of specific information for the mixtures under analysis and the extensive research required, beyond this project's scope, for its application.

As mentioned in the previous chapter, the temperature was collected at different locations in the samples. It was expected that the internal locations would always present higher temperatures than external locations within the samples. However, such behavior was not observed in all cases. To analyze differential temperatures within the samples and assume a worst-case scenario, the maximum and minimum temperature recordings were used for every mixture regardless of their location. Figure 4.13 to Figure 4.17 show the temperature curves used to analyze the differential temperature for the various mixtures. The Figures include the differential temperature marked in red.

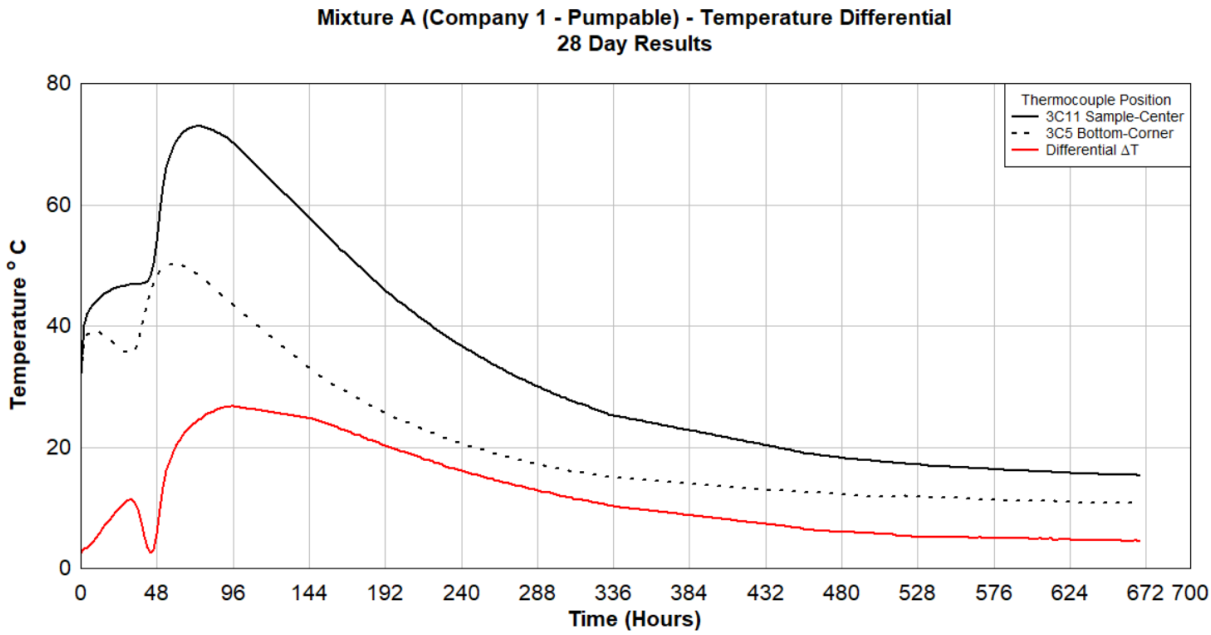

Figure 4.13 Internal restrain, temperature profile analysis for Mixture A

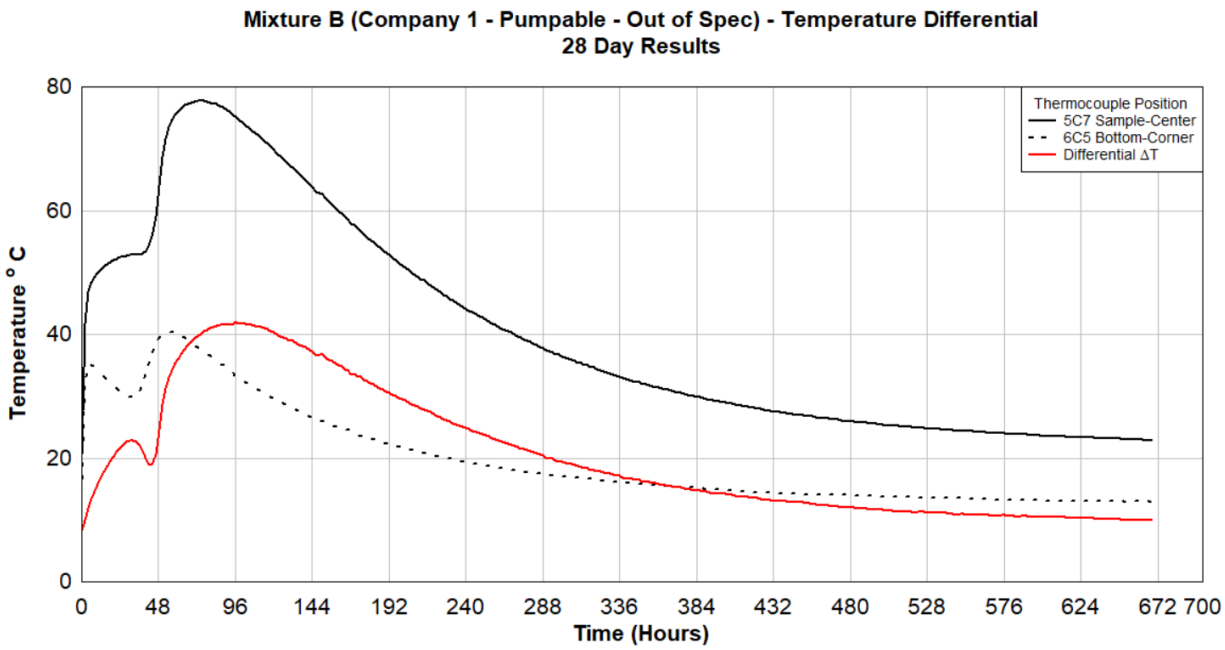

Figure 4.14 Internal restrain, temperature profile analysis for Mixture B

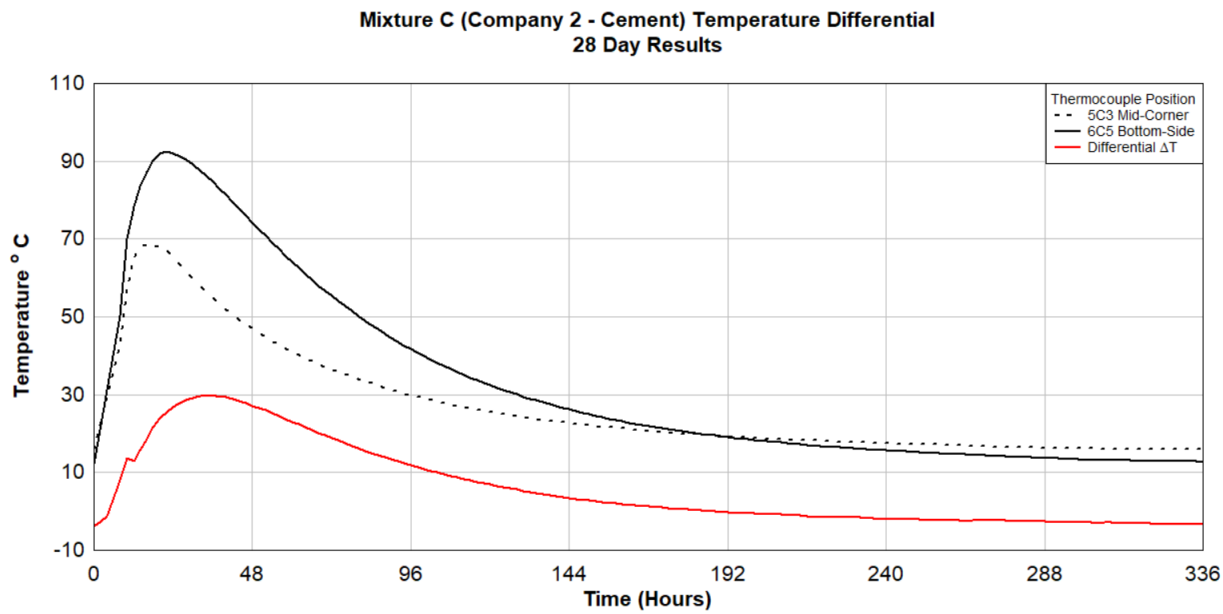

Figure 4.15 Internal restrain, temperature profile analysis for Mixture C

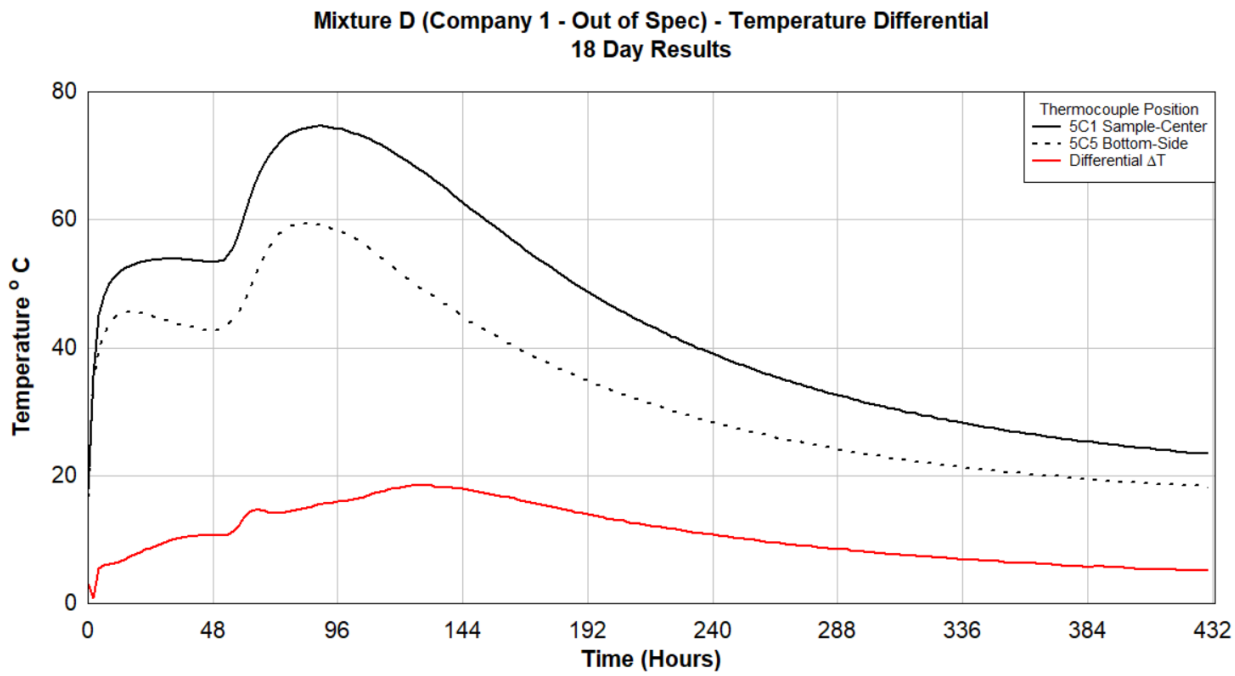

Figure 4.16 Internal restrain, temperature profile analysis for Mixture D

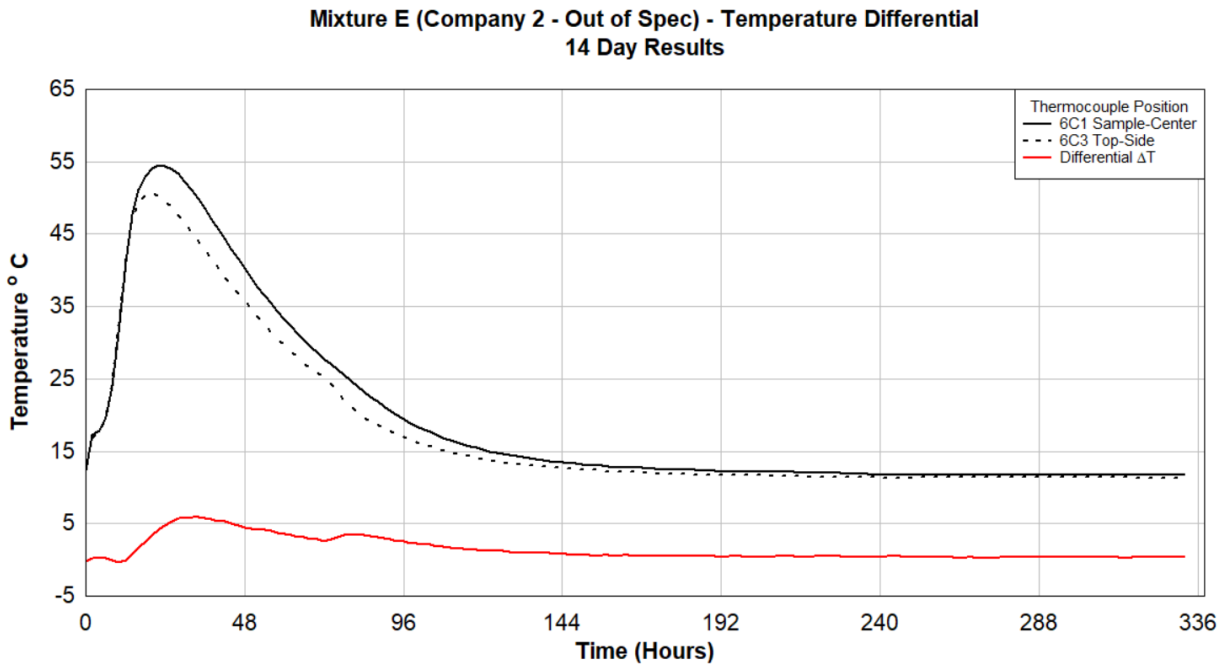

Figure 4.17 Internal restrain, temperature profile analysis for Mixture E

The following observations can be included using the results from previous graphs

- The peak for the differential temperature for mixtures of Company 2 is achieved within the first 48 hours, while the mixtures for Company 1 take a long time and occur after the first 48 hours.
- The maximum differential temperature recorded for standard (within specification) mixtures for Company 1 (Mixture A) is around 26.7 °C (80 °F), while for Company 2 (Mixture C) is 30 °C (86 °F).
- Changes in the powder/water ratio (Out of Spec) for Company 1 affect the maximum differential temperature recorded for its standard mixtures. When Figure 4.13 (Mixture A – 26.7 °C Diff) is compared against Figure 4.14, (Mixture B – 42 °C Diff) the increment in the differential temperature is around 15.3 °C (60 °F).
- Temperatures in Figure 4.17 for Company 2 are affected by the size of the sample.

Finally, the explanation of changes in the differential temperature for the various mixtures can be associated with the chemical process occurring during the curing process. Its analysis and relation with the physical properties of the cured mixtures are beyond this project's scope.

4.2.1.2 *Strain Behavior – Different Seal Mixtures*

The following Figures show the strain behavior of the samples at the different locations where the gauges were installed.

As mentioned previously, the strain data for Mixture A (Company 1 – Pumpable) was lost when the samples were poured the first time due to a problem in the data acquisition system connected to that sample. Because of that problem, Mixture A was prepared again, and Figure 4.18 shows the strain data for the mixture prepared manually in June 2021.

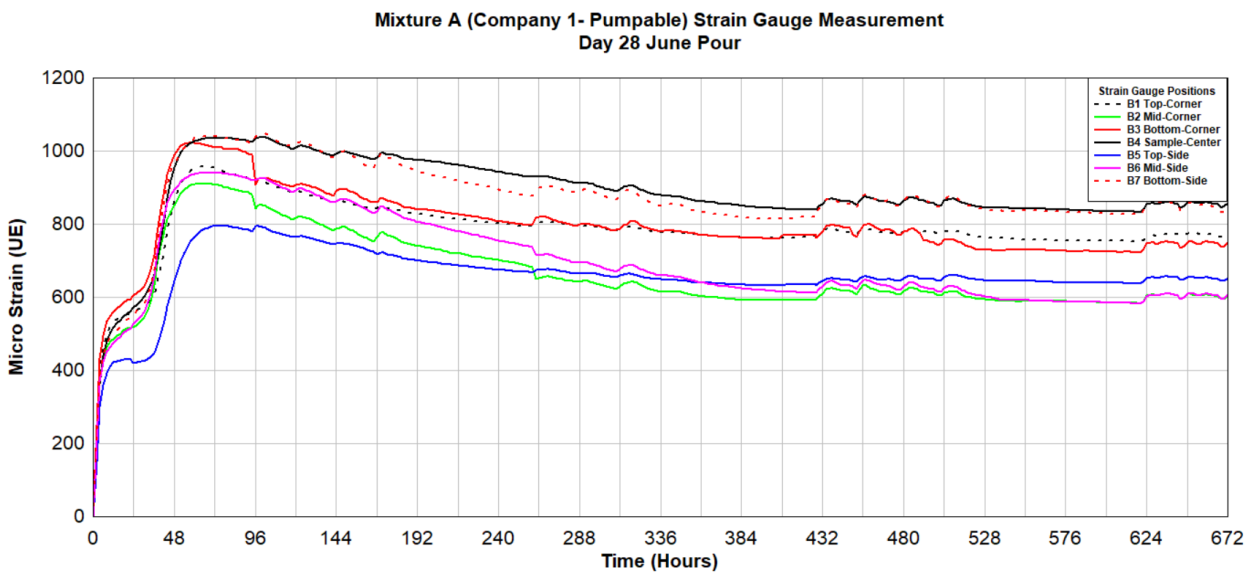

Figure 4.18 Mixture A (June Pour) – Strain gauge measurements

According to the data in Figure 4.18, the higher strain in the sample occurs at the center while there is less strain recorded at the top side of the sample. This is consistent with the internal restraint crack formation mechanism explained in Appendix III (Figure 9.6). According to such a mechanism, it is expected that the center of the sample is at higher temperatures than the sample's external zones. The higher temperatures in the center generate more expansion in those zones than in the external zones.

Figure 4.19 includes the strains measured in the sample for Mixture B (Company 1 – Pumpable – Out of Spec). The maximum strain was measured around 48 hours after pouring the sample, and its location was in the center. After reaching the peak, the strain in all the sensors goes down and becomes asymptotic to a particular value. In Figure 4.19 (and in all the strain figures), the vertical red line represents the instant when the wooden forms were removed.

In the case of the sample of Mixture B, two of the gauges showed changes in the trend after removing the form. Those gauges are located at the sample's bottom side (B7) and top corner (B1). Despite the behavior of these two gauges, the changes are minimal, and in practical terms, for Mixture B of Company 1, removing the form does not impart significant changes in the trend of the strains. This cementitious mixture exhibits a similar trend regarding the internal restrain crack formation mechanism.

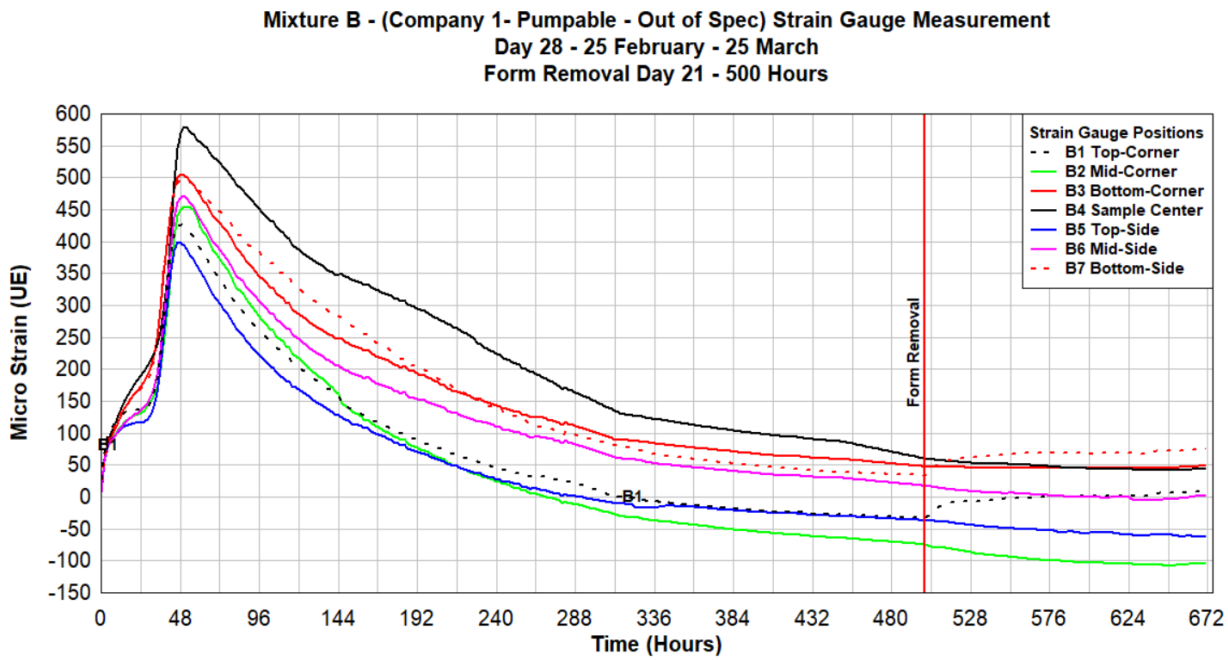

Figure 4.19 Mixture B – Strain gauge measurements

Figure 4.20, shows the behavior of the strain for Mixture C. When comparing Figure 4.18 and Figure 4.19 against Figure 4.20, it is evident that they are two different types of materials (Mixtures A and B are from Company 1, being the pumpable material while Mixture C is from Company 2). Additionally, it can be observed that Mixture C is more susceptible to strain changes when the form is removed. This is supported by observing the changes in the strain readings in Figure 4.20 after the form is removed. As seen in this Figure 4.20, the strains have a "re-activation." Finally, the strain readings at the final stages of the collected data are even higher than in the first 48 hours after pouring. The explanations of all these differences should be deeply associated with the complex chemical reactions happening during the curing process and the particular heat evolution curve for each mixture.

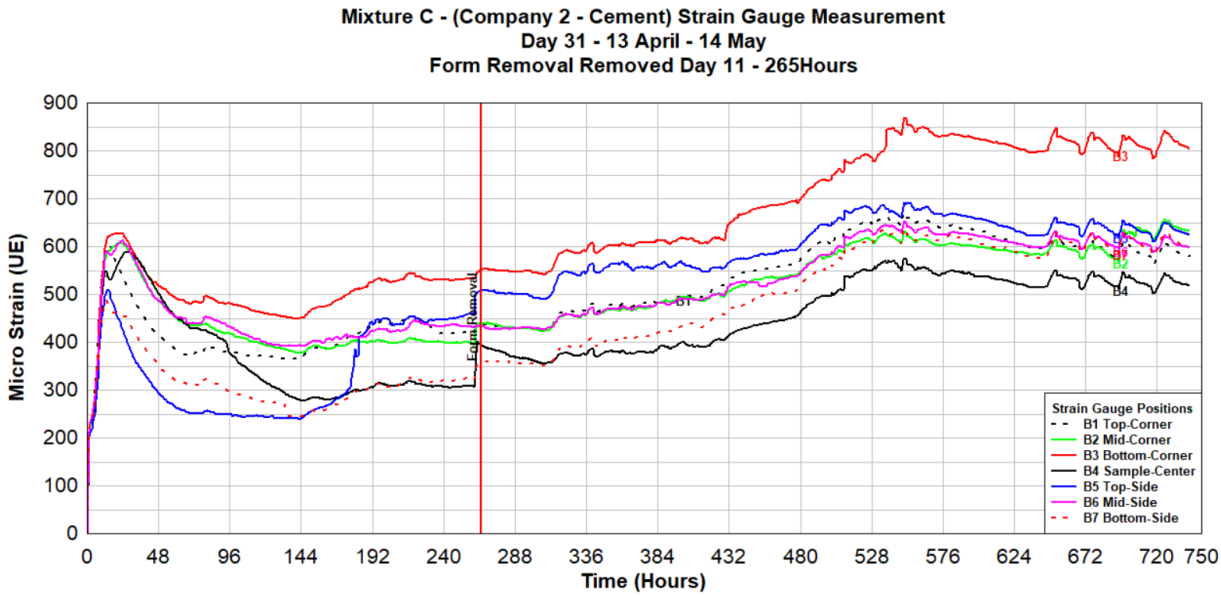

Figure 4.20 Mixture C – Strain gauge measurements

Another considerable difference compared to mixtures of Company 1 is that in the case of Mixture C (Company 2), the higher strains at the first peak (between the first 48 hours) are measured at the bottom corner (B3), while the minimum strains occur at the bottom side (B7). Despite that, the highest difference in strains is not between the center and the perimeters of the sample, as the crack formation mechanism of internal restraint suggests. There are differential strains between the center and other locations in the sample during the curing process.

Mixture D (Company 1 – Out of Spec) strain data is presented in Figure 4.21. As mentioned before, this sample was manually poured using materials from Company 1. The general shape of Figure 4.21 is similar, to figures from mixtures A and B. Additionally, a particular observation can be made regarding the behavior of the mixture when the form is removed (vertical red line after 96 hours from pouring, Figure 4.21). For the samples poured in February 2021, it was necessary to discuss the convenience of removing the form and the plastic film of the sample with the representative of Company 1 supporting the project. This was because the specifications for building the mine seals using the materials from Company 1 are very strict regarding keeping the plastic film as part of the recommended curing procedure. This is the reason why in Figure 4.19, the vertical line is almost at the end of the graph (after 480 hours). At that moment, it was thought that the strains did not change because the form was removed "too late." When analyzing Figure 4.21 where the form was removed after 96 hours, there is no increase in the rate of the strain, but the change in the behavior of the strains is almost imperceptible. In other words, strains developed in materials from Company 1 are not affected when the forms are removed when compared to strains developed in the material from Company 2.

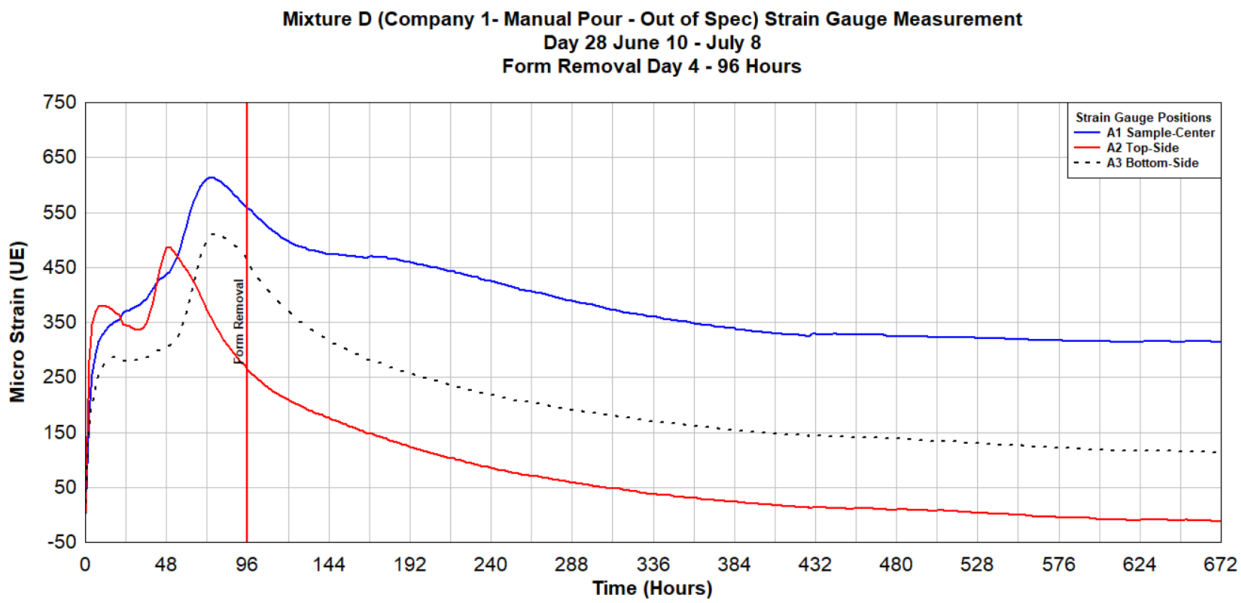

Figure 4.21 Mixture D – Strain gauge measurements

Similar to previous graphs from Company 1, differential values in the strains within the samples can contribute to cracking during the curing process.

Figure 4.22(a) shows the strain measurements from Mixture E (Company 2 Cement – Out of Spec). This sample was manually poured, and its dimensions are different from all the other samples. This sample dimensions are 4 x 4 x 2 ft. Several factors contributed to the change in the dimensions for this sample: the amount of available material from Company 2, the requirement to manually pour this sample, and one attempt to vary the conditions of this sample even more from the standard approved specification. For this particular sample, the effect of removing the form is only apparent for the strains measured at the center of the sample, but it is not of the same magnitude with respect to the changes observed in Mixture C. The strain information indicates that there are differential strains during the curing process.

This sample was poured using "out-of-spec" mix specifications. A visual inspection of the sample Figure 4.22(b) shows that there are different textures in the material. A detailed inspection shows that "sandy" areas migrate to the bottom of the sample, similar to a separation process where the heavier materials (sand) precipitate to the bottom of the sample.

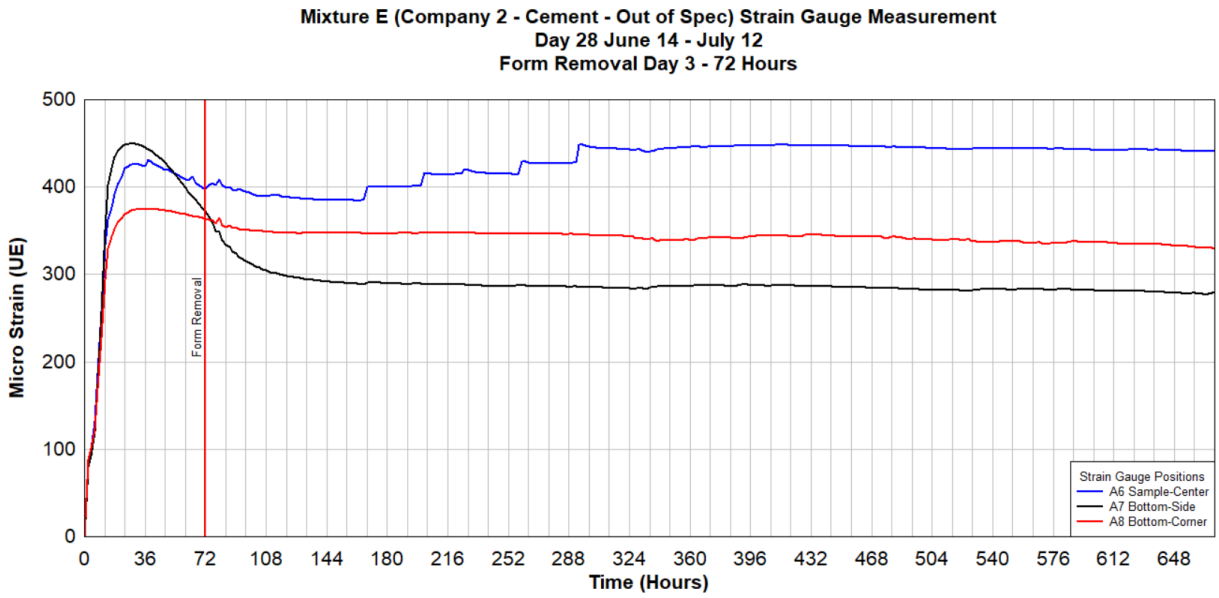

a) Strain data

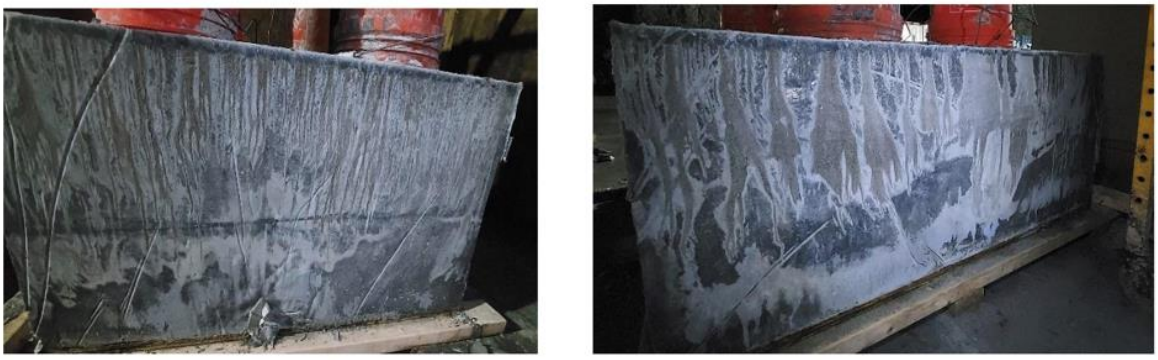

b) Visual inspection of the sample mixture E

Figure 4.22 Mixture E – Strain gauge measurements and visual inspection

4.2.1.3 *Strain versus Temperature Comparisons*

This section discusses the evolution of recorded strain and temperature of the samples with time. The aim of these graphs is to observe if there is an evident relationship between changes in temperature and the measured strain. The main hypothesis is that any temperature change will produce a change in the strains in the sample. If this hypothesis is proven true, the strains are directly related to thermal stresses, and any crack could be attributed to such stresses.

Figure 4.23 shows the strain versus temperature comparisons for Mixture A. The selected locations shown in the figure are the mid-corner and the center of the sample. As seen in Figure 4.23, temperature and strain follow the same trend. Temperature and strain increases relate to thermal stresses and expansion. In this Figure 4.23 strains are in black, while temperature records are in blue. Another observation in Figure 4.23 is that the rate of change in temperature is similar to the rate of change in strain, specifically for the first 72 hours (when the peak in both temperature and strain is reached). After the peak, the rate of change in temperature is more pronounced than the rate of change in strain. The reduction in strain implies material shrinkage from its peak values when temperatures and expansion were at their highest.

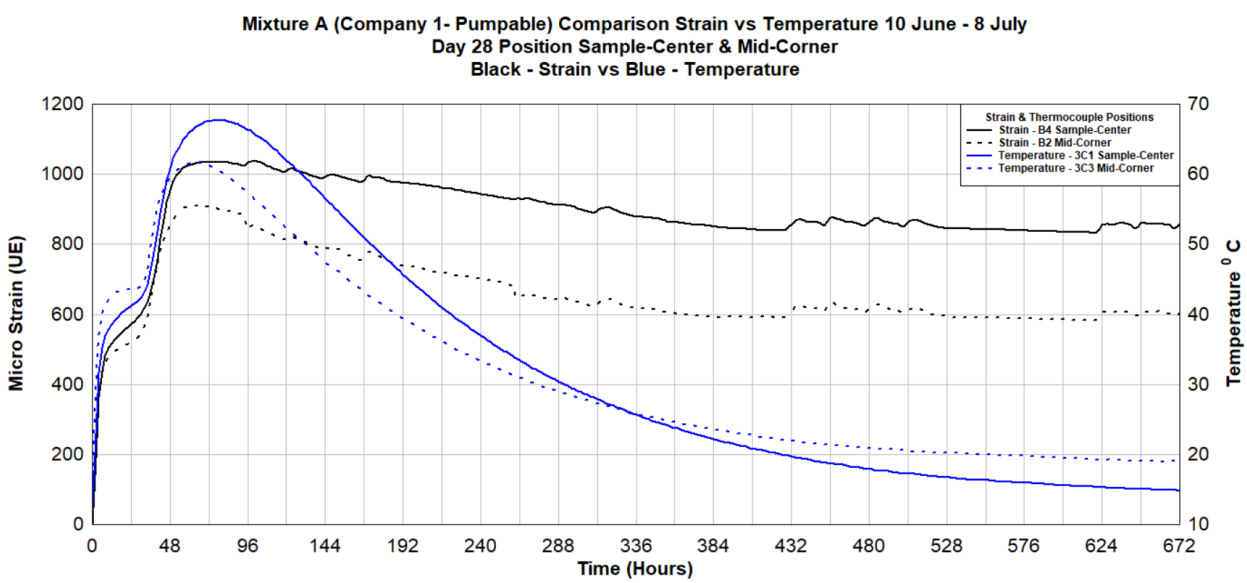

Figure 4.23 Mixture A – Comparison of strain versus temperature for the sample center and mid-corner

Figure 4.24 to Figure 4.26 shows the comparison curves for Mixture B (Company 1 – Out of Spec) at different sample locations, top-corner, center, and bottom-side, respectively. As seen in these figures, temperature and strain follow the same trend during the entire period of recorded data. As mentioned before, removing the forms affected strain at the bottom corner and bottom side, but no significant changes were observed in temperature related to removing the form. The only current hypothesis related to the strain graphs reducing to a negative strain supports the theory that the strain increased with expansion and temperature rises, and as the seal sample cooled down, the strain reduced due to material shrinkage.

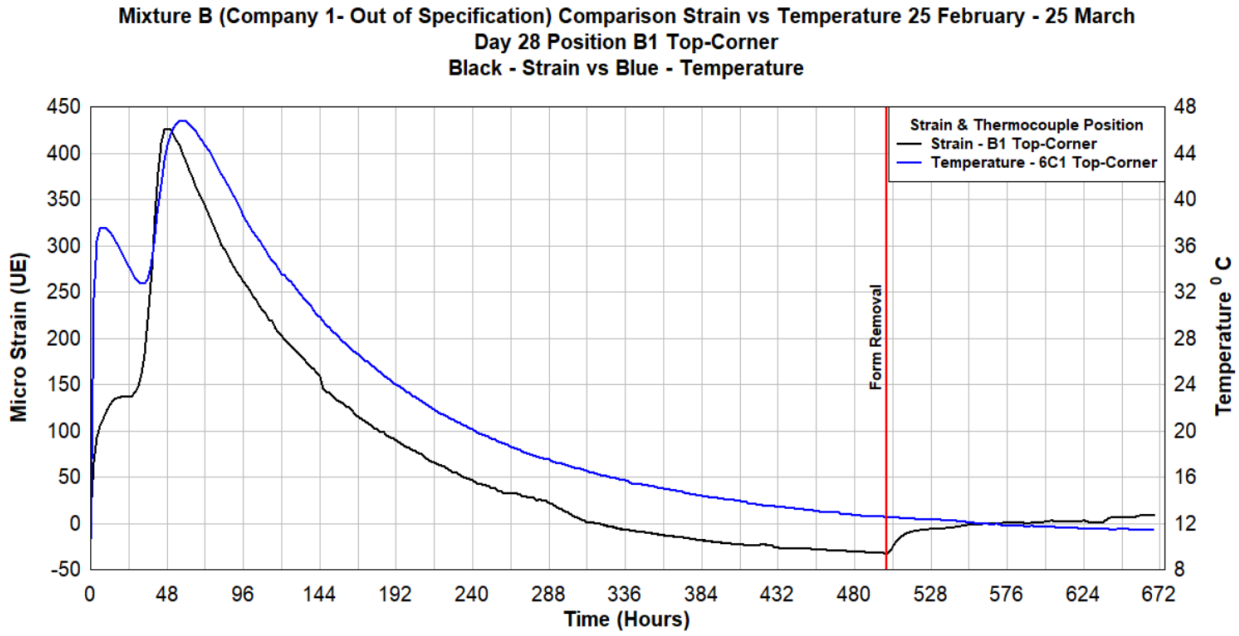

Figure 4.24 Mixture B – Comparison of strain versus temperature for the top-corner position

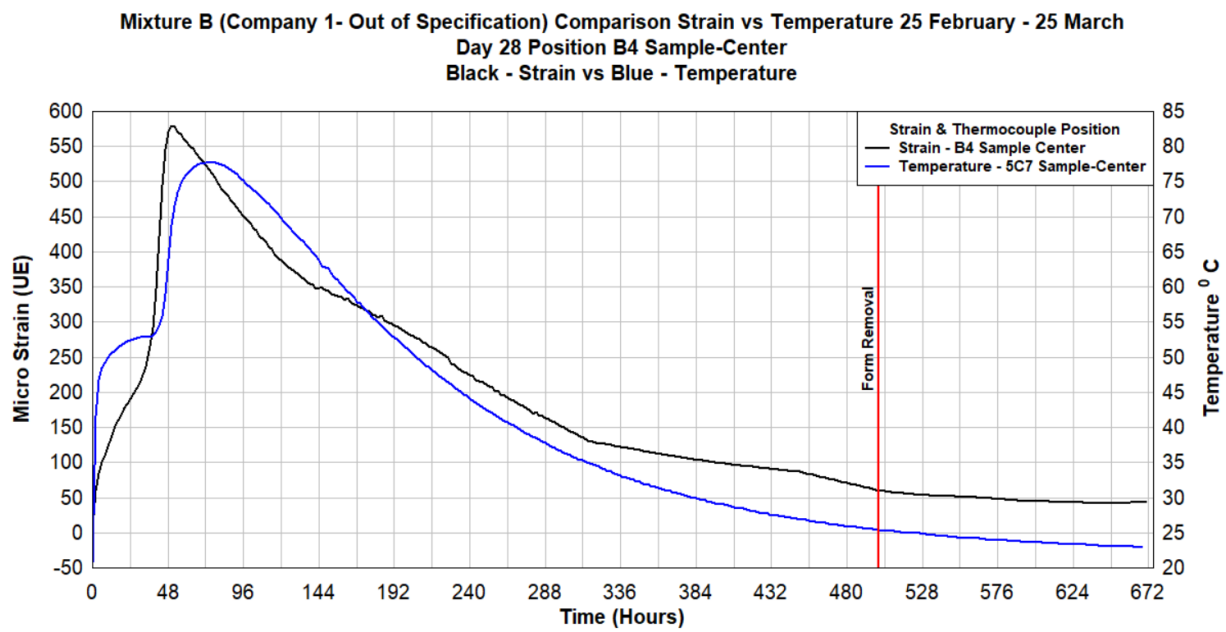

Figure 4.25 Mixture B – Comparison of strain versus temperature for the sample-center

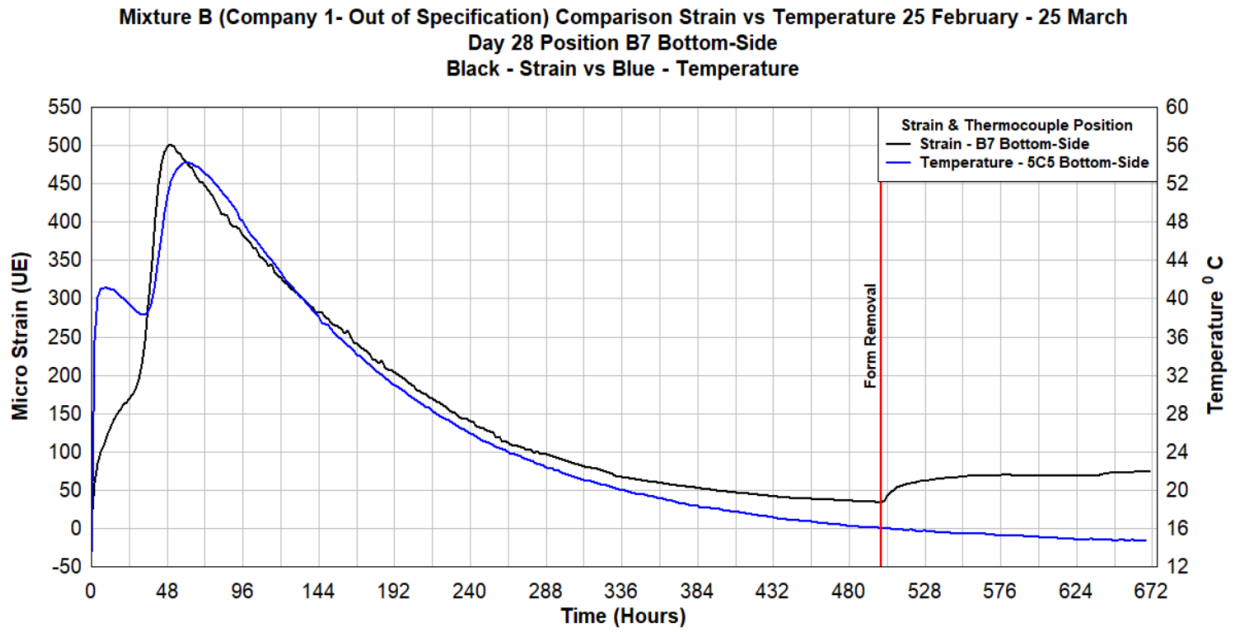

Figure 4.26 Mixture B – Comparison of strain versus temperature for the bottom-side position

For Mixture C (Company 2 – Cement), the curves for the sample's top-corner, center, and bottom-side locations are included in Figure 4.27 to Figure 4.29, respectively.

For this mixture, there is a clear concordance between strain and temperature for the first 72 to 144 hours after pouring. After such time, the sample keeps cooling at all locations while the strains increase again. The strain reaches a second peak about 528 hours after pouring.

In the cases of the corner and side positions (Figure 4.27 and Figure 4.29, respectively), the second peak amplitude is even higher than the first peak, while for the gauges at the center of the sample, the first and second strain peaks are of similar amplitude.

The figures include the time when the form was removed. It is observed that the strain curve shows an instantaneous change in all samples. However, it is not clear if the change is due to manipulating the form during the stripping operation or the changes in the sample's environmental conditions (humidity). As mentioned before, after 144 hours, there is no clear relation between the strain and temperature, which suggests that the stresses producing the strains are not thermal stresses. The source or the stress generation should have a different origin than the differential in temperature. This certainly could be a result of shrinkage (dehydration) or expansion of the sample due to changes in the samples' moisture content because of its exposure to the environmental changes (humidity).

After finding that temperature is not the only variable affecting the stress condition of the sample, it is suggested that another variable could influence the stress condition as expressed by the changes in the moisture content of the material. Moisture content significantly influences the chemical reaction during the curing process. It affects the expansion and shrinkage during dehydration, specifically when the seal samples have the opportunity to properly dry out with the forms removed. As such, this variable was not considered in the design of the tests, and moisture content was not measured.

Finally, in the analysis of the readings of strains of Mixture C after 624 hours of pouring the sample, the graph shows a series of cycles; these cycles follow intervals of 24 hours. The conclusion at this point is that these changes in strain are related to changes in the environment of the mine where the samples were built (changes in temperature and humidity). This is interesting given that all the locations of the sample show this behavior, supporting the idea that factors other than temperature, such as humidity, can induce stresses that will create volumetric changes in the samples. This behavior was not observed for materials supplied by Company 1.

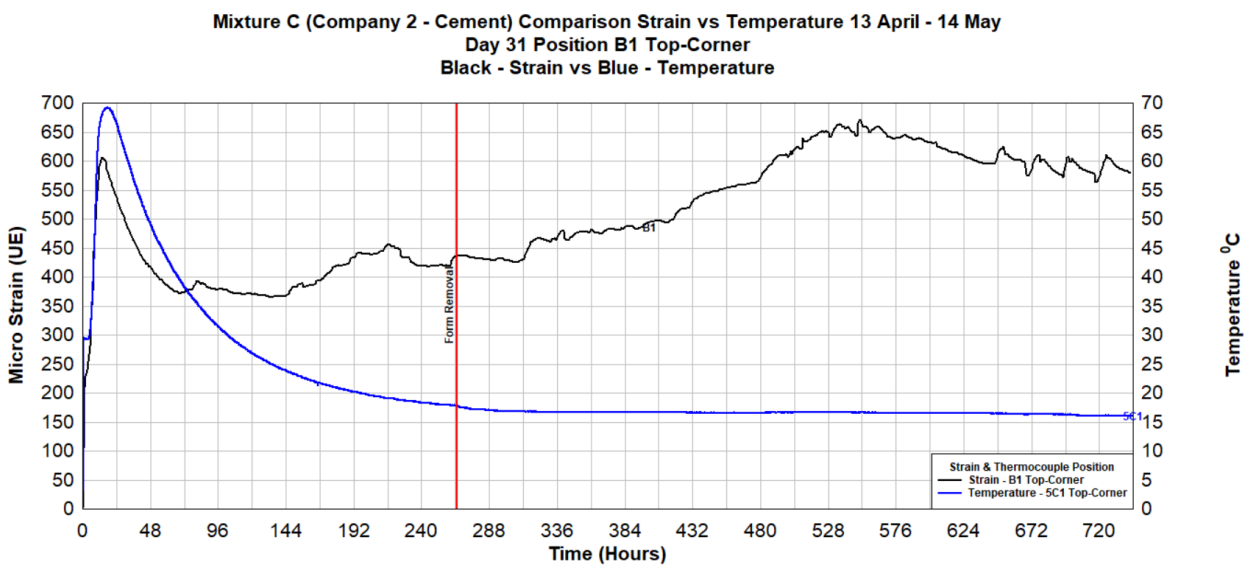

Figure 4.27 Mixture C – Comparison Strain versus Temperature for the top-corner position

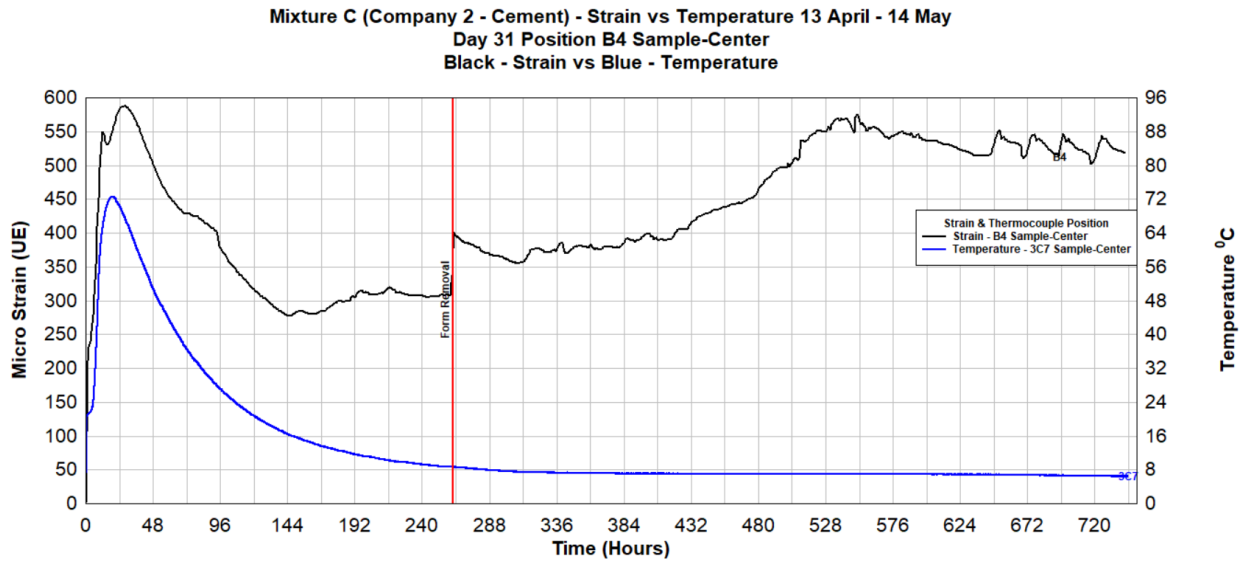

Figure 4.28 Mixture C – Comparison Strain versus Temperature for the sample-center

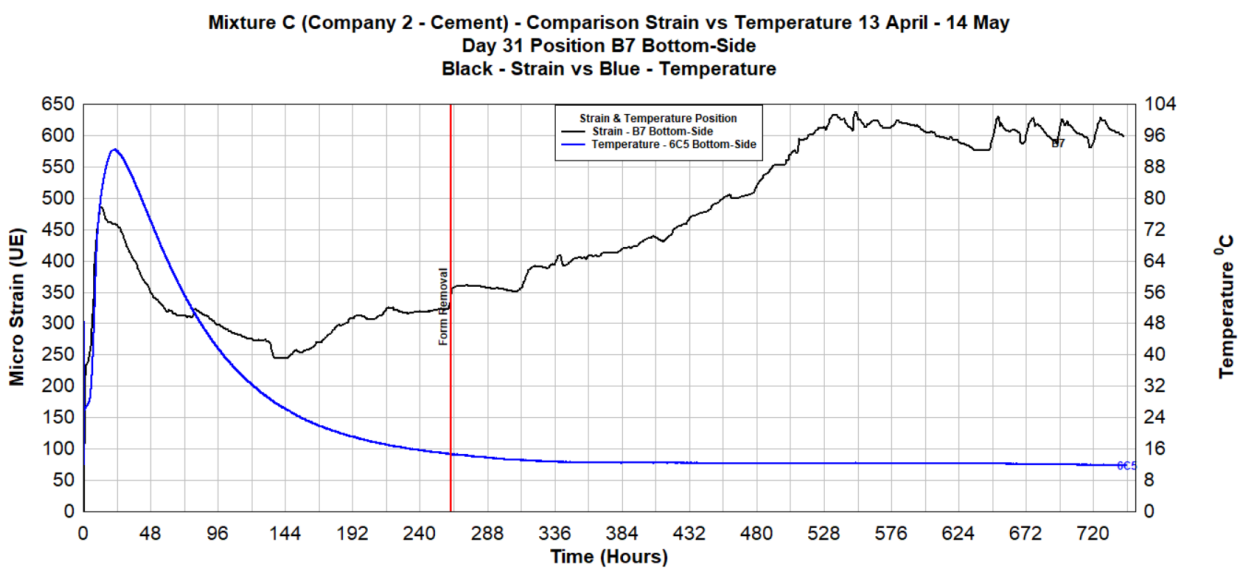

Figure 4.29 Mixture C – Comparison Strain versus Temperature for the bottom-side position

Mixture D comparison between strain and temperature is shown in Figure 4.30, the locations in the graph are for the center and the bottom-side of the sample. This mixture is using materials from Company 1 but in out of specification proportions. Despite the proportions used for the sample being different than the standard proportions, overall, the behavior is similar to Mixtures A and B. This indicates a concordance between strain and temperature during the tests.

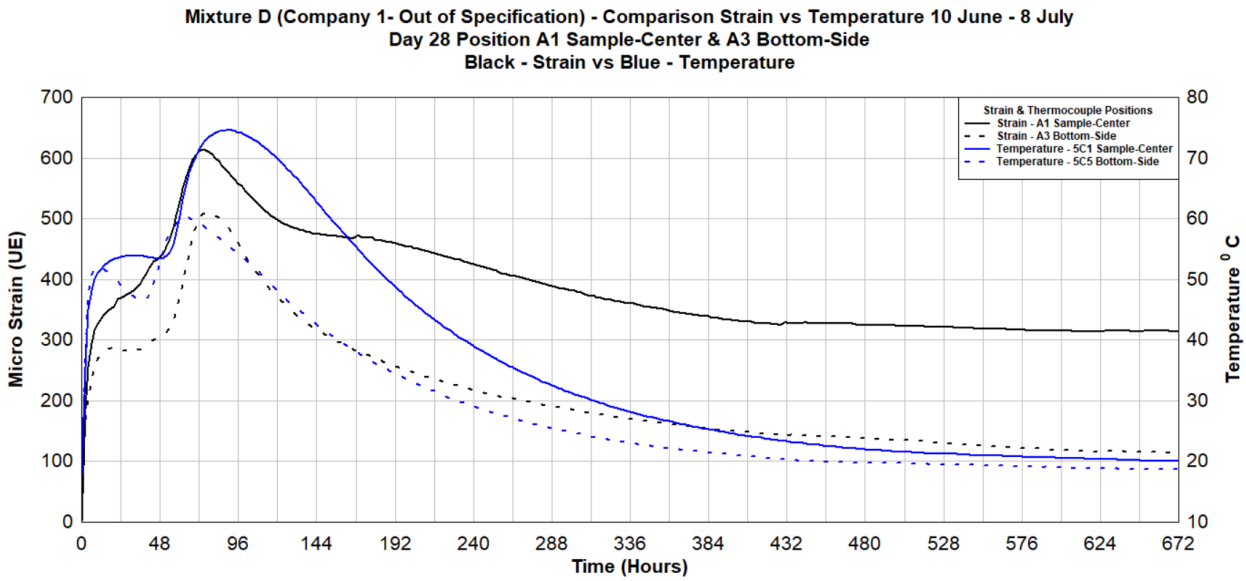

Figure 4.30 Mixture D – Comparison of strain versus temperature for the sample center and bottom-side

The strain versus temperature comparison for Mixture E (Company 2 – Cement – Out of Spec), is very similar to Mixture C and is included in Figure 4.31. The graph was done for the bottom-side and sample center location. The trend indicates that both variables follow a similar behavior for the initial 24 hours after pouring, but after 168 hours the strain starts to increase, at least at the center of the sample.

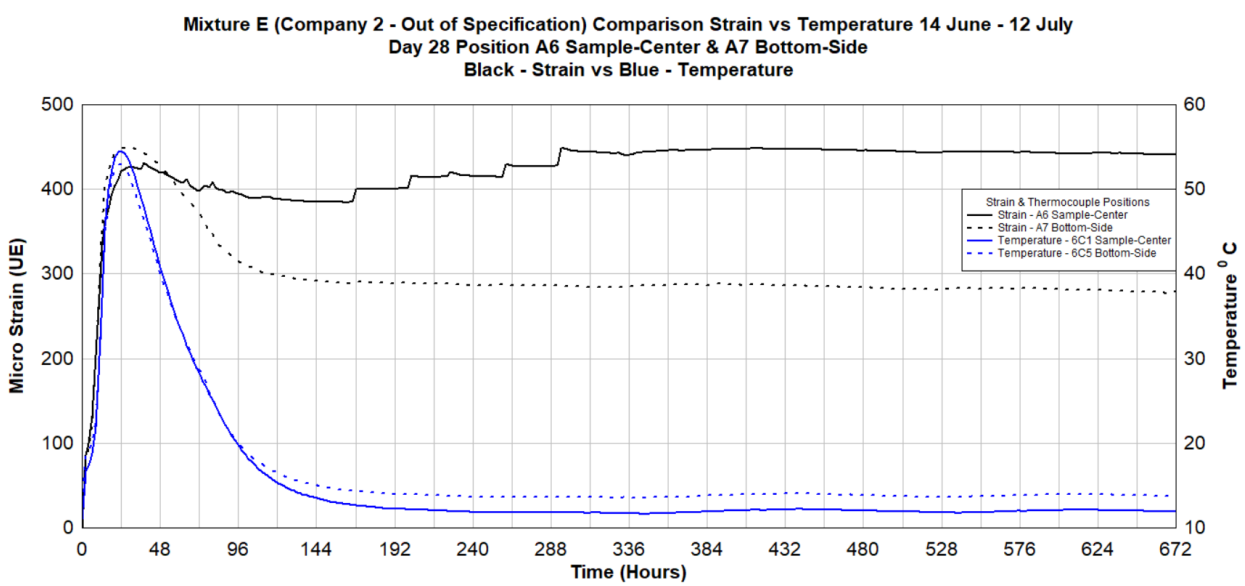

Figure 4.31 Mixture E – Comparison of strain versus temperature for the sample center and bottom-side

4.2.1.4 *Strength of the mixtures – Results for all samples.*

Every time a cube or seal sample was poured, a smaller batch of samples was collected for uniaxial compressive strength (UCS) testing. UCS testing was performed in these samples at 7, 14, and 28 days after pouring.

Table 4.1, Table 4.2, and Table 4.3 are a complete summary of all 41 seal samples tested for uniaxial compression strength (psi) in the laboratory. The tables represent 7, 14, and 28-day testing, respectively.

Table 4.1 – Seal Sample – Uniaxial Compression Strength (UCS) (psi) @ 7 days

4ft*4ft*4ft	Seal Sample – Uniaxial Compression Strength (UCS) (psi) (7 days)					
SEAL SAMPLE	Mixture A (Company 1 - Within Spec)	Mixture B (Company 1 - Out of Spec)	Mixture C (Company 2 - Within Spec)	Mixture A (Company 1 - Within Spec - Manual Pour June)	Mixture D (Company 1 - Out of Spec - Manual Pour)	Mixture E (Company 2 - Out of Spec - Manual Pour) (4 x 4 x 2 ft)
TRACER GAS	757	514	-	-	-	-
STRAIN GAUGES	453	659	5641	924	245	1958
THERMO COUPLE	642	682	5441	-	-	-
CONTROL SAMPLE	716	523	5015	-	-	-
Average	642	594	5366	924	245	1958

Table 4.2 – Seal Sample – Uniaxial Compression Strength (UCS) (psi) @ 14 & 18 days

4ft*4ft*4ft	Seal Sample – Uniaxial Compression Strength (UCS) (psi) (14 & 18 days)					
SEAL SAMPLE	Mixture A (Company 1 - Within Spec)	Mixture B (Company 1 - Out of Spec)	Mixture C (Company 2 - Within Spec)	Mixture A (Company 1 - Within Spec - Manual Pour June)	Mixture D (Company 1 - Out of Spec - Manual Pour)	Mixture E (Company 2 - Out of Spec - Manual Pour) (4 x 4 x 2 ft)
TRACER GAS	808	818	6516	-	-	-
STRAIN GAUGES	785	705	6549	1878	1682	1807
THERMO COUPLE	886	680	-	-	-	-
CONTROL SAMPLE	849	836	6674	-	-	-
Average	832	760	6580	1878	1682	1807

Table 4.3 – Seal Sample – Uniaxial Compression Strength (UCS) (psi) @ 28 days

4ft*4ft*4ft	Seal Sample – Uniaxial Compression Strength (UCS) (psi) (28 days)					
SEAL SAMPLE	Mixture A (Company 1 - Within Spec)	Mixture B (Company 1 - Out of Spec)	Mixture C (Company 2 - Within Spec)	Mixture A (Company 1 - Within Spec - Manual Pour June)	Mixture D (Company 1 - Out of Spec - Manual Pour)	Mixture E (Company 2 - Out of Spec - Manual Pour) (4 x 4 x 2 ft)
TRACER GAS	716	771	6867	-	-	-
STRAIN GAUGES	783	921	-	1122	1390	5300
THERMO COUPLE	1015	883	8411	-	-	-
CONTROL SAMPLE	888	1059	-	-	-	-
Average	850	908	7639	1122	1390	5300

Figure 4.32 shows the UCS at seven days comparison between Mixture A (Within Spec) and Mixture B (Out of Spec).

Figure 4.33 shows the UCS at seven days for all samples of mixture A (first and second round). It was also decided to include the results for mixture D material from the same supplier Company 1 (out of spec sample), in the graph.

As seen in Figure 4.33, despite the second sample of mixture A being manually poured, the UCS at seven days is showing slightly higher peak values than samples poured using all the equipment provided by the supporting company to the project. Another observation is that the sample of Mixture D (out of spec) shows peak values almost three (3) times lower than Mixture A at seven days (7).

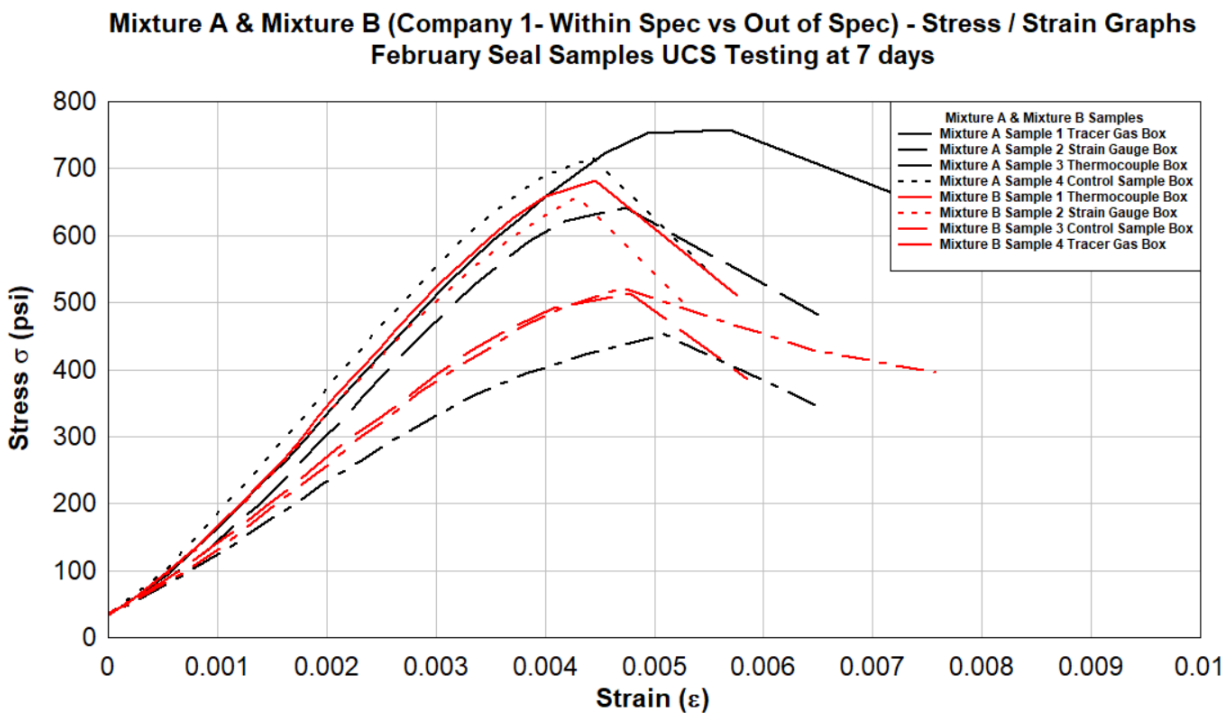

Figure 4.32 Mixtures A & B – Stress / Strain comparisons for the February pour for 7-day testing

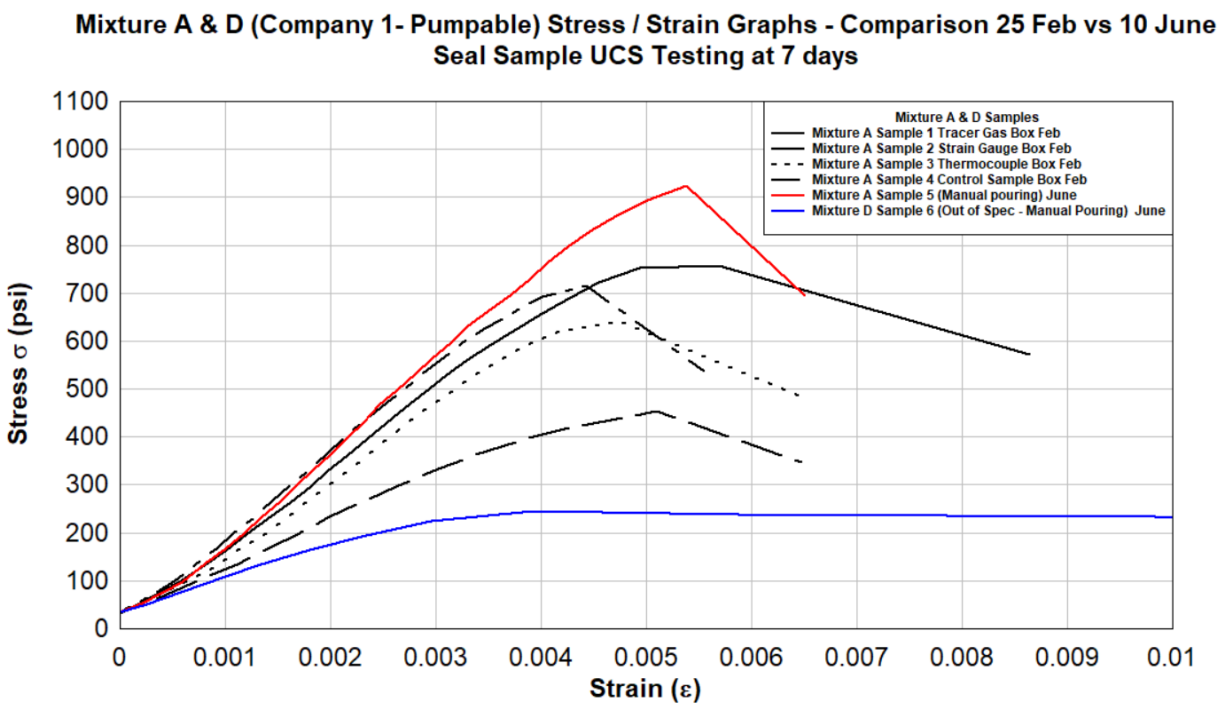

Figure 4.33 Mixtures A & D – Stress / strain comparisons between February and June pour for 7-day testing

Figure 4.34 is similar to the previous one and includes UCS testing results at 14 days. It should be noted that the mine was not accessible for the collection of the samples at 14 days (for the June pour), and the testing was done at 18 days instead of 14 days. The June pour tested at 18 days now clearly shows a higher UCS value than the February pour at 14 days.

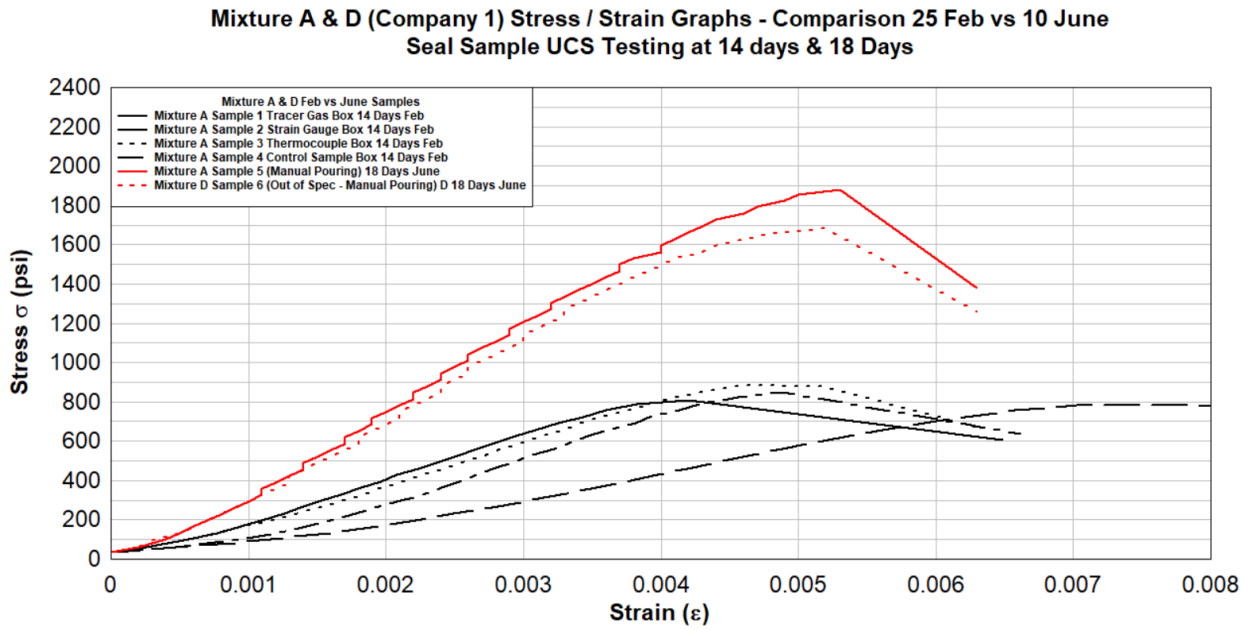

Figure 4.34 Mixtures A & D – Stress / strain comparisons between February and June pour for 14–18-day testing

Figure 4.35 includes the results for Mixtures C and E for Company 2 at seven (7) days. The out of specification sample exhibits a much lower UCS value than the standard and approved Mixture C from Company 2.

Figure 4.36 includes the results for mixtures C and E for Company 2 at 14 days. As noted for the 7-day test results, the out of spec sample exhibits a much lower UCS value.

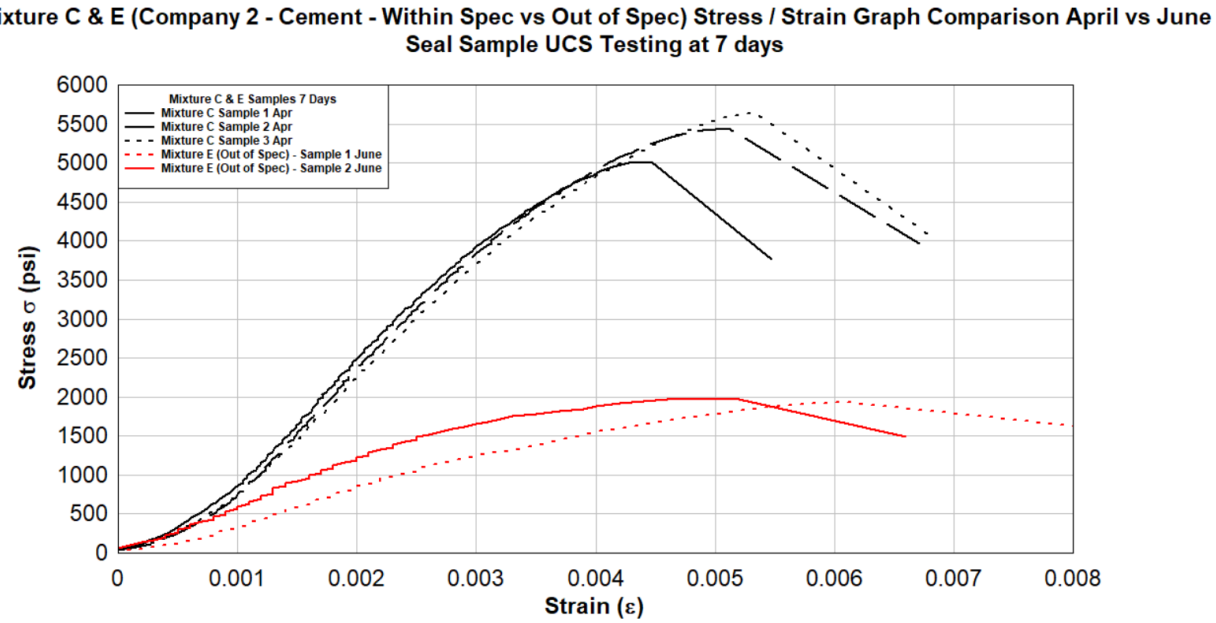

Figure 4.35 Mixtures C & E – Stress / Strain graphs comparison between April and June pour for 7-day testing

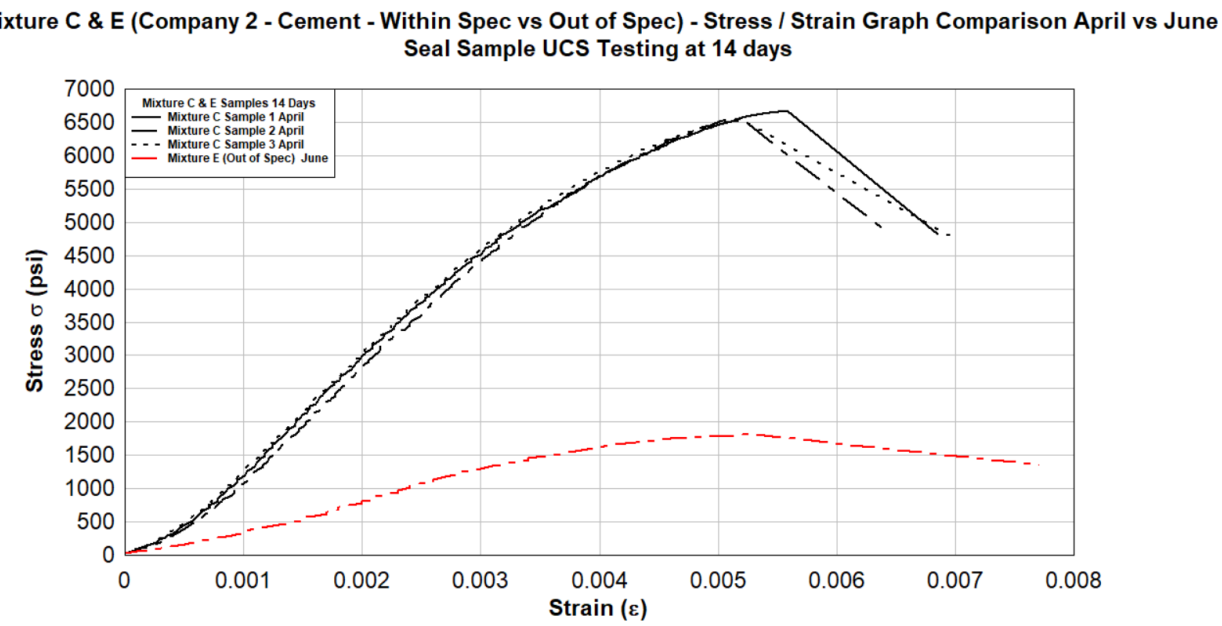

Figure 4.36 Mixture C & E – Stress / Strain graphs comparison between April and June pour for 14-day testing

Figure 4.37 through to Figure 4.40 shows all the UCS and comparisons for the 28 days test results.

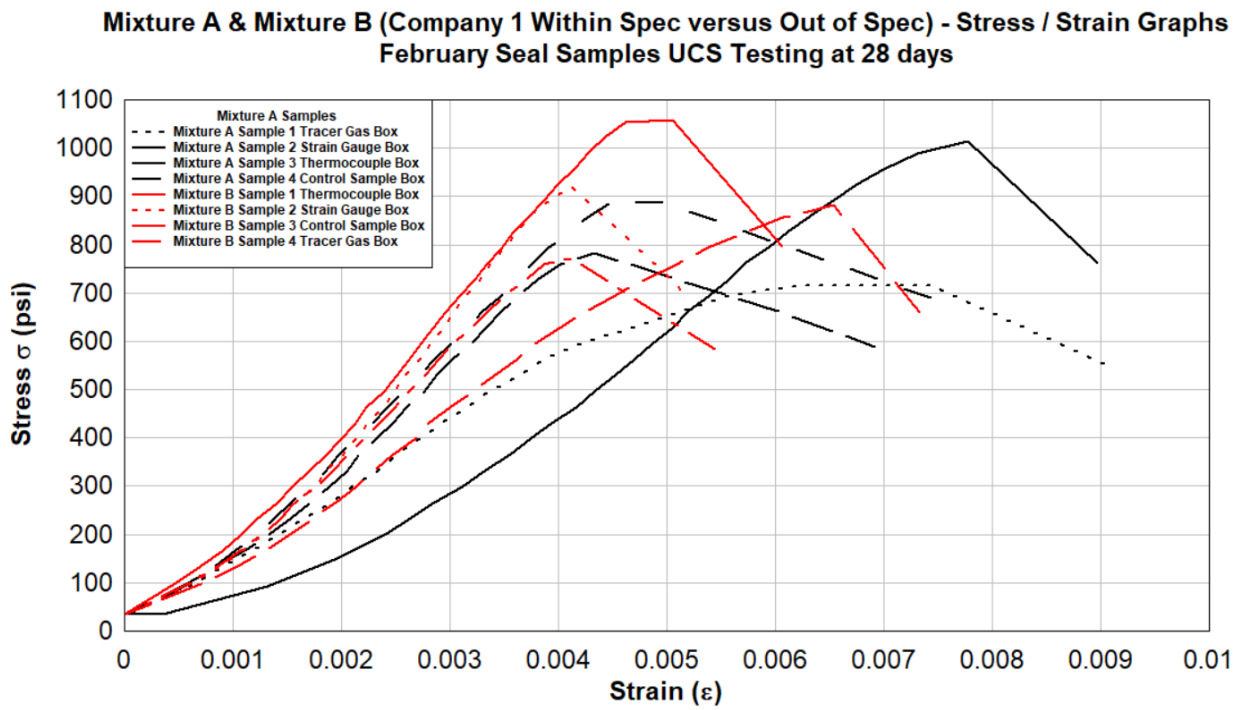

Figure 4.37 Mixture A & B – Stress / Strain graphs comparison on 28 days – Company 1 Within Spec vs Out of Spec February Pour.

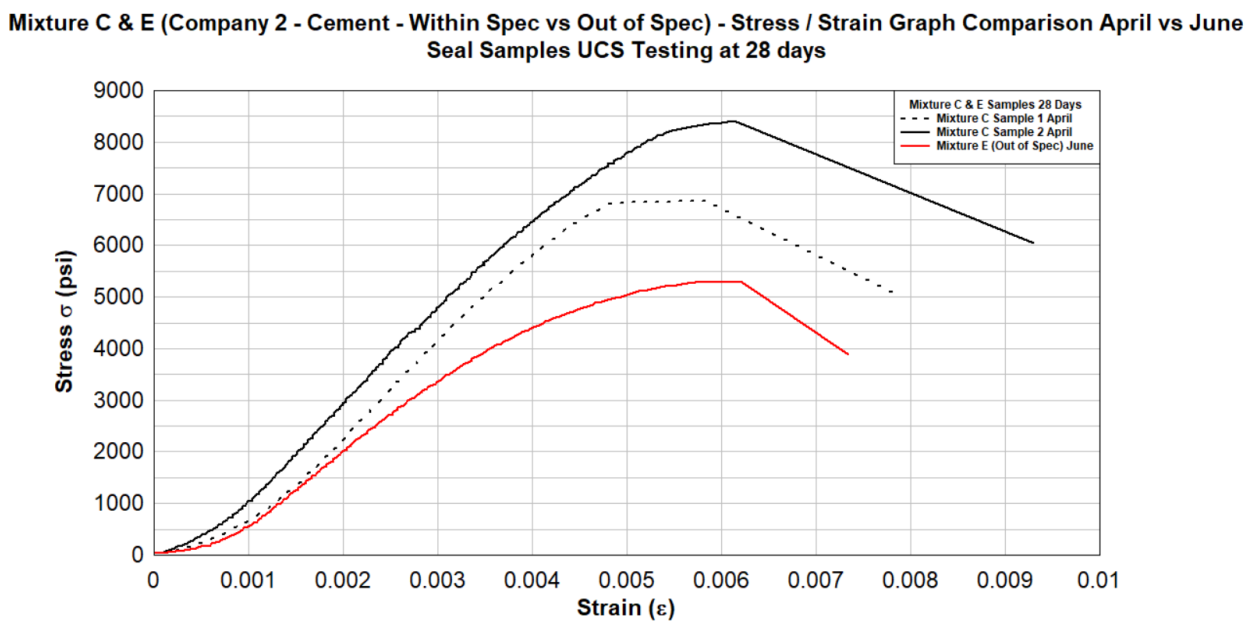

Figure 4.38 Mixture C & E – Stress / Strain graphs comparison between April and June pour for 28-day testing

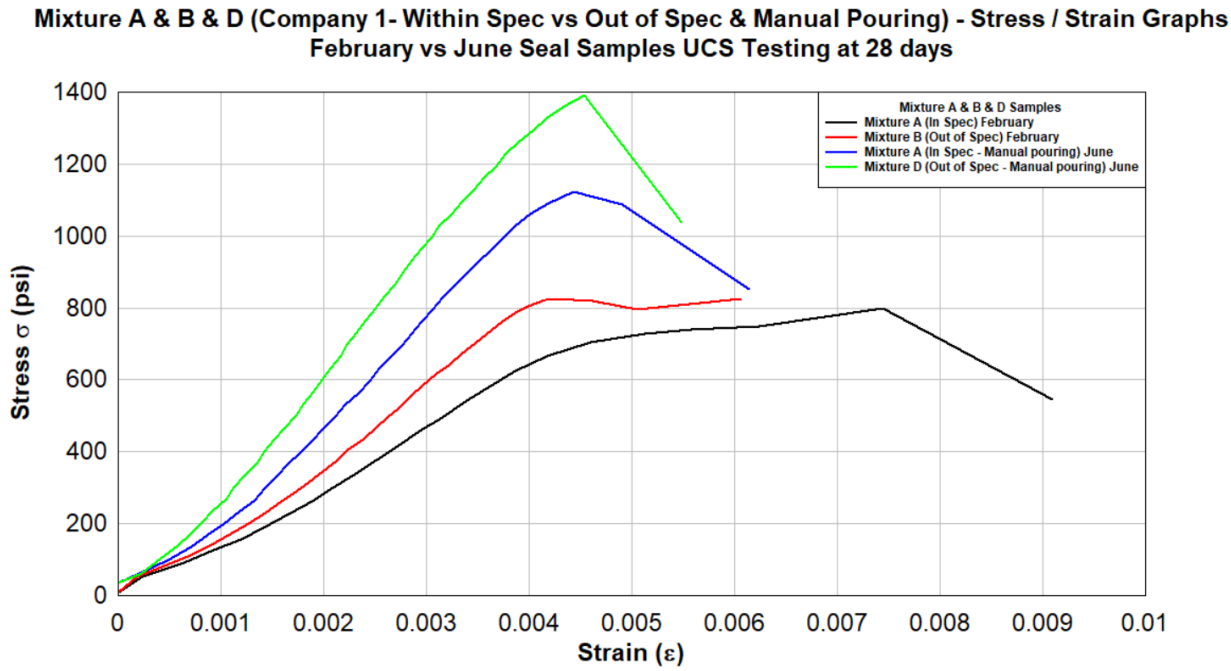

Figure 4.39 Mixture A & B & D – Stress / Strain graphs comparison between February and June pour for 28-day testing

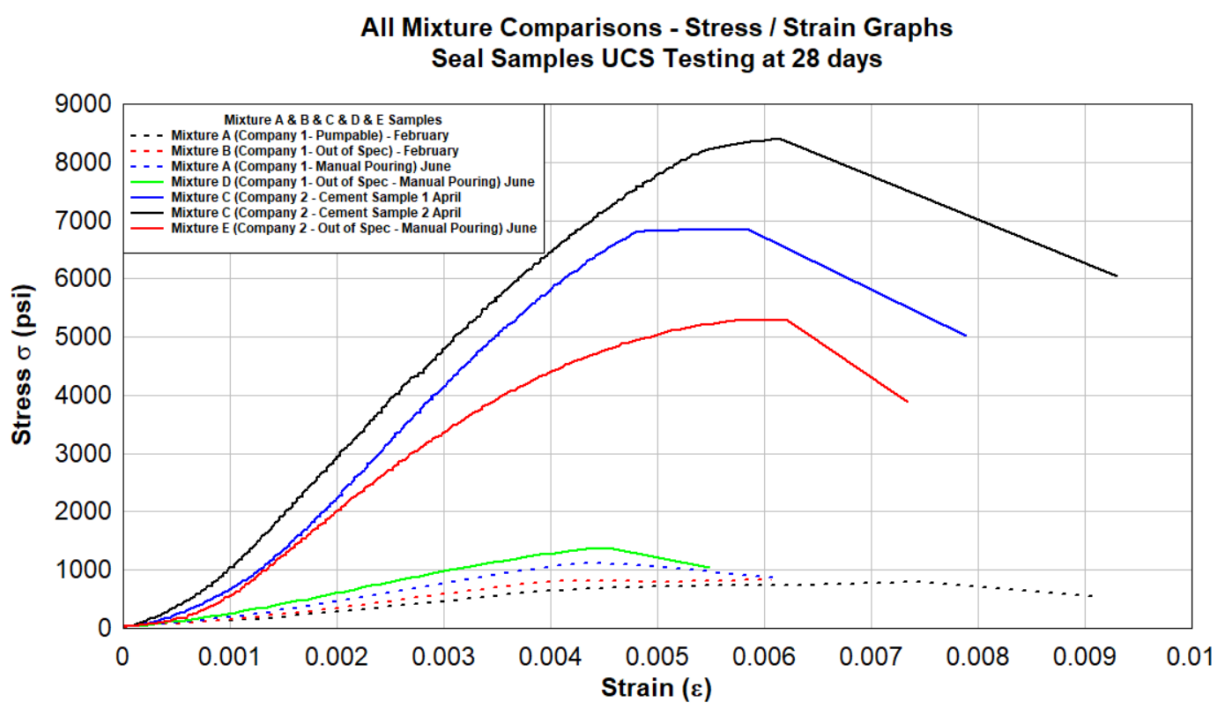

Figure 4.40 Mixture A & B & C & D & E – Stress / Strain graphs comparison between February, April and June pour for 28-day testing

The strain information and the strength information presented in previous sections were used to analyze the samples during the curing process. The following section describes the analysis performed with the data.

4.2.1.5 *Analysis of the strain-strength information.*

As included in Appendix III, a crack index for concrete can be defined as the ratio between the tensile strength of the material and the stresses produced during the curing process. Estimating the stresses produced by the curing process (internal and external restraint) is generally done using numerical modeling (FE). The stresses during the curing process can be related to the heat evolution curve of the cementitious material. On the other hand, the assessment of the tensile strength can be performed using lab tests such as the Brazilian test or estimated based on the compressive strength of the material. The collected strain gauges information, and the uniaxial compressive tests were used to visualize the evolution of the strength and the stress with the time for each mixture.
The obtained results can be used to identify the critical periods during the curing process where cracks can be generated, but because of the number of assumptions adopted, they cannot be used to assess the likelihood of crack generation.

Figure 4.41 shows the principles of the curves developed in this section. The main assumptions or considerations are listed as follows:

- The tensile strength for all the mixtures is ten percent (10%) of their compressive strength value. This assumption is reasonable for conventional concrete, but it will be necessary to validate it for the mine seal mixtures.
- The information collected in the gauges is assumed as tensile strains. Since the stresses are computed from the strains, this assumption plays a critical role in the analysis. This assumption can be an overestimation of the tensile strains in the sample and will need to be validated using numerical modeling.
- Shear stresses are not considered in the analyses.
- There is no consideration regarding the direction of the strains,
- The use of the elasticity theory is valid,
- The elastic modulus in compression measured in the UCS tests is similar or the same as that when the material is under tension.
- The strength of the material in the function of time follows a curve given by [14]

$$f_c = A * ln\,(t) + \mathrm{B} \qquad \text{Eq. 1}$$

Where:
f_c=compressive strength
t=time (days)
A, B=are constants to fit the curve to the lab data.

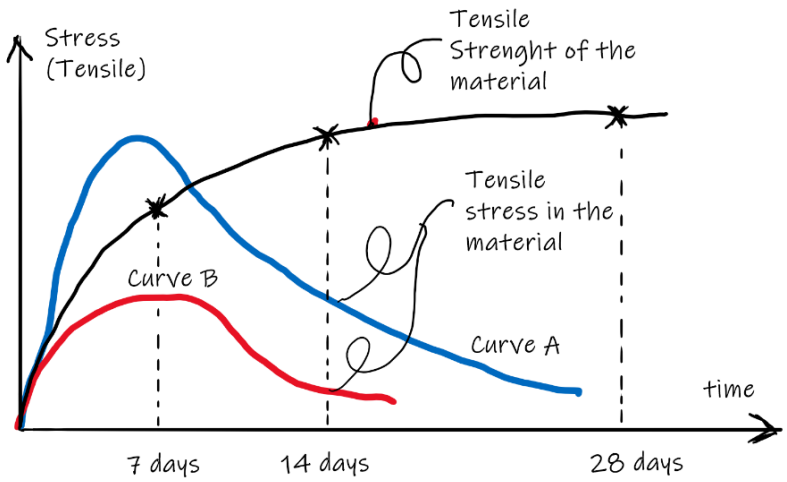

Figure 4.41 Development of strength and stress curves, with the strength and strain information collected through this project

According to Figure 4.41 and considering the assumptions stated above, the evolution of the material's tensile strength with time was calculated as being equal to 10% of the compressive strength. This was possible as there are UCS tests that are available for 7, 14, and 28 days (the respective points are denoted with asterisks in Figure 4.41).

The tensile stress of the material was calculated using the theory of elasticity and the basic equation that relates stress and strain (Hooke's Law) given by:

$$\sigma_t(t) = E * \varepsilon_t(t) \qquad \text{Eq. 2}$$

Where:
$\sigma_t(t)$: Tensile stress in the material at any given time,
E: Young's modulus,
$\varepsilon_t(t)$: Tensile strain in the material at the same time

To apply Equation 2, the Young's modulus from the USC tests was used. Table 4.4 (7 Days), Table 4.5 (14 Days), and Table 4.6 (28 Days) includes the values for the different UCS tests.

Table 4.4 Young's modulus calculated from the source of UCS specimen (psi) for 7 days Testing.

4ft*4ft*4ft	Average Young's Modulus 7 days (psi)					
SEAL SAMPLE	Mixture A (Company 1 - Within Spec)	Mixture B (Company 1 - Out of Spec)	Mixture C (Company 2 - Within Spec)	Mixture A (Company 1 - Within Spec - Manual Pour June)	Mixture D (Company 1 - Out of Spec - Manual Pour)	Mixture E (Company 2 - Out of Spec - Manual Pour) (4 x 4 x 2 ft)
Tracer gas	173,347	122,632	-	-	-	-
Strain Gauges	95,394	167,061	1,431,397	204,621	43,210	511,293
Thermocouple	164,032	180,982	1,528,938	-	-	-
Control sample	185,162	119,664	1,785,879	-	-	-
Average	**154,484**	**147,585**	**1,582,071**	**204,621**	**43,210**	**511,293**

Table 4.5 Young's modulus calculated from the source of UCS specimen (psi) for 14 days Testing.

4ft*4ft*4ft	Average Young's Modulus 14 & 18 days (psi)					
SEAL SAMPLE	Mixture A (Company 1 - Within Spec)	Mixture B (Company 1 - Out of Spec)	Mixture C (Company 2 - Within Spec)	Mixture A (Company 1 - Within Spec - Manual Pour June)	Mixture D (Company 1 - Out of Spec - Manual Pour)	Mixture E (Company 2 - Out of Spec - Manual Pour) (4 x 4 x 2 ft)
Tracer gas	233,368	237,063	1,977,113	-	-	-
Strain Gauges	140,055	196,385	1,443,801	463,407	428,109	526,400
Thermocouple	226,109	192,597	-	-	-	-
Control sample	233,781	239,229	1,593,870	-	-	-
Average	**208,328**	**216,318**	**1,671,595**	**463,407**	**428,109**	**526,400**

Table 4.6 Young's modulus calculated from the source of UCS specimen (psi) for 28 days Testing.

4ft*4ft*4ft	Average Young's Modulus 28 days (psi)					
SEAL SAMPLE	**Mixture A (Company 1 - Within Spec)**	**Mixture B (Company 1 - Out of Spec)**	**Mixture C (Company 2 - Within Spec)**	**Mixture A (Company 1 - Within Spec - Manual Pour June)**	**Mixture D (Company 1 - Out of Spec - Manual Pour)**	**Mixture E (Company 2 - Out of Spec - Manual Pour) (4 x 4 x 2 ft)**
Tracer gas	149,045	226,591	1,905,382	-	-	-
Strain Gauges	220,784	279,941	-	308,736	374,152	1,336,702
Thermocouple	179,470	175,360	1,762,696	-	-	-
Control sample	223,653	266,766	-	-	-	-
Average	**193,238**	**237,165**	**1,834,039**	**308,736**	**374,152**	**1,336,702**

As illustrated in Figure 4.41, two cases were considered with respect to stress development: Curve A and Curve B. Curve A represents a situation where the tensile stress is higher than the tensile strength, so there is the likelihood of cracking in the material. On the other hand, if the situation is represented by curve B, the probability of cracking is lower.

The curves obtained during the project for the different mixtures are included in Figure 4.42 through Figure 4.46. Despite the fact that in some cases, the stress curve is above the strength curve, the results cannot be used to assess the likelihood of crack generation, given all the assumptions made for their development.

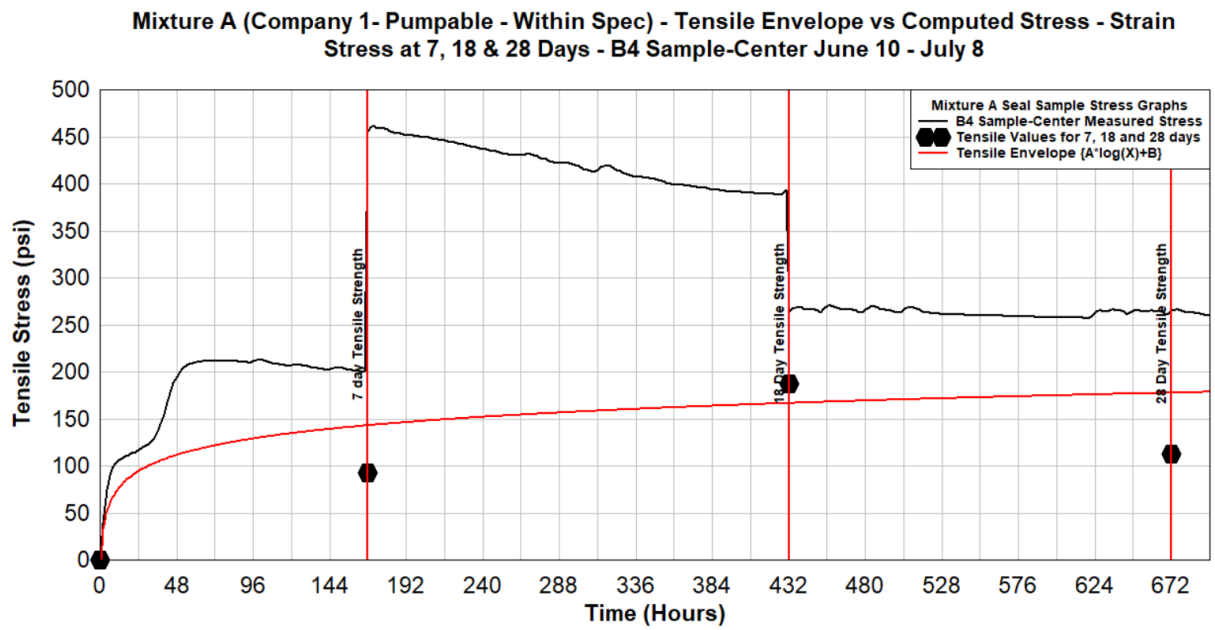

Figure 4.42 Mixture A – Tensile envelope versus computed stress-strain for sample center

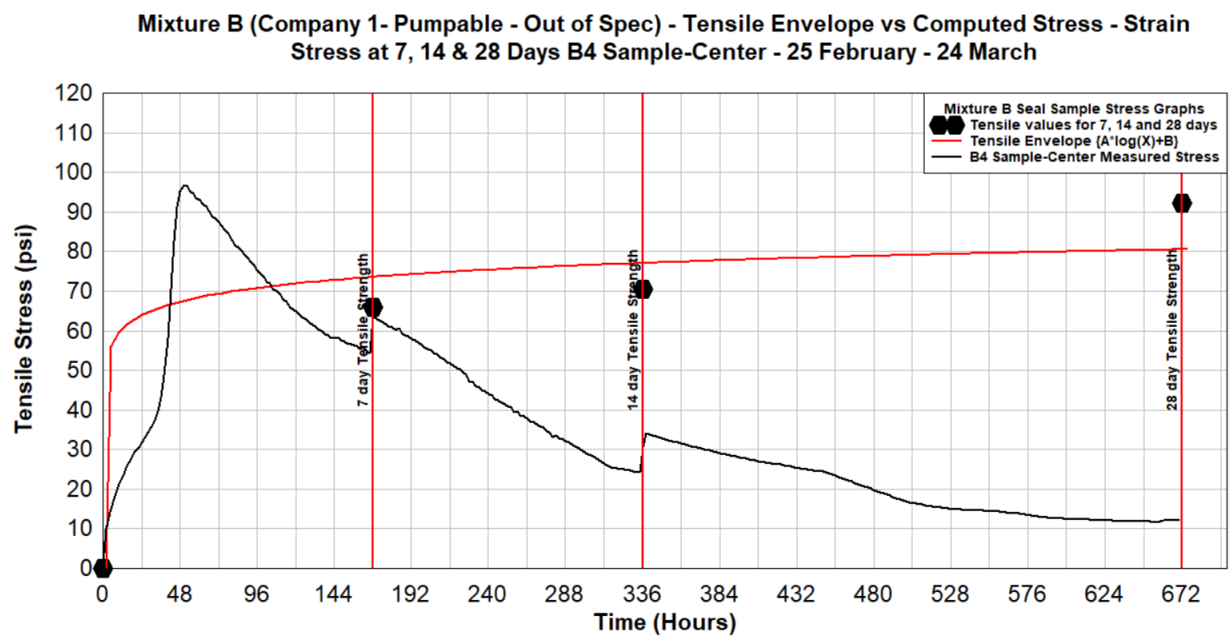

Figure 4.43 Mixture B – Tensile envelope versus computed stress-strain for sample center

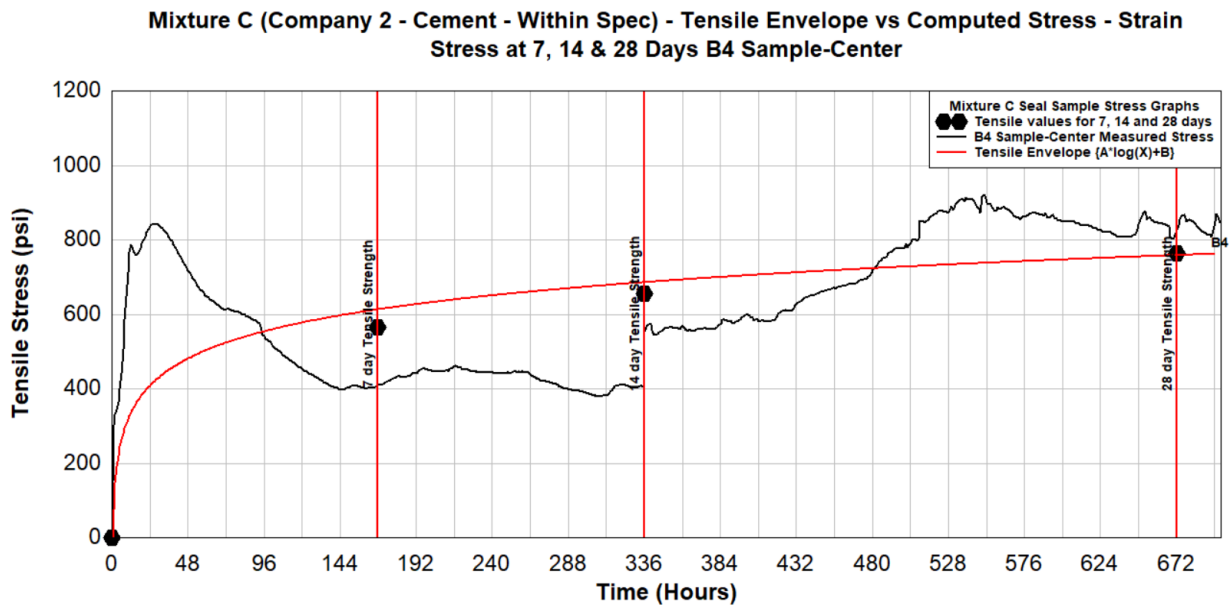

Figure 4.44 Mixture C – Tensile envelope versus computed stress-strain for sample center

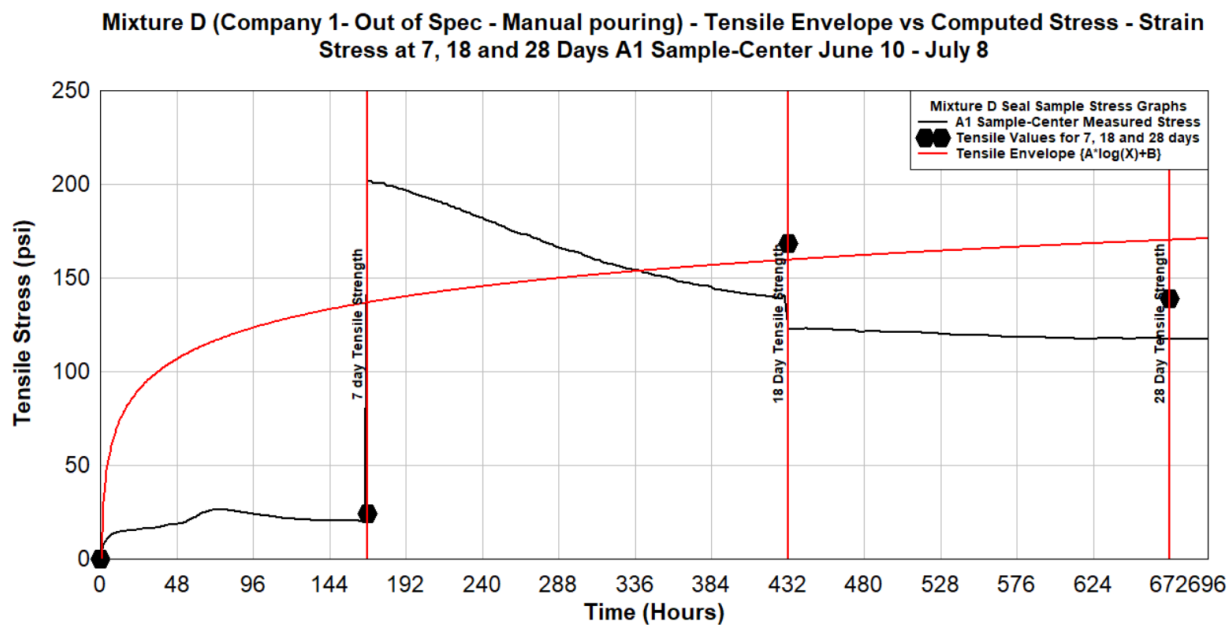

Figure 4.45 Mixture D – Tensile envelope versus computed stress-strain for sample center

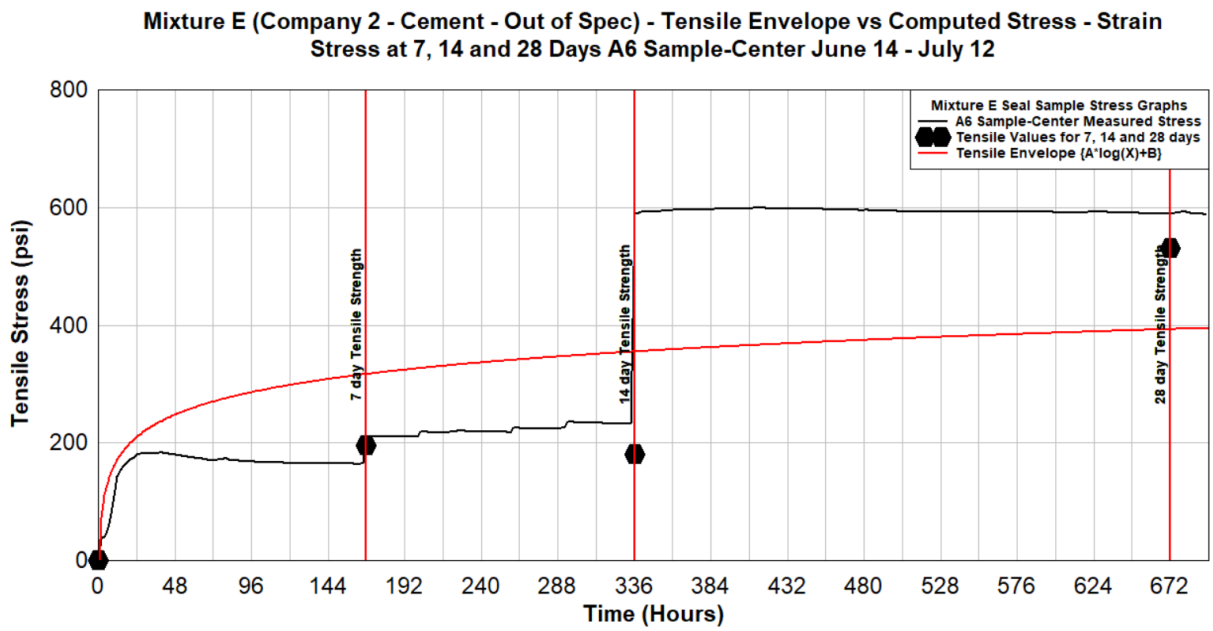

Figure 4.46 Mixture E – Tensile envelope versus computed stress-strain for sample center

The stress curves in Figures 4.42 to Figure 4.46, are not continuous (there are some "jumps") because of the changes in the value of the Young's modulus used to calculate the tensile stress. Additionally, and as indicated in the Figures and the assumptions, the data points at 7, 14, and 28 days are the 10% of the Uniaxial Compression Strength test value.

It can be concluded from this analysis that for all mixtures, that the early curing stages are when most susceptible to crack generations the materials are due to curing, matching the period when the strain, stress, and temperature changes occur dramatically. This is approximately on the first 144 hours after pouring the mixtures.

4.3 Analysis of Acoustic Emission information

The acoustic emission (AE) technique has been recognized as a promising non-destructive method for structural health monitoring [15]. This approach is mainly based on measuring the activity rate and the acoustic emission features, which are sensitive to the severity of certain damage mechanisms. When using the AE technique, one of the tasks is to associate each AE signal with a specific damage mechanism. In this report, a quantitative methodology was developed to detect and classify the crack signals, among all the collected signals that can be associated with cracks, during the curing process of the samples. This classification is required given that the AE emission signals can be generated by other mechanisms, different than cracking, such as impacts, and in general, any rubbing action on the structure under monitoring. As an example, it should be mentioned that the AE data collected included a signal that was attributed to the operation of the mine ventilation fan. That information was identified and removed from the possible signals related to cracking.

Equipment and Software

The instrumentation of the AE system used in this study includes two (2) low-frequency sensors, Figure 4.47(a), and two (2) very-low-frequency AE sensors, Figure 4.47(b), a computer-based data acquisition device and a preamplifier linking the AE sensor and the data acquisition device, Figure 4.47(c). The AE system used in this study was procured from the Mistras Group Inc. The system was purchased using a different funding source for use in this project. Some of the characteristics of the sensors used to collect data are included in Table 4.7.

Table 4.7 Sensor characteristics used for this project.

Channel	Sensor model	Sensor type	Frequency
CH1	PK3I	Low frequency	30 kHz
CH2	PK3I	Low frequency	30 kHz
CH3	R.45	Very low frequency	4.5 kHz
CH4	R.45	Very low frequency	4.5 kHz

a) Sensor PK3I b) Sensor R.45 c) Micro-SHM node

Figure 4.47 AE system used in this project

AE Signal Features

The AE signal may be generated through a number of different activities within the structure. As a result, there is a high probability of falsely attributing a signal to crack generation. The presence and magnitude of the damage are assessed by different signal parameters. The parameters generally used to characterize the AE signal are included in Figure 4.48.

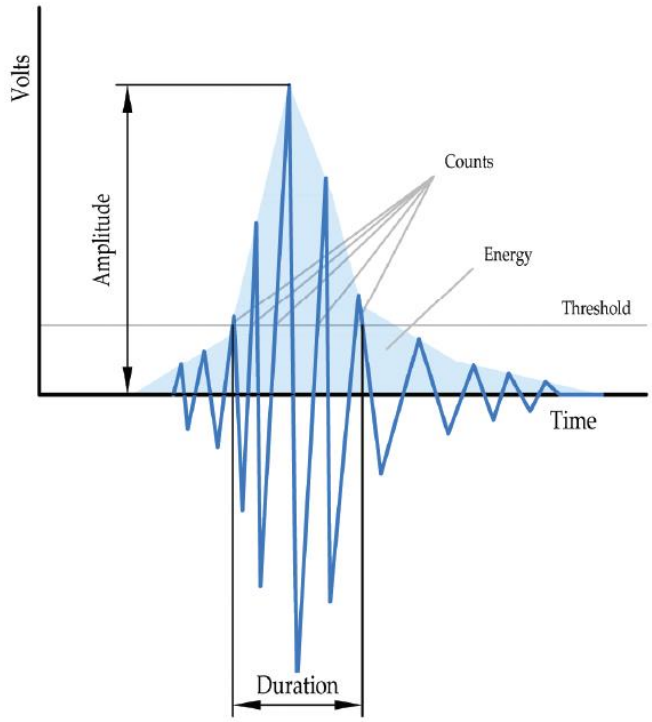

Figure 4.48 AE Hit feature extraction drawing (Source: Adapted from reference [15])

The most important terminology used in the analysis of AE information, and included in Figure 4.48, is described below:

- **Threshold**: Signal recording is triggered when the threshold value is reached. This value should be carefully set to remove the maximum possible noise as well as eliminate the weaker signals.
- **Hit**: AE signal data are recorded by a system channel when they meet the threshold value.
- **Amplitude**: The largest voltage peak in the AE signal waveform; customarily expressed in decibels.
- **Rise time**: The time duration between the signal triggering time and the moment when the signal reaches its peak amplitude is termed rise time.
- **Duration**: This is the time duration between the signal triggering time and the moment when the signal falls below the threshold value.
- **Energy**: The energy content of the signal can be correlated to the AE source strength.
- **Event**: The set of numbers used to describe an event pursuant to data processing that recognizes that a single event can produce more than one hit.
- **Counts**: It is the total number of times when the signal exceeds and crosses the threshold value in a determined duration.
- **Time of arrival**: The time when the first threshold is crossed.
- **Peak time**: The time when the maximum signal voltage is reached.
- **Frequency centroid**: Also known as the first moment of inertia, is a 2-byte value reported in kHz. It is a real-time frequency-derived feature.
- **Peak frequency**: It is the frequency of maximum signal contribution. A 2-byte value, reported in kHz, is defined as the point in the Power Spectrum at which the peak magnitude occurs.
- **Average frequency**: It is determined by the ratio of counts to duration and the reverberation frequency which is the "fade away" frequency of the wave after stopping of the source sound.
- **Counts to peak**: The number of threshold crossings between the time of arrival and peak time.

The AE system was installed to collect information from mixtures C and D. All the procedures and analysis are included in detail in this report for mixture D, and the results are presented for both mixtures.

Detailed analysis of AE system installed in the sample from Mixture D (Company 1 – Out of Spec).

4.3.1.1 *Mixture D Sensor Installation Setup*

The installation of the four sensors in the sample from Mixture D is shown in Figure 4.49.

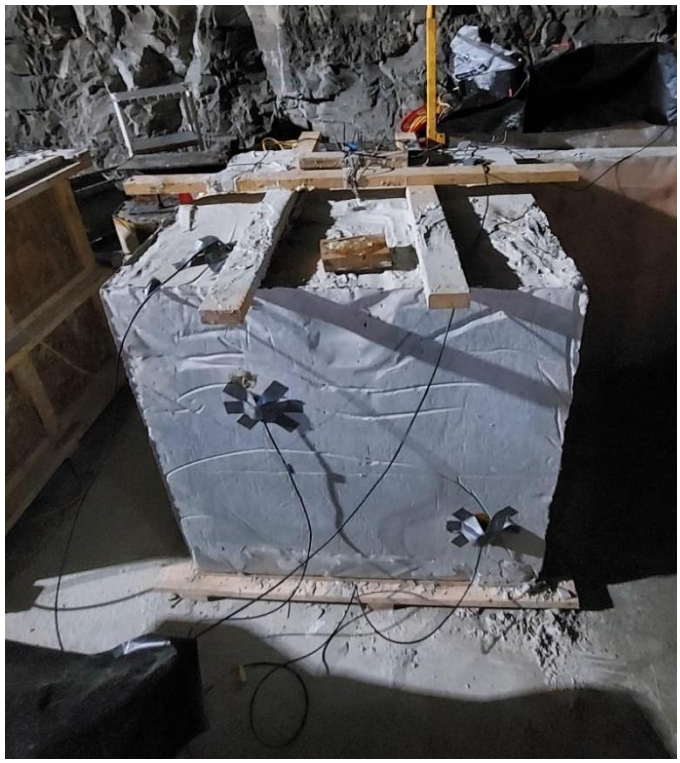

Figure 4.49 Sensors installed on the sample of Mixture D (Company 1 – Out of Spec)

4.3.1.2 *Analysis and filtering of data collected in the sample from Mixture D*

The system was installed for 16 days (from 11 June to 27 June). In this period, a total of 2,238,423 hits (waveforms) were recorded. Figure 4.50 shows all the hits in space-time in seconds versus peak frequency in kHz.

Figure 4.50 Peak frequency (kHz) vs time (sec)

Figure 4.50 shows a range of frequencies from almost zero to 400 kHz. The configuration of the data acquisition system allows the distinction of the data every 24 hours. In the figure, there are 15 columns of data matching the number of days the system was collecting information. The presence of very low and very high frequencies in the data was studied and was the base for the classification of useful information relating to the possible crack generation mechanism and the AE recordings.

A detailed examination of the waveforms for frequencies at 0, 301, and 396 kHz is included in Figure 4.51. The waveforms at these frequencies are more like white-noise signals, and they were removed from the database. In total, such types of waveforms account for almost 1.5 million records. Unfortunately, after analyzing this information, it was concluded that most of the records from frequencies at 301 kHz correspond with records from channel 4. An examination of the database showed that the setup of the equipment for channel 4 was not done correctly, and basically all the information from channel 4 was not useful for the analysis of potential cracks for Mixture D. This situation is discussed later as well as the implications of this on the location of the cracks inside the sample.

Figure 4.52 shows the database once the frequencies of 0, 301 and 396 kHz have been removed. In this graph, it is observed that the maximum frequency after filtering is around 140 kHz.

Peak Freq (khz)	# Hits	Typical waveform		
0	11,014	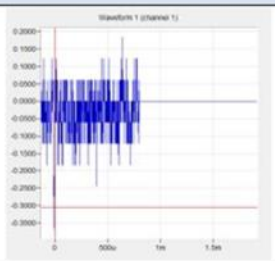	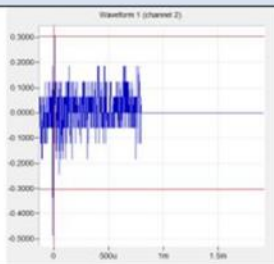	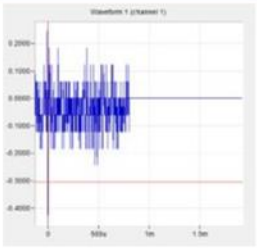
301	1,444,740	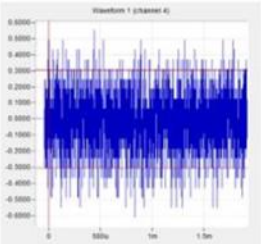	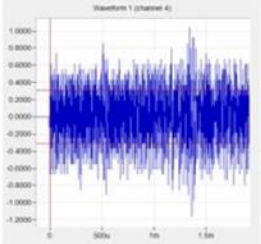	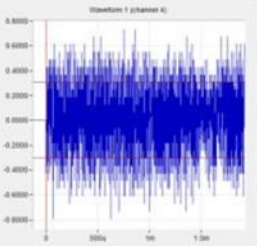
396	244	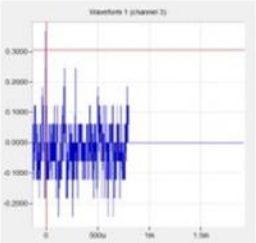	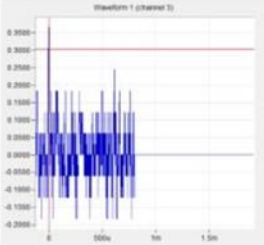	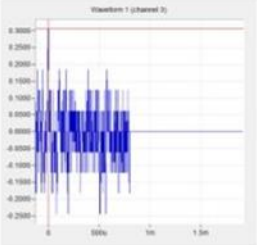

Figure 4.51 Detailed analysis for frequencies at 0, 301 and 396 kHz.

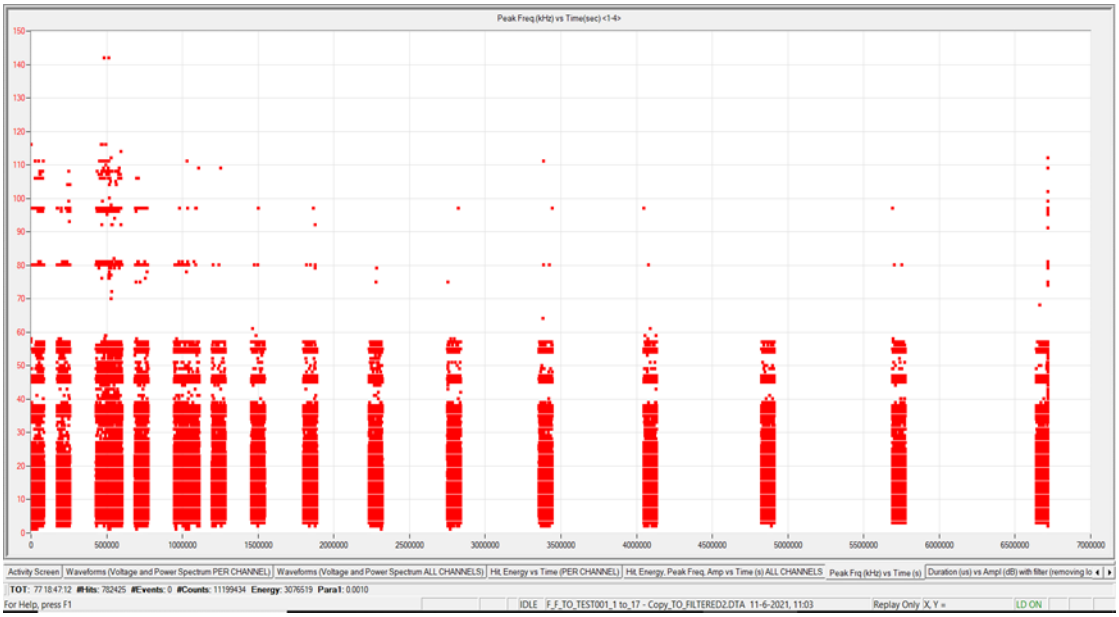

Figure 4.52 Peak frequency (kHz) vs time (sec) graph with the hits after the first filter

To focus more on the analysis while considering that thermal stresses, as discussed in previous sections, are more likely to generate cracking due to internal restraints, the AE database was filtered again, accounting for the AE data that match the period when the sample starts to cool down. Figure 4.53 shows this behavior for Mixture D. As seen in this figure, the mixture reached its highest temperature, around 86 hours after pouring, and then cooled down. The interval of data used in the AE system matches the vertical lines in Figure 4.53.

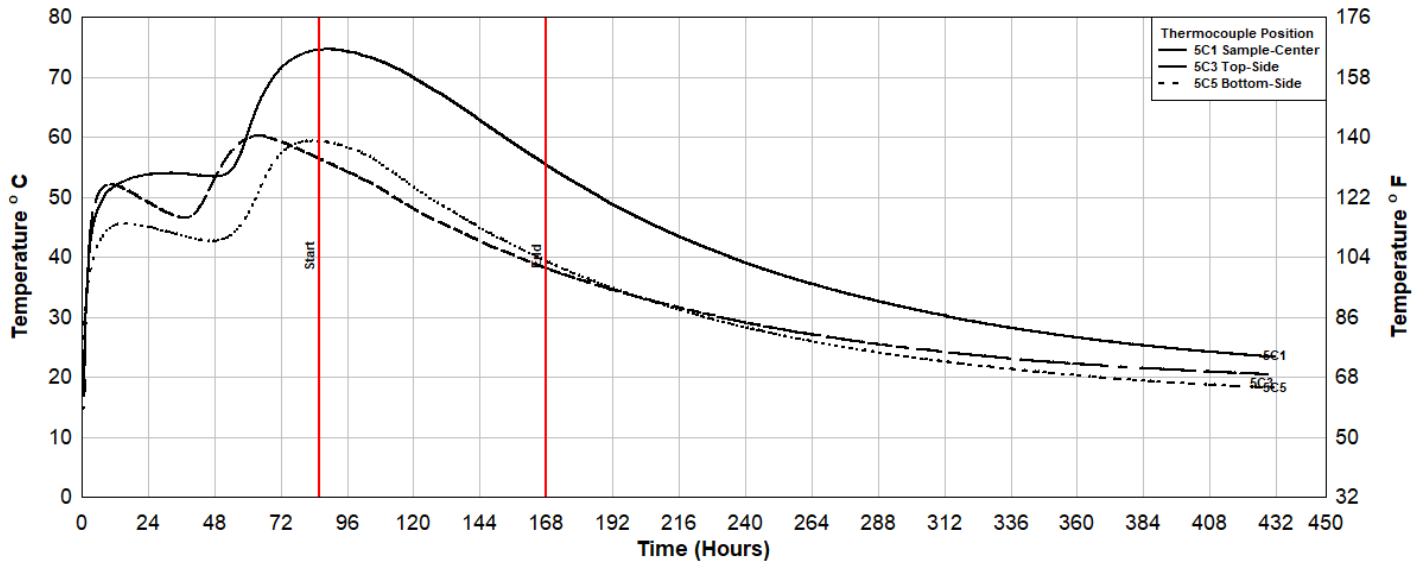

Figure 4.53 Temperature vs time for mixture D

In order to use the interval of AE selected in Figure 4.53, it was required to account for the different installation timeline of the AE in the sample. The timeline of the pouring of the sample and the installation of the AE system is included in Figure 4.54.

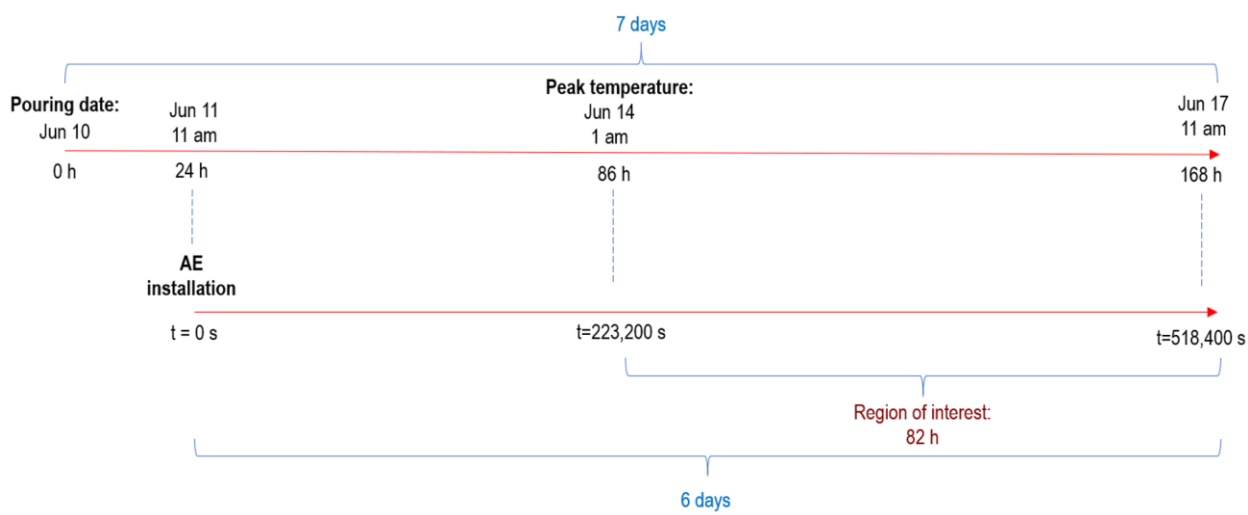

Figure 4.54 Timeline of the pouring of Mixture D and Acoustic Emission installation

Figure 4.55 includes the database after applying the restrictions explained before. In this way, the resulting number of hits was 146,827 as shown in Figure 4.55.

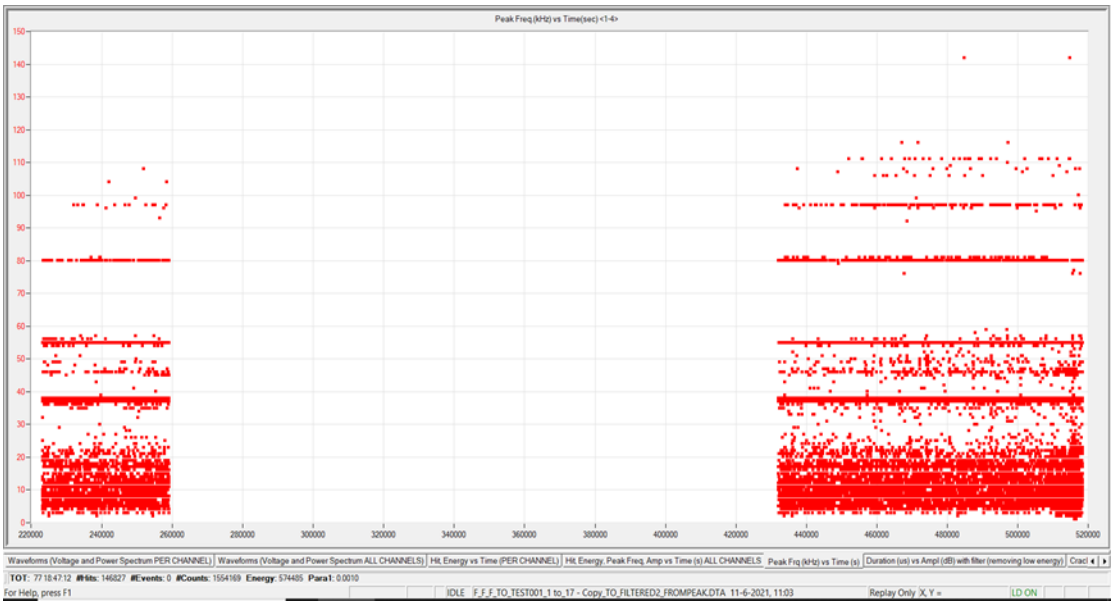

Figure 4.55 Peak frequency (kHz) vs time (sec) graph with the hits after the time filter

This information was again reviewed and some frequencies such as the frequencies of 37, 38 and 55 kHz were identified as frequencies with a waveform similar to that of white-noise. Figure 4.56 shows the typical waveform for the mentioned frequencies.

Peak Freq (khz)	# Hits	Typical waveform		
37	4949	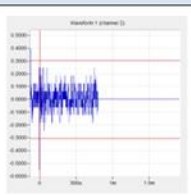	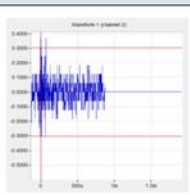	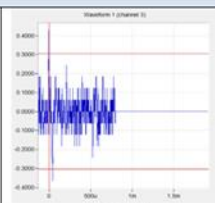
38	2639	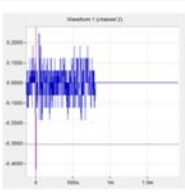	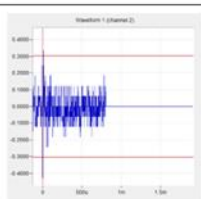	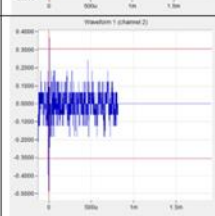
55	1613	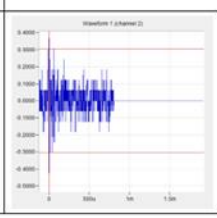	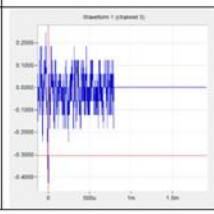	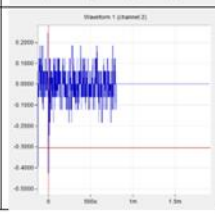

Figure 4.56 Peak frequency characterization based on waveform geometry, mixture D

Figure 4.57 shows the information that was developed after removing all white noise and filtering for the proper time interval. This information is used to identify the most likely signals related to cracking in mixture D. There are in total 137,626 waveforms in Figure 4.57.

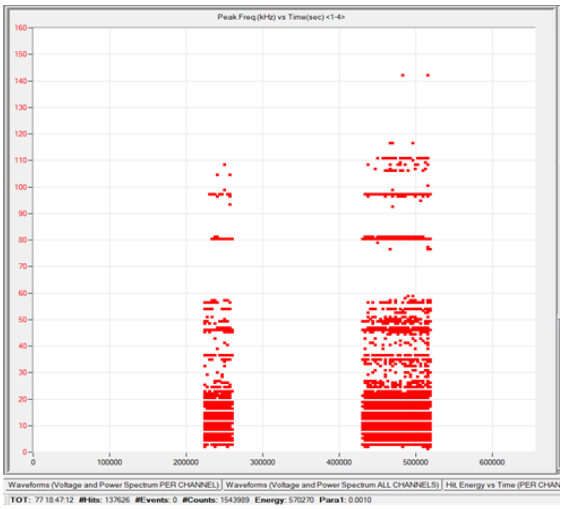

Figure 4.57 Peak frequency (kHz) vs time (sec) graph with the hits after the peak frequency filter

4.3.1.3 *Analysis of signals most likely related to cracking in Mixture D.*

Before determining from the database shown in Figure 4.57 what signals are more likely events related to cracking in the sample, it is necessary to discuss some concepts used in the AE analysis. It is accepted that the AE burst signals are asymmetric and are characterized by their Amplitude (dB), Duration (μs) and Rise Time [16]. The determination of high probability zones where hits are related to crack events can be seen in logarithmic plots of duration (μs) vs Amplitude (dB). As an example, from the paper of the reference [17], Figure 4.58 shows a plot where different mechanical processes (classes) are identified as occurring during crack generation

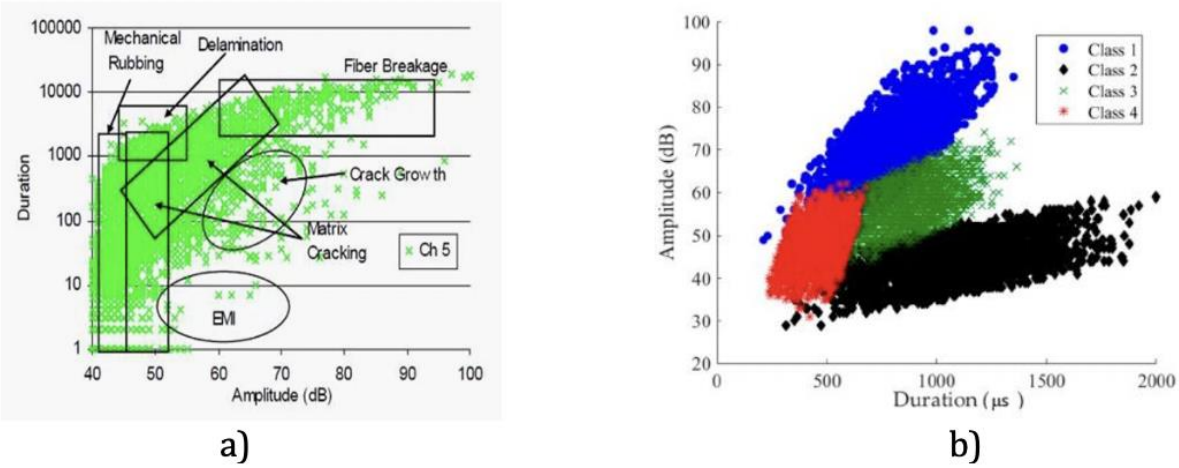

Figure 4.58 Identification of zones using AE data related to different mechanism of cracking (Source: a) Mistras: Training material, b) Adapted from Reference [17])

Figure 4.59 was created, following a similar procedure with the data from Mixture D (Company 1 – Out of Spec – Manual June Pour).

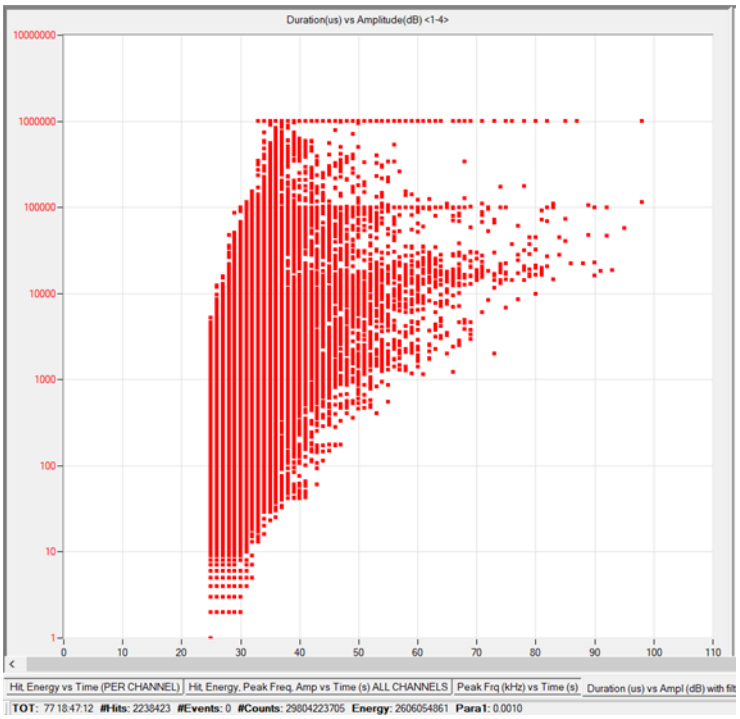

Figure 4.59 All the hits displayed in a Duration (µs) vs Amplitude (dB)

The analysis of the waveforms for five (5) different areas in Figure 4.59 shows that the waveforms can be grouped according to the limits provided in Table 4.8.

Table 4.8 Peak frequency characterization based on waveform geometry

Order of Filtering	Variable	Values
1	Peak Frequency (kHz)	Reject =0
2	Peak Frequency (kHz)	Reject >=150 and <=400
3	Time Frame (s)	Accept >=223 200 and <=518 400
4	Peak Frequency (kHz)	Reject >=37 and <=38
5	Peak Frequency (kHz)	Reject =55

Figure 4.60 shows the areas that can be defined when the limits in Table 4.8 are applied to the data of Mixture D (Company 1 – Out of Spec).

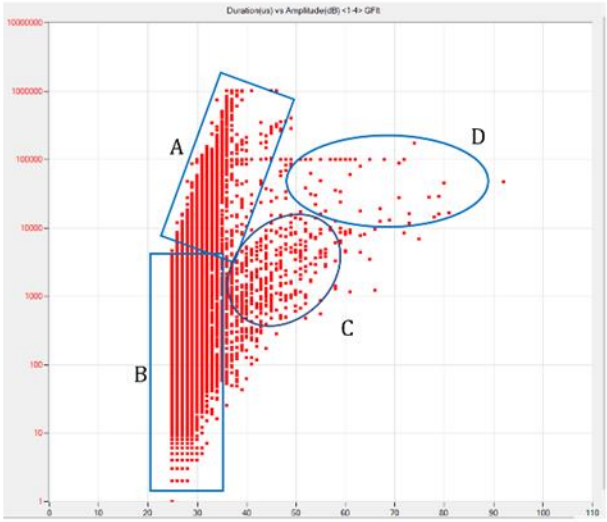

Figure 4.60 Cloud point grouped by amplitude (dB) and duration (µs)

The analysis of the shape of the waveforms in the areas of Figure 4.60 is included in Figure 4.61.

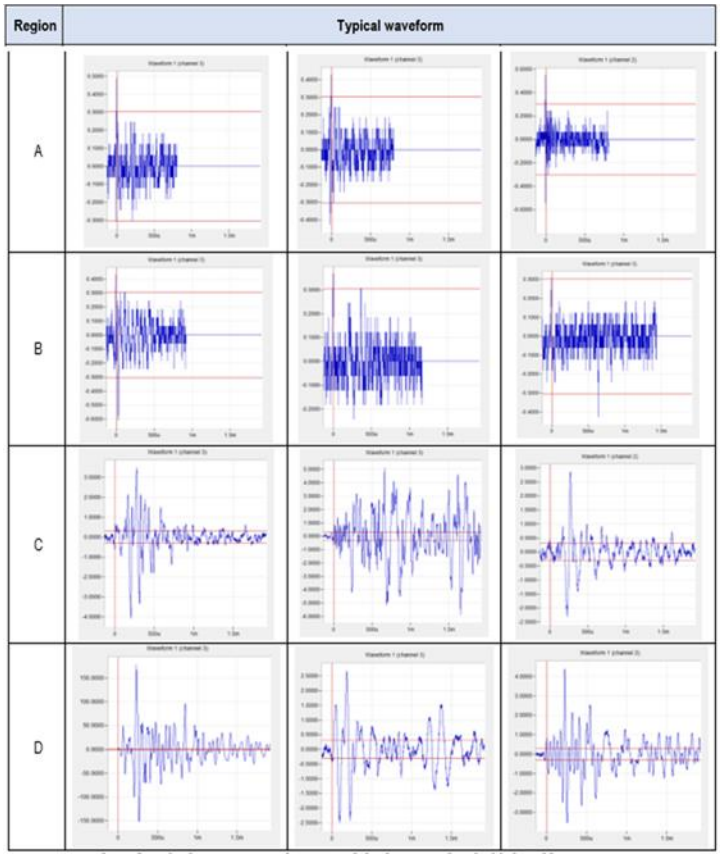

Figure 4.61 Typical waveforms for areas of interest in Figure 4.60

The hits in area D were selected to do an analysis for the locations of such events in the sample. Figure 4.62 shows the selected hits in area D.

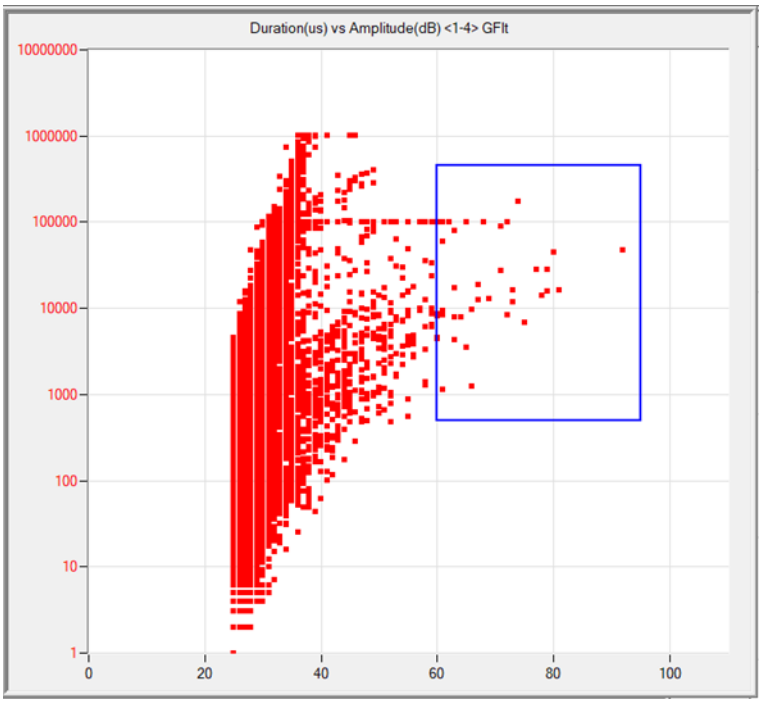

Figure 4.62 Selected hits with high amplitude and long duration in the duration (μs) vs Amplitude (dB) plot

Figure 4.63 shows those hits (acoustic signals) in a Peak Frequency vs. Time graph

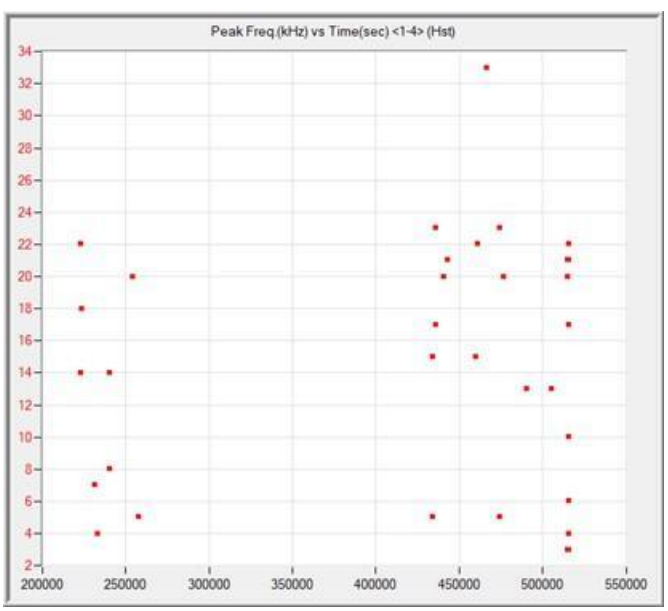

Figure 4.63 Selected hits with high amplitude and long duration in the Peak Frequency (kHz) vs Time (s) plot

As mentioned before, an Event occurs when a series of hits are linked in each period of time. Table 4.9 shows hits of Figure 4.63 grouped into 10 possible events based on very similar starting arrival times. All these hits correspond to the region with high amplitude and long duration.

Table 4.9 Hits grouped into high-probability events based on arrival time to the sensors

Hit Id	Possible Event	Time of arrival (s)	Channel	Energy	Duration (µs)	Amplitude (dB)	Peak Frequency (kHz)	Δ time (s)
1	I	223,291.1140600	3	588	15668	79	14	
2		223,291.1153753	2	79	9237	61	22	0.0013153
7	II	240,662.3504810	3	453	14158	78	14	
8		240,662.3507852	2	86	8646	60	8	0.0003042
13	III	434,289.9380950	3	309	12812	69	5	
14		434,289.9381953	2	197	11660	73	15	0.0001003
15	IV	436,132.5893400	3	6269	46802	92	17	
16		436,132.5904457	1	1234	28261	79	23	0.0011057
17		436,132.5922213	2	1343	27894	77	17	0.0028813
23	V	474,160.9370160	3	1713	44683	80	5	
24		474,160.9421607	1	382	18806	67	23	0.0051447
30	VI	515,215.8447957	1	316	33660	59	22	
31		515,215.8960792	2	46	4542	60	20	0.0512835
32		515,215.9761838	1	143	9889	59	22	0.1313881
36	VII	515,522.7464640	3	1819	172136	74	4	
37		515,522.7470823	2	458	100001	62	10	0.0006183
43	VIII	515,781.2553590	2	2955	99999	59	21	
44		515,781.3568468	2	3694	100001	61	6	0.1014878
45		515,781.4582483	2	2404	100001	60	21	0.2028893
46	IX	515,782.8625232	2	7715	100001	72	17	
47		515,782.9636278	2	4255	88063	71	22	0.1011046
48	X	515,783.6456395	2	1761	100001	59	5	
49		515,783.7476078	2	1531	100001	59	21	0.1019683
50		515,783.8488033	2	2146	100001	62	21	0.2031638

The main purpose of grouping the hits into events, as shown in Table 4.9 is to be able to estimate potential cracks in the sample.

The following section provides a brief overview of the math behind location determination. The fundamental basis for the calculation of the location is the time-distance relationship implied by the velocity of the wave. The absolute arrival time, (t), of a hit in an event, can be combined with the velocity, (v), of the sound wave to yield the distance, (d), from the sensor to the source. This is shown in Equation 3:

$$d = v * t \qquad \text{Eq. 3}$$

To find the unknown coordinates of the source, Equation 4 is used:

$$t_i - t_1 = \frac{\sqrt{(x_i - x_s)^2 + (y_i - y_s)^2 + (z_i - z_s)^2} - \sqrt{(x_1 - x_s)^2 + (y_1 - y_s)^2 + (z_1 - z_s)^2}}{v} \qquad \text{Eq. 4}$$

Where:

t_i=	time of arrival of the hit to the ith sensor
t_1=	time of arrival of the hit to the 1st sensor
(x_i, y_i, z_i) =	coordinates of ith sensor
(x_1, y_1, z_1) =	coordinates of 1st sensor (used as reference point)
(x_s, y_s, z_s) =	coordinates of the <u>source</u>
v =	velocity of the acoustic wave

Based on Equation 3, the following system of three (3) unknown variables is set up in three (3) simultaneous equations. To solve this system, a minimum of four (4) hits are needed, i.e., the signal from four (4) sensors:

$$t_2 - t_1 = \frac{\sqrt{(x_2 - x_s)^2 + (y_2 - y_s)^2 + (z_2 - z_s)^2} - \sqrt{(x_1 - x_s)^2 + (y_1 - y_s)^2 + (z_1 - z_s)^2}}{v}$$

$$t_3 - t_1 = \frac{\sqrt{(x_3 - x_s)^2 + (y_3 - y_s)^2 + (z_3 - z_s)^2} - \sqrt{(x_1 - x_s)^2 + (y_1 - y_s)^2 + (z_1 - z_s)^2}}{v}$$

$$t_4 - t_1 = \frac{\sqrt{(x_4 - x_s)^2 + (y_4 - y_s)^2 + (z_4 - z_s)^2} - \sqrt{(x_1 - x_s)^2 + (y_1 - y_s)^2 + (z_1 - z_s)^2}}{v}$$

The velocity of signal waves in concrete ranges from 2500 to 3500 m/s [16], [18]. Sensor (channels) coordinates are shown in Table 4.10.

Table 4.10 Coordinates of the sensors on site (meters)

	x_i	y_i	z_i
Channel 1	0.30	0.00	0.90
Channel 2	0.90	0.90	1.20
Channel 3	0.30	0.30	1.20
Channel 4	0.90	0.00	0.30

As already mentioned, data from Channel 4 cannot be used due to a misconfiguration of that channel.

4.3.1.4 *Analysis of signals most likely related to cracking in Mixture C.*

The procedure to collect, classify and analyze the information for the Mixture C sample was the same as that of Mixture D. The following figures include the results of the analyses. Figure 4.64 shows the installation of the sensors on the sample for Mixture C.

Figure 4.64 On-site sensors setup for Mixture C

Some of the data collected are included in Figure 4.65.

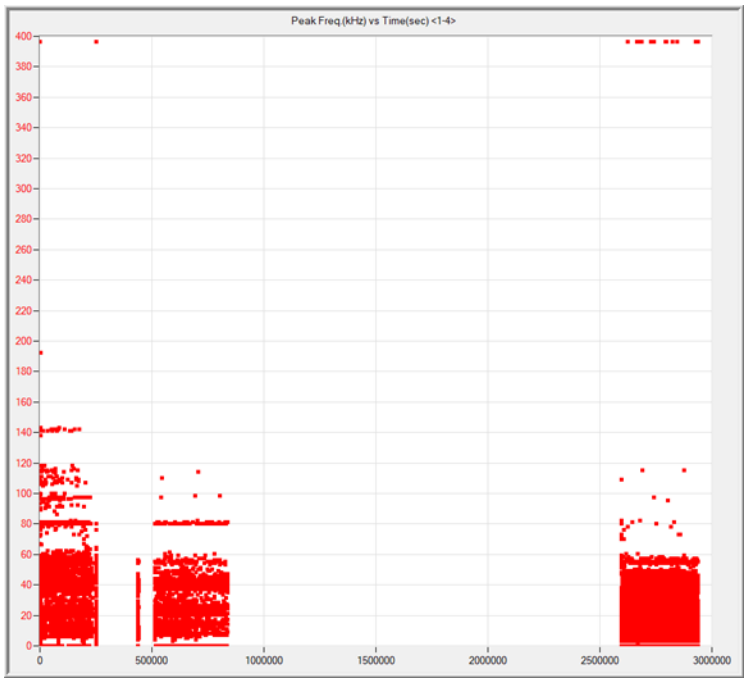

Figure 4.65 Peak frequency (kHz) vs time (sec) for data in Mixture C

Figure 4.66 includes the analysis of the waveforms filtered from the database.

Peak Freq (khz)	# Hits	Typical waveform		
0	2932	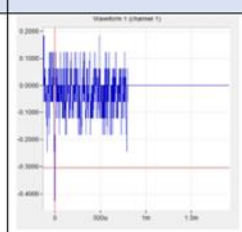	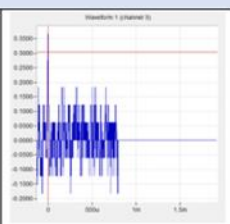	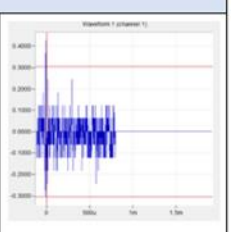
37-45	391,543	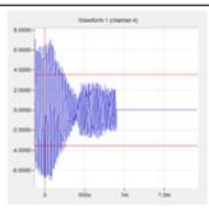	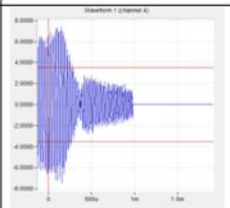	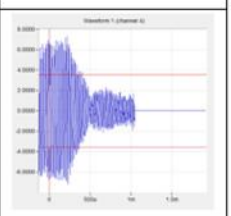
200-410	3396	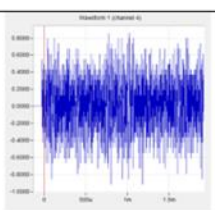	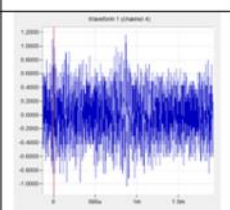	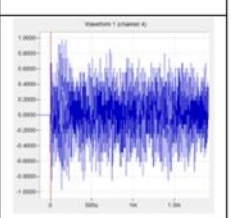

Figure 4.66 Peak frequency characterization based on waveform geometry, mixture C

Figure 4.67 includes the delimited zones where signals most likely may be related to cracking in the sample.

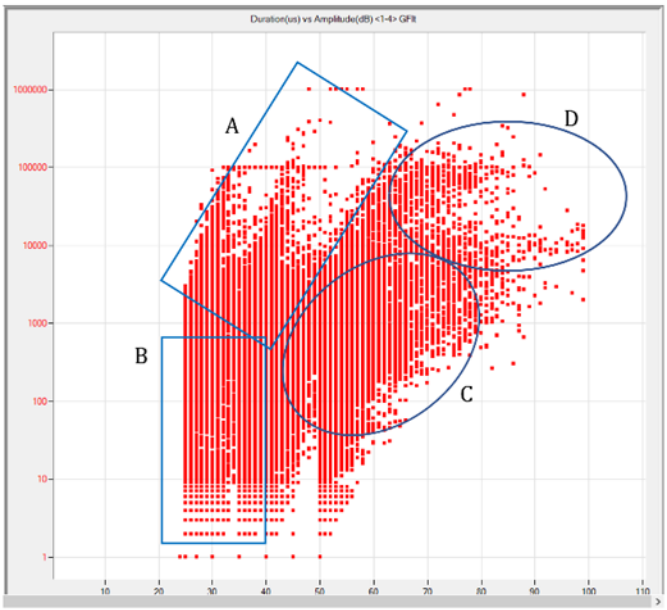

Figure 4.67 Cloud point grouped by amplitude (dB) and duration for Mixture C (Company 2 – Within Spec)

Some of the waveforms more likely related to cracking in the sample for Mixture C are included in Figure 4.68.

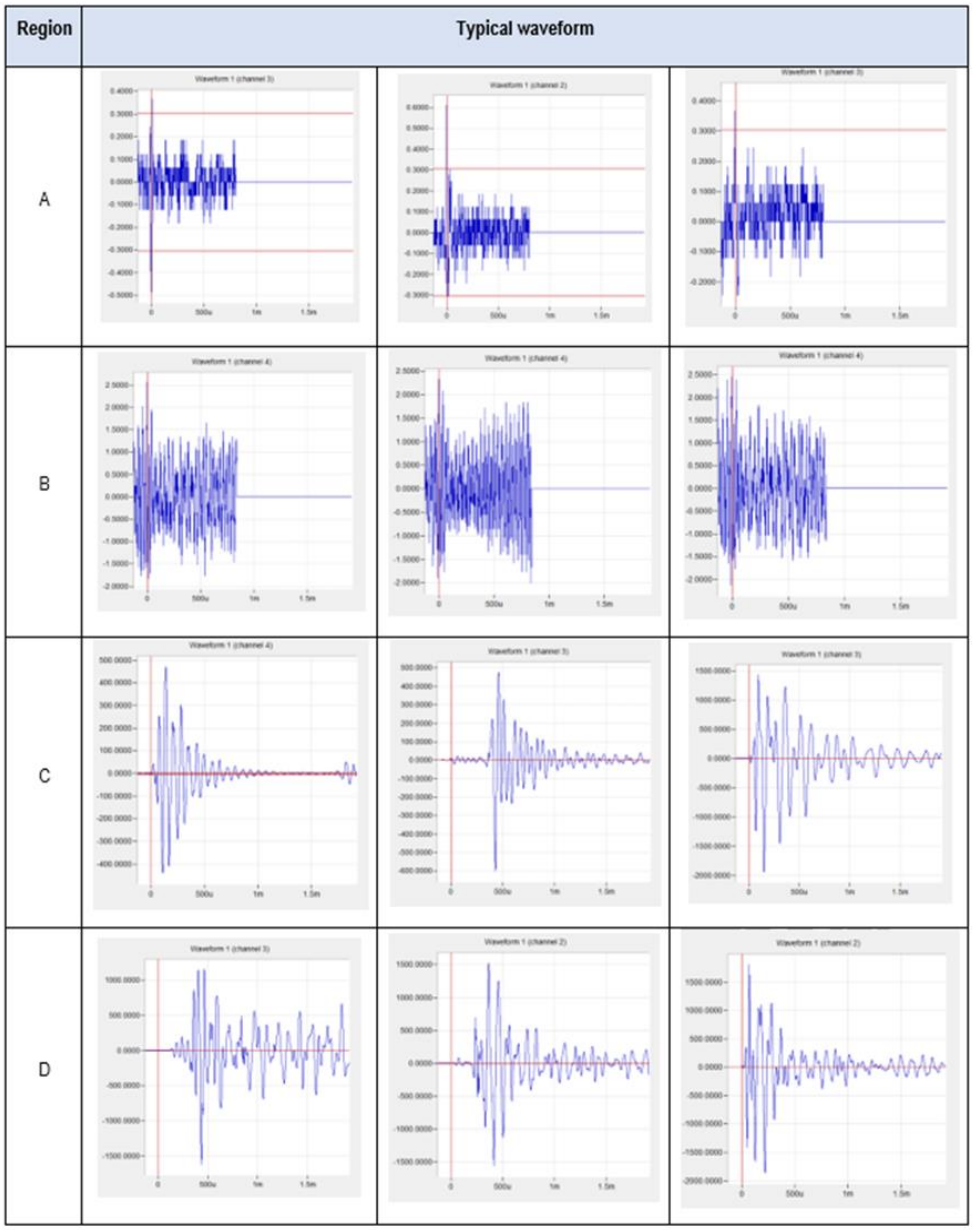

Figure 4.68 Typical waveforms for areas of interest in Figure 4.62.

The following are some of the conclusions after analyzing the collected AE information:

- Figures 4.61 and 4.68 show the typical waveforms recorded for mixtures from the two companies (Mixture D- Company 1 Out of Spec and Mixture C – Company 2-Cement). In both figures, the records with the waveforms in Region D are the most likely associated with cracks generation.
- Limitations in the equipment and procedural errors made the location of the source of the acoustic emissions difficult.
- The available information is not conclusive regarding the generation of macro-fractures in the mixtures tested in the project.

4.4 Analysis of the GPR information Research Goals

This section is a summary of a complete report of the GPR study that is included as an appendix to this report and is based on two site visits in May and June 2021 to acquire preliminary reconnaissance GPR data on the blocks. The goals of these 2-day and 1-day preliminary visits were a) to familiarize the GPR team with the imaging targets (blocks of concrete-like materials), b) to test and optimize GPR data acquisition for the targets, c) to determine whether GPR can detect fractures, and embedded objects within the blocks, and d) with this knowledge, plan future GPR studies for characterization of fractures within these materials.

The Ground-Penetrating Radar (GPR) study aimed to image and characterize macro-fractures within blocks constructed of mine ventilation seal materials. Characterization of the fractures was to support the goal of the larger project, which was to identify and investigate the effects of macro- fractures on the structural integrity of mine ventilation seals.

For this project, standard data processing was applied to produce GPR images for initial interpretation; this, however, does not include more detailed work to improve and quantify the images. Acquisition, processing, and initial results should be considered preliminary because both acquisition and processing can be improved to better quantify the imaging. However, such improvement will not be expected to change the conclusions of the findings using the GPR technique.

The only reason older blocks were used with already mechanical-induced cracks was to be able to calibrate the GPR system. The report differentiates between "older blocks" used and "new blocks" cast as part of this report and study. The older blocks used in the GPR study were built prior to 2020 as part of a previous research. These blocks have been cured and aged 1-4 years in the same underground mine environment. Most have been moved by forklift, which may have induced damage. Cognizance should be taken of references to "older blocks" and "new blocks" when interpreting the report.

Analysis for New Blocks

Mixture B (Company 1) Block: This block was built outside the approved standard for this material, using 1.25 times the standard powder to water ratio. Fractures were not visible on the exposed faces of the block. Quasi-linear horizontal alignments of air bubbles were visible on the sides of the block and are likely due to the pour method of the relatively viscous material. GPR data were acquired along the top and one side of a block of this mixture B that contained embedded strain gauges.

Mixture C (Company 2) Block: This block was built to standard for this material. Fractures are not visible on the exposed faces of this block. The material visually appears uniform, sometimes with one boundary between pours. GPR data were acquired along the top and one side of a block of this mixture that contains embedded strain gauges and along one side of a block that contains embedded thermocouple sensors.

GPR images acquired on the sides of these blocks show a hyperbolic diffraction from vertical strain gauge wires at <50 cm depth of penetration (Figure 4.69a and Figure 4.70a). Deeper wires were not observed in the radar images. The diffraction is stronger in Mixture C than in Mixture B, suggesting the media have different radar attenuation. The thinner thermocouple wires produce a weaker diffraction (Figure 4.70c) than the strain gauge wires. Although conducting metal is a strong scatterer/reflector, the thinness of the sensor wires weakens the diffraction. Wire diffraction amplitudes have not been quantified to calibrate attenuation and expected fracture amplitudes.

No fractures are observed in any of the GPR images of these blocks. This may be due to radar attenuation or weak reflection amplitudes from thin fractures. However, no fractures were observed on the exposed faces of the blocks, and it is likely that the blocks contain no macro fractures for the GPR to image. Deep, low-frequency, sloping layering in the images may be due to weak air-wave reflections from objects surrounding the mine-seal blocks.

GPR data acquired on the tops of the blocks (Figure 4.69(b) and Figure 4.70(b) have a different character than data acquired on the sides.

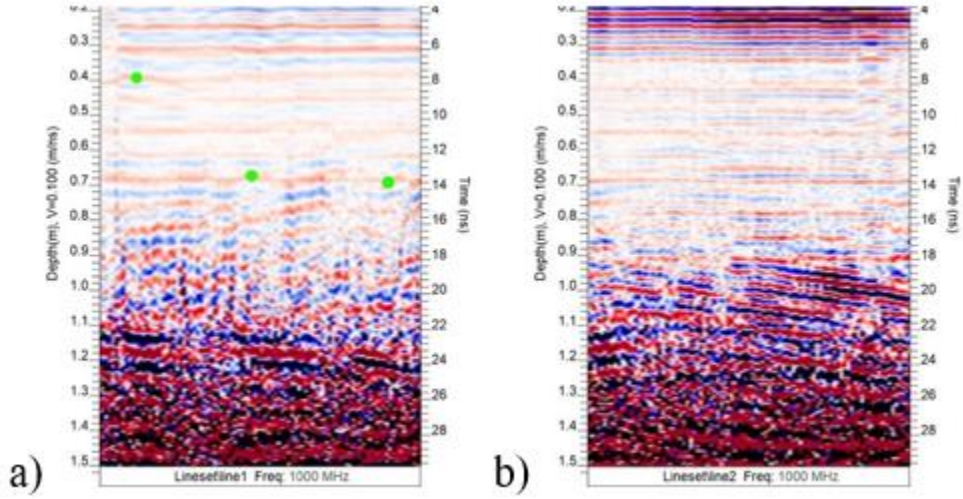

Figure 4.69 GPR sections in a block of Mixture B containing vertical wires and strain gauges. a) GPR section acquired along the front face of the block, 30 cm from the top. Green dots indicate interpreted or expected locations of wires. b) GPR section acquired along the front face of the block, 30 cm from the top. Green dots indicate interpreted or expected locations of wires. b) GPR section acquired along the top of the block, 20 cm from the back edge (source VT team)

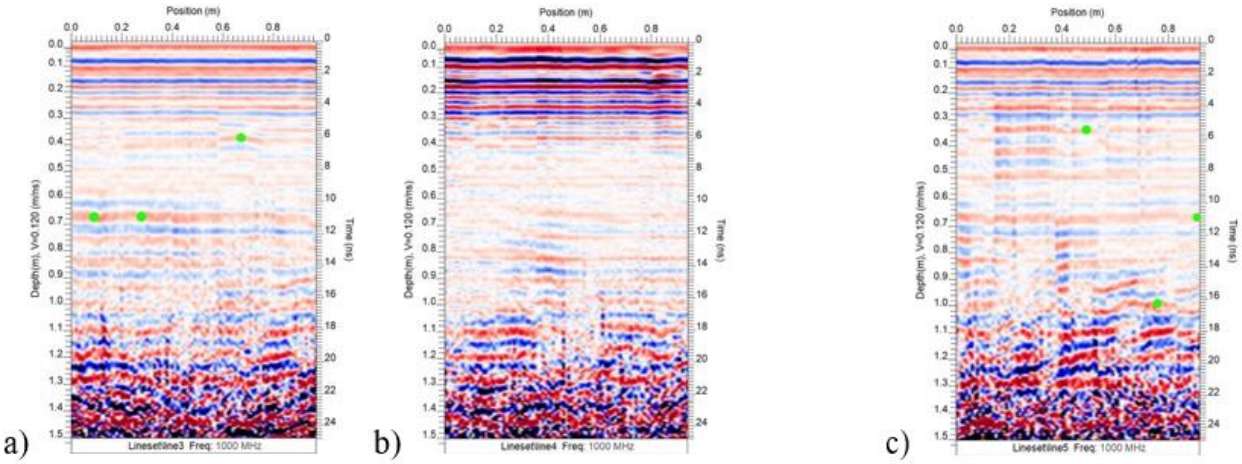

Figure 4.70 GPR sections in two blocks of Mixture C containing vertical wires. a) GPR section acquired along the left face of the block containing strain gauges, 30 cm from the top. Green dots indicate interpreted or expected locations of wires. b) GPR section acquired along the top of the block containing strain gauges, 20 cm from the right edge. c) GPR section acquired along the back face of the block containing thermocouples, 30 cm from the top (source VT team)

In summary, GPR data acquisition, processing, and initial results are preliminary. Both acquisition and processing can be improved to better quantify the imaging. However, such improvement will not be expected to change the conclusions regarding no macro fractures detected in the blocks.

Block G ("older block") is the only block imaged with GPR that has known fractures deep within the block. These fractures produce strong 1-GHz radar reflections. Fractures are imaged to more than half the 4-ft (1.22 m) thickness of the block. These fractures are open at the cm-scale; narrower fractures would have weaker amplitudes.

The hairline fractures in Blocks A and C were not imaged by the GPR. These data were acquired during the first visit that used poorer acquisition methods. The lack of imaged fractures may be due to radar attenuation, due to the fractures being too thin to image, or because the surface fractures do not extend deep into the block.

No fracture reflections were observed from within new blocks of Mixture B, nor C. Thin metal wires were observed within these blocks as point diffractions to >40 cm depth of penetration (corresponding with the instrumentation). The lack of radar reflections from fractures is likely due to a lack of fractures in these blocks.

As a conclusion for the GPR section, and in summary, the complete GPR report in the addendum, Appendix VI, needs to be read and interpreted in conjunction with this summary.

4.5 Tracer Gas Analysis

Two unique tracer gases in two passive sources were embedded in each of the three seal samples:

- perfluoromethylcyclohexane (PMCH) and
- perfluoromethylcyclopentane (PMCP).

One source was embedded at the centroid of the samples and the other centered at a depth of 12 inches from the top surface.

Tracer gas samples were collected from the three seal materials (Mixture A, Mixture B, and Mixture C) at the frequencies prescribed in Table 4.11. The samples were collected in the mine and stored in a climate-controlled environment until sampling was complete. The samples were then shipped in bulk for testing. A total of 39 tracer gas samples were collected from the three seal materials.

Table 4.11 Tracer Gas Sampling Schedule

Sample Schedule	Frequency
1	2 days from casting seal material sample
2	Daily samples from day 2 until day 12
3	Weekly samples from day 13 until day 28
4	Monthly samples after day 28

Once the samples were received, gas chromatography - mass spectrometry testing (GC/MS) was used to sense the presence or absence of the two tracer gases collected from the sampling apparatus. The GC/MS analysis focused on sensing the two different types of tracer gases embedded in the seal material and sudden spikes or upward trends of tracer gas content collected during sampling.

The 39 tracer gas samples in TEDLAR® bags were provided to the testing laboratory and used as received. Hexane organic solvent was obtained from Sigma-Aldrich (St. Louis, MO) and used as received. GC/MS qualitative analyses were performed using a 7890 GC equipped with a 5975 Mass Selective Detector (MSD) from Agilent (Wilmington, DE). Separations were obtained using an RT-PLOT Alumina Bond/KCl capillary column (30 m long x 250 µm I.D. with a film thickness of 4 µm) from Restek (Bellefonte, PA).

The following operating parameters were used for each GC/MS analysis:

Injection Port Temp.	200°C
Purge Valve	3 mL/min
Purge Time	1 min
Total Flow	19 mL/min
Constant Flow	1.5 mL/min
Injection Volume	100µL, split 1:10

Column Oven Initial Temp.	100°C
Column Oven Initial Time	1 min
Column Oven Ramp Rate	30°C/min to 195°C
Column Oven Final Temp.	195°C
Column Oven Final Time	8 min
MSD Transfer line Temp.:	200˚C
SIM Detection Ions:	131 and 181

Figure 4.71 shows MS spectra of PMCH in scan mode. As can be observed two ions of 131 and 181 were used for all detection and quantification.

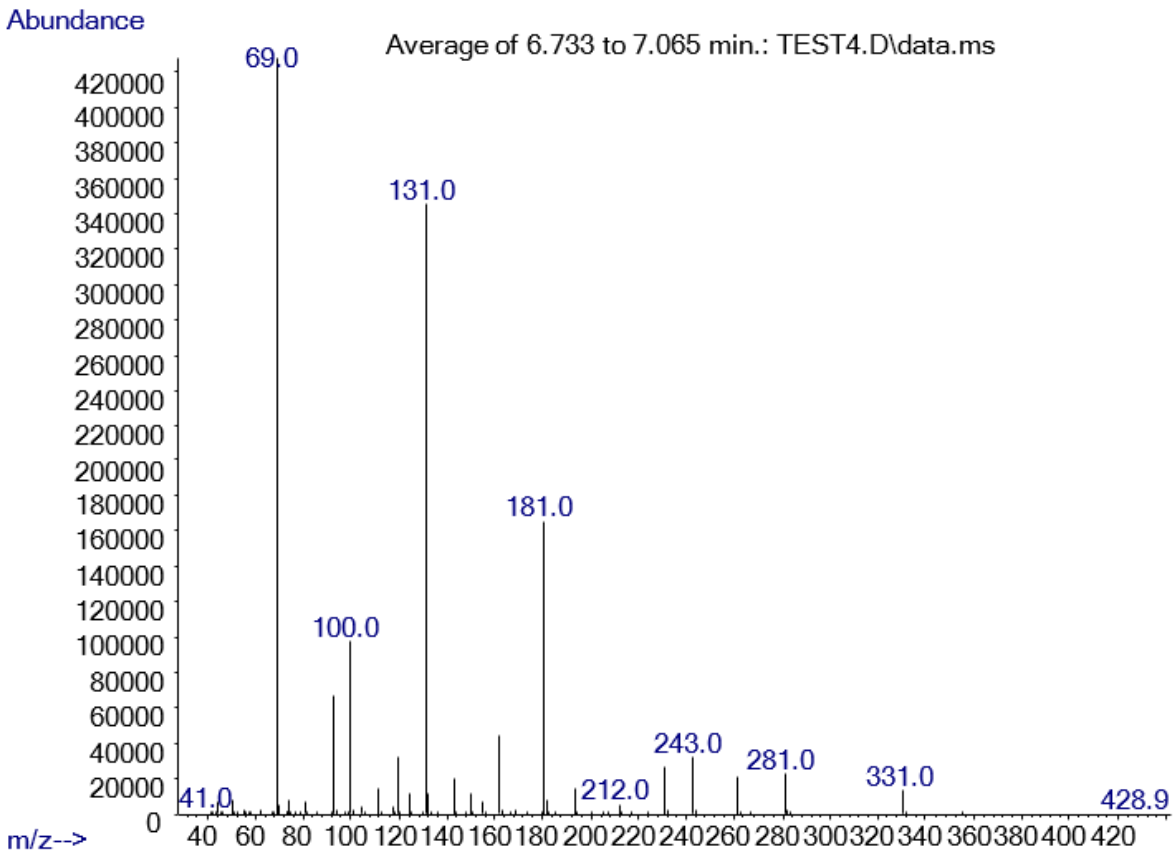

Figure 4.71 MS spectrum of PMCH

Quantitative analyses of PMCH of the thirty-nine samples were obtained using GC/MS in a single ion monitor (SIM) in positive mode using ions of 131 and 181 atomic mass units (amu). Detection of PMCP was obtained using the same ions with different retention time.

From a quantitative perspective, the amount of PMCH determined via an external calibration curve standard ranged in concentrations between ~1 and 1,116 pg/mL. The associated %RSD values of the quantitative experiments for samples above the limit of quantification were less than 5% indicating excellent analytical precision. The results from the GC/MS analyses are summarized in Table 4.12.

Table 4.12 Concentration of PMCH and PMCP using GC/MS

Sample ID	Run 1	Run 2	Run 3	Avg.	%RSD	PMCH Conc., pg/mL	PMCP
Sample 1	4	3	3	3.3	17.3	ND*	ND*
Sample 2	0	0	0	0.0		ND*	ND*
Sample 3	0	0	0	0.0		ND*	ND*
Sample 4	20	18	17	18.3	8.3	38.2	ND*
Sample 5	0	0	0	0.0		ND*	ND*
Sample 6	46	39	32	39.0	17.9	113.8	ND*
Sample 7	0	0	0	0.0		ND*	ND*
Sample 8	36	34	34	34.7	3.3	97.9	ND*
Sample 9	38	42	38	39.3	5.9	115.0	ND*
Sample 10	9	8	8	8.3	6.9	1.6	ND*
Sample 11	256	266	274	265.3	3.4	941.9	ND*
Sample 12	3	3	3	3.0	0.0	BDL***	D**
Sample 13	102	104	105	103.7	1.5	350.4	ND*
Sample 14	0	0	0	0.0		ND	D**
Sample 15	65	67	70	67.3	3.7	217.5	ND*
Sample 16	0	0	0	0.0		ND*	D**
Sample 17	237	244	257	246.0	4.1	871.2	D**
Sample 18	7	8	11	8.7	24.0	2.8	D**
Sample 19	260	257	260	259.0	0.7	918.8	D**
sample 20	5	1	2	2.7	78.1	BDL***	D**
Sample 21	351	358	352	353.7	1.1	1,265.2	D**
Sample 22	12	14	15	13.7	11.2	21.1	D**
Sample 23	190	199	190	193.0	2.7	677.3	D**
Sample 24	5	8	6	6.3	24.1	BDL***	D**
sample 25	585	583	590	586.0	0.6	2,115.3	D**
Sample 26	32	35	33	33.3	4.6	93.1	D**
Sample 27	437	436	458	443.7	2.8	1,594.5	D**

Sample 28	59	61	62	60.7	2.5	193.1	D**
sample 29	160	157	162	159.7	1.6	555.3	D**
Sample 30	4	4	5	4.3	13.3	BDL***	ND*
Sample 31	11	9	10	10.0	10.0	7.7	D**
Sample 32	45	47	46	46.0	2.2	139.4	D**
Sample 33	7	8	10	8.3	18.3	1.6	D**
Sample 34	6	5	5	5.3	10.8	BDL***	D**
Sample 35	20	21	22	21.0	4.8	47.9	D**
Sample 36	15	15	17	15.7	7.4	28.4	D**
sample 37	28	35	30	31.0	11.6	84.5	D**
Sample 38	12	10	11	11.0	9.1	11.3	D**
Sample 39	5	7	8	6.7	22.9	BDL***	D**

* ND - Not detected ** Detected *** Below Detection limit

All standards and samples were injected in triplicate analysis for statistical data analysis. Table 4.13 shows a list of calibration curve standards and their results. Figure 4.72 shows (TIC) overlaid of all standards ranging from 5.58-1116.88 pg/mL. Figure 4.73 shows a calibration curve that was used to calculate the concentration of PMCH in each sample. The R2 value for the calibration curve was greater than 0.998 indicating excellent linear correlations between MS area counts and analyte concentration. Also, low relative standard deviations for the injections displayed in Table 4.13 show that the methodology used to create the curve is robust. Standard 1 (1.40 pg/mL) was not detected due to the low concentration. Therefore, one can conclude that system Level of Detection (LOD) is in the range of 3-4 pg/mL.

Table 4.13 Calibration Curve Results for PMCH

Level	pg/mL	Area	%RSD
Std 1	1.40	ND*	
Std 2	5.58	6	9.52
Std 3	39.09	26	3.85
Std 4	83.77	31	5.04
Std 5	139.61	41	2.44
Std 6	279.22	86	4.65
Std 7	558.44	161	1.08
Std 8	1,116.88	310.7	3.44

* - Not Detected

Figure 4.72 shows the overlay TIC for all standards ranging from 5.58-1116.88 p/mL.

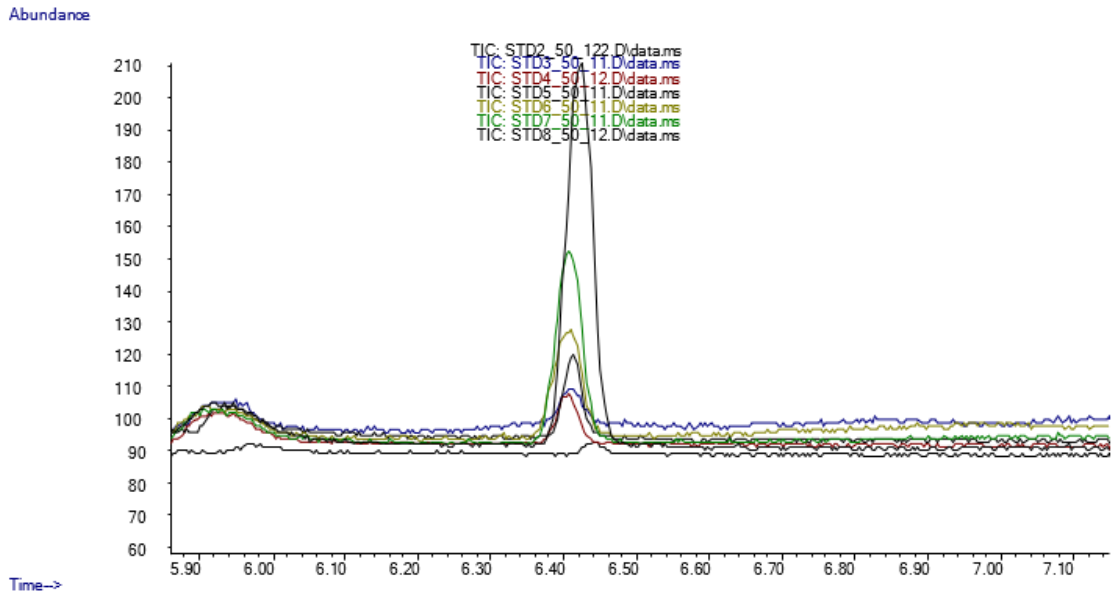

Figure 4.72 Overlay TIC for all standards

Each sample was injected in triplicates and the quantity of PMCH was obtained using the calibration curve in Figure 4.73. The calculated concentrations of PMCH in each sample with the %RSD are provided in Appendix IV. The GC/MS analysis data of each sample in triplicate is provided in Appendix V.

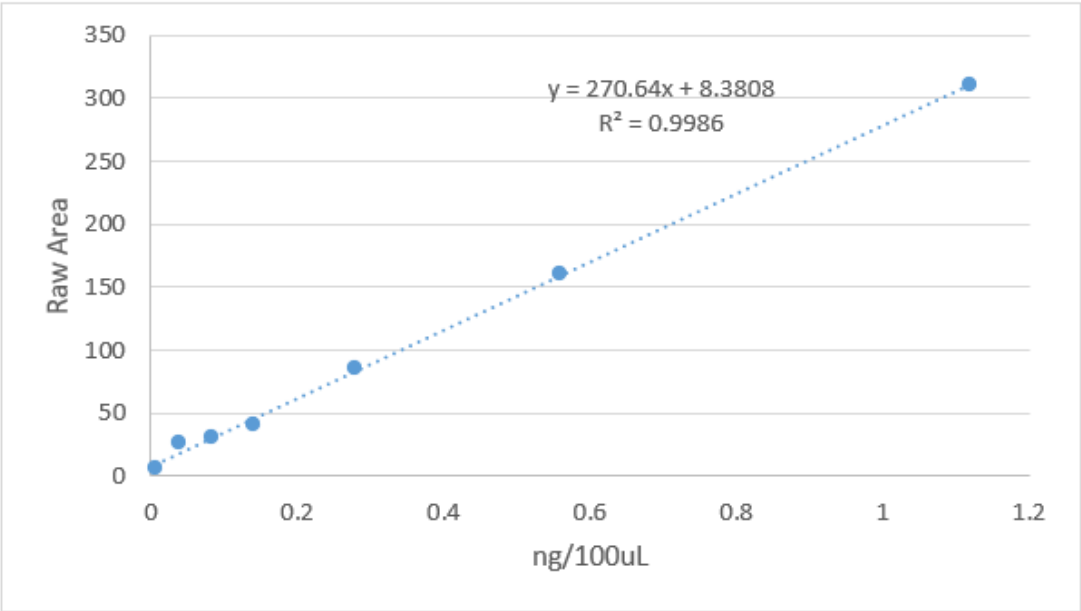

Figure 4.73 Calibration curve for determination of PMCH

Small-scale and large-scale laboratory testing indicates that the tracer gases can permeate the seal material matrix at variable rates, but this doesn't necessarily mean from macro fractures. Further testing of scaled sample transmission rates will need to be performed to determine if extended periods of sampling in the future will yield either increased or decreased concentrations of the gases. Further testing may also provide information regarding the movement of tracer gases through micro- and macro-fractures that develop while the seal material is curing and when the cured seal material is introduced to external loading.

5 Publication Record and Dissemination Efforts

This project has been presented in the following meetings:

34th Annual – Kentucky Professional Engineers in Mining Seminar P.E.M – August 27, 2021 – Presentation - Jaco van den Berg – Graduate Research Assistant – Department of Mining Engineering – University of Kentucky - *Analysis of Information Collected During the Curing Process of Materials Used for Underground Coal Mine Seals.*

SME Pittsburgh Section – Pittsburgh Coal Mining Institute of America (PCMIA) - Student Short Presentation Contest – September 10, 2021 - Participant – Jaco van den Berg – Graduate Research Assistant – Department of Mining Engineering – University of Kentucky – 3rd Place with publication of Abstract in SME's Mining Engineering Magazine - *Investigation into, and analysis of information collected during the curing process of materials used for underground coal mine seals in an attempt to identify possible micro and or macro cracks formation.*

Additionally, the collected information will be used for the master's thesis work of the student Jaco van den Berg. Once the student completes his work, the Alpha Foundation will be notified.

6 Conclusions and Impact Assessment

After the analysis of the collected data the following conclusions can be derived:

- No macro-fractures were detected using the two crack detection techniques selected for the project (GPR and Tracer Gases techniques).
- If the proportions, quality, and standard procedures developed by the two companies that provided materials for these mine seals are followed, there is currently no probability of macro-cracks forming or indications of any problems with the seals during the curing stage.
- The cementitious materials used for mine seals applications that were tested in this project can be classified into two types: (a) the first type corresponds to a standard supplier-specific powder which is mixed with water denominated in this report as Company 1-pumpable material, and b) the second type corresponds to seals that use traditional materials for regular concrete such as aggregates, water, cement, and additives, denominated as Company 2-concrete. The two suppliers that provided the material and know-how to this project have developed rigorous and particular procedures for their mixtures and the construction of the seals.
- The curing process of cementitious materials is a complex phenomenon given the chemical, physicochemical, and thermochemical reactions taking place in the solidification of a substance that initially is a fluid. This phenomenon is known as hydration. A rigorous study of the hydration process of seal materials was outside the scope of this project.
- Every cementitious material has its own hydration process. In other words, the heat evolution, and the probability of cracking changes between mixtures, even for mixtures using the same material proportions.
- The study of standard Portland concretes used in civil engineering applications uses the cracking index concept to assess the generation of cracks during the curing process of those materials. The cracking index is related to the heat evolution curve for a particular cementitious mixture. A rigorous study of the hydration process is required to obtain the heat evolution curve for any cementitious material. A rigorous study of the hydration process of seal materials was outside this project's scope, and the assessment of cracking generation and macro-fractures in this project was planned and executed using tracer gases and GPR techniques.
- The theoretical analyses in this report were based on parameters, variables, and theories developed based on the research of the hydration process of traditional Portland cement and concrete. However, the reader should be aware that Company 1 material is not traditional Portland cement, and despite the fact that Company 2 uses Portland cement in its formulation, the chemistry used in the proprietary additive can considerably modify the mixture from a traditional Portland cement mixture.
- The importance of constructability and quality control during the initial pouring and curing of these seals was explored, collecting data at different strength, temperature, and strain behaviors for similar and different mixtures and similar and different construction methods (industrial and manual pouring).

- The quality control during the early stages is highlighted as a major factor that may affect the integrity and performance of the seals, both for the tested materials as well for materials provided by other suppliers which were not tested during this project. In general, and according to the collected information, the first 144 hours after pouring are critical for the curing process. In this period, the most dramatic and active changes in strains, temperature, and acoustic sounds occur for the mixtures used in this project.

7 Recommendations for Future Work

It should be mentioned that the properly constructed seal samples used in this project have not exhibited any visually apparent macro-fractures from the time of pouring until the submission of this report. Moreover, the seals observed during the site mine visit that had already been in operation for more than five years, also did not show any evidence of macro-fractures. As per construction guidelines, the seals at the mine have been kept isolated from the environment by keeping them wrapped. However, if the isolation is lost, the seals may experience changes due to environmental factors. It is recommended to study the behavior of these seals over an extended period of time when subjected to environmental factors. Of course, the findings will only be representative of a situation where the isolation of the seal has been lost.

The mine seals can be affected by cracks generated during other stages besides the curing process. Some of the events that can generate cracks include convergence, environmental changes, water impacts, etc. A study considering the previous factors will increase the knowledge database regarding mine seals for underground coal mines.

Tracer gas results indicated that gas does move through the seal blocks. However, with the available data, it cannot be concluded whether the tracer gases moved through the seal material itself or whether it moved through micro fractures within the seal material. In any case the gas will move through the path of least resistance.

8 References

[1] Winter, Nicholas B. (2009). *Understanding Cement: An Introduction to cement production, cement hydration and deleterious processes in concrete.* London: WHD Microanalysis Consultants Ltd.

[2] Sidney Mindess, J.F.Y. and D. David, *Concrete 2nd Edition*. Technical Documents.

[3] Nocuń-Wczelik, W., Stok, A. & Konik, Z. (2010). *Heat evolution in hydrating expansive cement systems.* J Therm Anal Calorim 101: 527–532. doi:10.1007/s10973-010-0846-1

[4] Kim, Soo Geun. *Effect of heat generation from cement hydration on mass concrete placement*" (2010). Graduate Theses and Dissertations. 11675. doi:10.31274/etd-180810-763

[5] William A., *Temperature matched curing systems.* (1986), *Properties of concrete at early stages. American Concrete Institute*. ACI- SP-95. J. Francis Young Editor.

[6] Emborg, Mats; Bernander, Stig., (1994), *Assessment of Risk of Thermal Cracking in Hardening Concrete. Journal of Structural Engineering, Vol. 120, No. 10.*

[7] ACI (2007). *Report on Thermal and Volume Change Effects on Cracking of Mass Concrete*. ACI 207.2R-07. Reported by ACI Committee 207.

[8] ASTM C1679-17, *Standard Practice for Measuring Hydration Kinetics of Hydraulic Cementitious Mixtures Using Isothermal Calorimetry*. ASTM International, West Conshohocken, PA, 2017, www.astm.org

[9] Noorzaei, J., et al. (2006). *Thermal and stress analysis of Kinta RCC dam. Engineering Structures*, 28, 1795-1802.

[10] Jaafar, M.S, et al. (2007). *Development of finite element computer code for thermal analysis of roller compacted concrete dams*. Advances in Engineering Software, 38, 886-895

[11] Korea Concrete Institute. (2003). *Standard Specification for Concrete*. Korea Concrete Institute, Seoul, Korea

[12] K.C. Tayade, et al., (2018), *A Case Study on Measurement of Temperature Rise in Concrete and Assessment of Probability of Cracking Due to Heat of Hydration*., International Journal of Research in Engineering and Technology., Volume: 07 Special Issue: 01

[13] Jeon, S.J., (2008), *Advanced Assessment of Cracking due to Heat of Hydration and Internal Restraint*. ACI materials Journal, Title 105-M37, July-August 2008, pp.325-333

[14] Metwally abd allah Abd elaty. (2013). *Compressive strength prediction of Portland cement concrete with age using a new model*. HBRC Journal. doi: 10.1016/j.hbrcj.2013.09.005

[15] Shiotani, T., D. G. Aggelis, et al. (2007). *Global monitoring of concrete bridge using acoustic emission*. Journal of Acoustic Emission 25: 308-315.

[16] López Pumarega MI. (2003). *Relation between amplitude and duration of acoustic emission signals*. In: AIP Conference Proceedings. AIP.

[17] Godin N., Reynaud P., Fantozzi G. (2018). *Challenges and Limitations in the Identifications of Acoustic Emission Signature of Damage Mechanisms in Composite Materials*. MDPI: Molecular Diversity Preservation International. MDPI. doi:10.3390/app8081267

[18] Mukherjee A., Banerjee A (2020). *Analysis of the Acoustic Emission Signal for Crack Detection and Distance Measurement*. Australian Acoustical Society. doi: 10.1007/s40857-020-00208-z

9 Appendices

*9.1 **Appendix I**: Mine Seals Information*

<u>Approved Seals under the Final Rule</u>

Seals Designed to Withstand an Overpressure of 50 psi

- 50M-01.1 - Strata Mine Services Plug Seal- For Entry Dimensions Up To 16 ft. High & 40 ft. Wide
- 50M-02.2 – Minova Main Line Tekseal® - For Entry Dimensions Up To 30 ft. High & 30 ft. Wide
- 50G-04.0 - MICON Gob Seal - For Entry Dimensions Up To 20 ft. High & 28 ft. Wide
- 50M-05.0 - MICON Main Line Seal - For Entry Dimensions Up To 20 ft. High & 28 ft. Wide
- 50G-06.1 - JennChem Gob Isolation J-Seal - For Entry Dimensions Up To 30 ft. High & 30 ft. Wide
- 50M-07.0 - JennChem Mainline J-Seal - For Entry Dimensions Up To 30 ft. High & 30 ft. Wide
- 50M-08.0 – Micon Hybrid II Main Line Seal with or without Door - For Entry Dimensions Up To 20 ft. High & 28 ft. Wide

Seals Designed to Withstand an Overpressure of 120 psi

- 120M-01.3 - Strata Mine Services Plug Seal - For Entry Dimensions Up To 16 ft. High & 100 ft. Wide
- 120M-02.2 – Minova Main Line Tekseal® - For Entry Dimensions Up To 30 ft. High & 30 ft. Wide
- 120M-03.0 - BHP Billiton Concrete Main Line Plug Seal- For Entry Dimensions Up To 20 ft. High & 26 ft. Wide
- 120M-04.1 - Precision Mine Repair (PMR) 8x40 Concrete Seal- For Entry Dimensions Up To 8 ft. High & 40 ft. Wide
- 120G-05.1 – Minova Gob Isolation Tekseal® - For Entry Dimensions Up To 30 ft. High & 30 ft. Wide
- 120M-06.1 - MICON Mainline Hybrid Seal- For Entry Dimensions Up To 20 ft. High & 28 ft. Wide
- 120M-07.1 - Precision Mine Repair (PMR) Concrete Seal- For Entry Dimensions Up To 6 ft. High & 40 ft. Wide
- 120M-08.1 - Precision Mine Repair (PMR) Concrete Seal- For Entry Dimensions Up To 10 ft. High & 40 ft. Wide
- 120M-09.1 - Precision Mine Repair (PMR) Concrete Seal- For Entry Dimensions Up To 12 ft. High & 40 ft. Wide
- 120M-10.1 – Minova Main Line Tekseal® - For Entry Dimensions Up To 30 ft. High & From 30 ft. to 40 ft. Wide
- 120M-11.3 - MICON Mainline Hybrid II Seal - For Entry Dimensions Up To 32.5 ft. High & 28 ft. Wide
- 120G-12.0 - MICON Gob Isolation Hybrid II Seal - For Entry Dimensions Up To 20 ft. High & 28 ft. Wide

- 120M-13.0 - MICON Mainline Hybrid III Seal - For Entry Dimensions Up To 20 ft. High & 28 ft. Wide
- 120M-14.0 - Strata Mine Services Reinforced StrataCrete Seal - For Entry Dimensions Up To 12 ft. High & 40 ft. Wide
- 120M-15.1 - JennChem Mainline J-Seal- For Entry Dimensions Up To 30 ft. High & 30 ft. Wide
- 120G-16.0 - JennChem Gob Isolation J-Seal- For Entry Dimensions Up To 30 ft. High & 30 ft. Wide
- 120M-17.0 - JennChem Mainline 1-Day J-Seal- For Entry Dimensions Up To 30 ft. High & 30 ft. Wide
- 120M-18.0 - Strata Mine Services Reinforced StrataCrete Seal - For Entry Dimensions Up To 8 ft. High & 40 ft. Wide

Seals Designed to Withstand an Overpressure > 120 psi
Currently, no seals have been approved under this category.

Manufacturer	MSHA Approval	Seal Type	Overpressure	Material
Strata Mine Services	50M-01.1	Plug	50psi	M.S. Stratacrete®
Minova	50M-02.2	Plug	50psi	Tekseal®
Micon	50G-04.0	Flexural	50psi	HybriBond &70
Micon	50M-05.0	Flexural	50psi	HybriBond &70
JennChem	50G-06.1	Plug	50psi	J-Seal®
JennChem	50M-07.0	Plug	50psi	J-Seal®
Micon	50M-08.0	Flexural	50psi	Hybribond & SIGNUM
Strata Mine Services	120M-01.3	Plug	120psi	M.S. Stratacrete®
Minova	120M-02.2	Plug	120psi	Tekseal®
BHP Billiton	120M-03.0	Plug	120psi	Portland Cement Concrete
Precision Mine Repair	120M-04.1	Flexural	120psi	Portland Cement and Sand
Minova	120G-05.1	Flexural	120psi	Tekseal®
Micon	120M-06.1	Flexural	120psi	HybriBond &70
Precision Mine Repair	120M-07.1	Flexural	120psi	Portland Cement and Sand
Precision Mine Repair	120M-08.1	Flexural	120psi	Portland Cement and Sand
Precision Mine Repair	120M-09.1	Flexural	120psi	Portland Cement and Sand
Minova	120M-10.1	Plug	120psi	Tekseal®
Micon	120M-11.3	Flexural	120psi	Hybribond & SIGNUM
Micon	120M-12.0	Flexural	120psi	Hybribond & SIGNUM
Micon	120M-13.0	Flexural	120psi	Hybribond & PU37A

Strata Mine Services	120M-14.0	Flexural	120psi	H.S. Stratacrete®
JennChem	120M-15.1	Plug	120psi	J-Seal®
JennChem	120G-16.0	Plug	120psi	J-Seal®
JennChem	120M-17.0	Plug	120psi	1 Day J-Seal®
Strata Mine Services	120M-18.0	Flexural	120psi	H.S. Stratacrete®

Notes to the approved seals

Approved Seals under the Final Rule

Seals Designed to Withstand an Overpressure of 50 psi

50M-01.1 - Strata Mine Services Plug Seal- For Entry Dimensions Up To 16 ft. High & 40 ft. Wide

- Quality control procedures: Site prep, Formwork, Aggregate, Convergence, Formwork, Slump, Joints, and Sampling for uniax-comp testing.
- No heating or thermal testing included

50M-02.2 – Minova Main Line Tekseal® - For Entry Dimensions Up To 30 ft. High & 30 ft. Wide

- Quality control procedures: Site prep, surrounding strata properties, Formwork, Training, Mix water compatibility, Penetration test, Surface drying effects, Voids, Strata fractures, Convergence, Material storage, Joints, and Sampling for uniax-comp testing.
- Recommended mix water temperature, no heating or thermal testing included

50G-04.0 - MICON Gob Seal - For Entry Dimensions Up To 20 ft. High & 28 ft. Wide

- Quality control procedures: Packaging/storage, Training, Samples prep and lab testing (direct shear), CMU testing ASTM C-140-97, Hybricrete block testing ASTM D-1621-04a, Convergence.
- No heating or thermal testing included

50M-05.0 - MICON Main Line Seal - For Entry Dimensions Up To 20 ft. High & 28 ft. Wide

- Quality control procedures: Packaging/storage, Training, Samples prep and lab testing (direct shear), CMU testing ASTM C-140-97, Hybricrete block testing ASTM D-1621-04a, Convergence.
- No heating or thermal testing included.

50G-06.1 - JennChem Gob Isolation J-Seal - For Entry Dimensions Up To 30 ft. High & 30 ft. Wide

- Quality control procedures: Packaging and QC testing at plant; Shelf-life; Water compatibility, Penetration test, Surface drying effects, Voids, Strata fractures, Convergence, Material storage, Joints, and Sampling for uniax-comp testing.
- Recommended mix water temperature, no heating or thermal testing included.

50M-07.0 - JennChem Mainline J-Seal - For Entry Dimensions Up To 30 ft. High & 30 ft. Wide

- Quality control procedures: Packaging and QC testing at plant; Shelf-life; Water compatibility, Penetration test, Surface drying effects, Voids, Strata fractures, Convergence, Material storage, Joints, and Sampling for uniax-comp testing.

- Recommended mix water temperature, no heating or thermal testing included

50M-08.0 – Micon Hybrid II Main Line Seal with or without Door - For Entry Dimensions Up To 20 ft. High & 28 ft. Wide

- Quality control procedures: Packaging/storage, Training, Samples prep and lab testing (direct shear), Pump ratio tests, Pre-approved CMU supplier, Material storage, Convergence.
- No heating or thermal testing included.

Seals Designed to Withstand an Overpressure of 120 psi

120M-01.3 - Strata Mine Services Plug Seal - For Entry Dimensions Up To 16 ft. High & 100 ft. Wide

- Quality control procedures: Site prep, Formwork, Storage and re-testing admixtures, Batch testing ASTM C1611, Admixture testing ASTM C494 and 494M, Water testing ASTM C1602/C1602M-06, Convergence, Formwork, Slump, Joints, and Sampling for uniax-comp testing ASTM C31/C31M and ASTM C470-02A, Curing ASTM C171 or ASTM C309, Training.
- No heating or thermal testing included

120M-02.2 – Minova Main Line Tekseal® - For Entry Dimensions Up To 30 ft. High & 30 ft. Wide

- Quality control procedures: Site prep, surrounding strata properties, Formwork, Training, Mix water compatibility, Equipment calibration, Penetration test, Surface drying effects, Voids, Strata fractures, Convergence, Material storage, Joints, and Sampling for uniax-comp testing.
- Recommended mix water temperature, no heating or thermal testing included

120M-03.0 - BHP Billiton Concrete Main Line Plug Seal- For Entry Dimensions Up To 20 ft. High & 26 ft. Wide

- Quality control procedures: Site prep, Formwork, Concrete provider manifest; PPE, Training, Slump test, Convergence, and Sampling for uniax-comp testing.
- No heating or thermal testing included

120M-04.1 - Precision Mine Repair (PMR) 8x40 Concrete Seal- For Entry Dimensions Up To 8 ft. High & 40 ft. Wide

- Quality control procedures: Roof and floor pull tests, Site prep, Material storage, Formwork, Test Panels ASTM C1140 for core samples, mix water compatibility ASTM C1602 or Article 1002.02 of the Illinois Department of Transportation Standard Specifications for Road and Bridge Construction (Adopted Jan. 1, 2007), including all addenda, Training – ACI 506.3R, Convergence.
- No heating or thermal testing included

120G-05.1 – Minova Gob Isolation Tekseal® - For Entry Dimensions Up To 30 ft. High & 30 ft. Wide

- Quality control procedures: Site prep, surrounding strata properties, Formwork, Training, Mix water compatibility, Equipment calibration, Penetration test, Surface drying effects, Voids, Strata fractures, Convergence, Material storage, Joints, and Sampling for uniax-comp testing.

- Recommended mix water temperature, no heating or thermal testing included

120M-06.1 - MICON Mainline Hybrid Seal- For Entry Dimensions Up To 20 ft. High & 28 ft. Wide

- Quality control procedures: Packaging/storage, Site prep, Training, Samples prep and lab testing (direct shear), CMU testing ASTM C-140-97, Hybricrete block testing ASTM D-1621-04a, Convergence.
- MICON 70 and Hybribond temp range 40°F to 105°F, no heating or thermal testing included.

120M-07.1 - Precision Mine Repair (PMR) Concrete Seal- For Entry Dimensions Up To 6 ft. High & 40 ft. Wide

- Quality control procedures: Roof and floor pull tests, Site prep, Material storage, Formwork, Test Panels ASTM C1140 for core samples, mix water compatibility ASTM C1602 or Article 1002.02 of the Illinois Department of Transportation Standard Specifications for Road and Bridge Construction (Adopted Jan. 1, 2007), including all addenda, Training – ACI 506.3R, Convergence.
- No heating or thermal testing included

120M-08.1 - Precision Mine Repair (PMR) Concrete Seal- For Entry Dimensions Up To 10 ft. High & 40 ft. Wide

- Quality control procedures: Roof and floor pull tests, Site prep, Material storage, Formwork, Test Panels ASTM C1140 for core samples, mix water compatibility ASTM C1602 or Article 1002.02 of the Illinois Department of Transportation Standard Specifications for Road and Bridge Construction (Adopted Jan. 1, 2007), including all addenda, Training – ACI 506.3R, Convergence.
- No heating or thermal testing included

120M-09.1 - Precision Mine Repair (PMR) Concrete Seal- For Entry Dimensions Up To 12 ft. High & 40 ft. Wide

- Quality control procedures: Roof and floor pull tests, Site prep, Material storage, Formwork, Test Panels ASTM C1140 for core samples, mix water compatibility ASTM C1602 or Article 1002.02 of the Illinois Department of Transportation Standard Specifications for Road and Bridge Construction (Adopted Jan. 1, 2007), including all addenda, Training – ACI 506.3R, Convergence.
- No heating or thermal testing included

120M-10.1 – Minova Main Line Tekseal® - For Entry Dimensions Up To 30 ft. High & From 30 ft. to 40 ft. Wide

- Quality control procedures: Site prep, surrounding strata properties, Formwork, Training, Mix water compatibility, Equipment calibration, Penetration test, Surface drying effects, Voids, Strata fractures, Convergence, Material storage, Joints, and Sampling for uniax-comp testing.
- Recommended mix water temperature, no heating or thermal testing included

120M-11.3 - MICON Mainline Hybrid II Seal - For Entry Dimensions Up To 32.5 ft. High & 28 ft. Wide

- Quality control procedures: Packaging/storage, Strata properties, Site prep, Training, Samples prep and lab testing (direct shear), Ratio testing, Voids, CMU testing ASTM C-140-97, Hybricrete block testing ASTM D-1621-04a, Convergence.
- SIGNUM and Hybribond temp range 40°F to 105°F, no heating or thermal testing included.

120G-12.0 - MICON Gob Isolation Hybrid II Seal - For Entry Dimensions Up To 20 ft. High & 28 ft. Wide

- Quality control procedures: Packaging/storage, Strata properties, Site prep, Training, Samples prep and lab testing (direct shear), Ratio testing, Voids, CMU testing ASTM C-140-97, Hybricrete block testing ASTM D-1621-04a, Convergence.
- SIGNUM and Hybribond temp range 40°F to 105°F, no heating or thermal testing included.

120M-13.0 - MICON Mainline Hybrid III Seal - For Entry Dimensions Up To 20 ft. High & 28 ft. Wide

- Quality control procedures: Packaging/storage, Strata properties, Site prep, Training, Samples prep and lab testing (direct shear), Voids, CMU testing ASTM C-140-97, Hybricrete block testing ASTM D-1621-04a, Convergence.
- PU37A and Hybribond temp range 40°F to 105°F, no heating or thermal testing included.

120M-14.0 - Strata Mine Services Reinforced StrataCrete Seal - For Entry Dimensions Up To 12 ft. High & 40 ft. Wide

- Quality control procedures: Site prep, pull test, Storage and handling, Admixture testing, Formwork, Training, Sample pre–ASTM C470-02a, Convergence, Slump, Joints, and Sampling for ACI 318 uniax-comp testing ASTM C31/C31M and ASTM C143/143M, Water testing ASTM C1602/1602M-06, Admixtures ASTM C494/494M, Curing ASTM C171 or ASTM C309, Panel testing ASTM C1140.
- No heating or thermal testing included

120M-15.1 - JennChem Mainline J-Seal- For Entry Dimensions Up To 30 ft. High & 30 ft. Wide

- Quality control procedures: Packaging and QC testing at plant; Storage, Shelf-life; Water compatibility, Site prep, Formwork, Training, Equip. calibration, Joints, Penetration test, Surface drying effects, Voids, Strata fractures, Convergence, and Sampling for uniax-comp testing.
- Recommended mix water temperature 55°F-75°F, no heating or thermal testing included

120G-16.0 - JennChem Gob Isolation J-Seal- For Entry Dimensions Up To 30 ft. High & 30 ft. Wide

- Quality control procedures: Packaging and QC testing at plant; Storage, Shelf-life; Water compatibility, Site prep, Formwork, Training, Equip. calibration, Joints, Penetration test, Surface drying effects, Voids, Strata fractures, Convergence, and Sampling for uniax-comp testing.
- Recommended mix water temperature 55°F-75°F, no heating or thermal testing included

120M-17.0 - JennChem Mainline 1-Day J-Seal- For Entry Dimensions Up To 30 ft. High & 30 ft. Wide

- Quality control procedures: Packaging and QC testing at plant; Storage, Shelf-life; Water compatibility, Site prep, Formwork, Training, Equip. calibration, Joints, Penetration test, Surface drying effects, Voids, Strata fractures, Convergence, and Sampling for uniax-comp testing.
- Recommended mix water temperature 55°F-75°F, no heating or thermal testing included

120M-18.0 - Strata Mine Services Reinforced StrataCrete Seal - For Entry Dimensions Up To 8 ft. High & 40 ft. Wide

- Quality control procedures: Site prep, pull test, Storage and handling, Admixture testing, Formwork, Training ACI C 660, Sample pre–ASTM C470-02a, Convergence, Slump, Joints, and Sampling for ACI 318 uniax-comp testing ASTM C31/C31M and ASTM C143/143M, Water testing ASTM C1602/1602M-06, Admixtures ASTM C494/494M, Curing ASTM C171 or ASTM C309, Panel sample prep ASTNC42/C42M or C513 and testing ASTM C1140.
- No heating or thermal testing included

Seals Designed to Withstand an Overpressure > 120 psi

Currently, no seals have been approved under this category

9.2 ***Appendix II:*** *Theoretical concepts – Heat Evolution Curves*

Most of the available information regarding the curing process of cementitious materials is related to concrete. This is because concrete is one of the materials used for infrastructure construction in our modern civilization. The most basic definition of concrete is a mixture made of Portland cement, coarse and fine aggregates of stone and sand, and water. For this project, Company 1 provided all the materials required to build the seals in the form of a powder where no aggregates were needed. Only water is added at a specific, predetermined temperature. On the other hand, Company 2 uses a standard concrete mix (it can be purchased from a concrete plant), and an additive (produced by the company) is added to the standard concrete mixture for the application in mine seals.

During the development of this project, the research team recognizes that the study of the curing process of cementitious materials, used for mine seals applications, and any other application, including the generation of micro and macro-fractures, is a very complex topic given all the physical and thermochemical interactions and reactions occurring during such a process. The following concepts are included in this report to provide some guidance for the interpretations of the data collected during the project.

9.2.1.1 *Concrete curing general concepts*

Curing in concrete, and in the case of the pumpable cementitious material, is to provide the right conditions (with respect to the environment and time) to the fresh mixture to gain strength properly. Curing serves the main purposes of:

- Helps retain moisture, so the material continues to gain strength.
- Delays drying shrinkage until the material is strong enough to resist shrinkage cracking.
- Allows the growth of crystals generated from a reaction between the Portland cement and the water. This reaction is known as hydration.
- Provides the proper temperature (material temperature) to the mixture for the hydration process to take place at the proper rate. If the temperature is too low, the hydration reaction will slow down and can eventually stop (below 40 °F). On the other hand, if the material is too hot, the crystals will not have time to grow, and the material will not develop the expected strength. Hot mixtures can also generate significant differential temperatures between different areas of the material that can lead to cracking.

There are different curing methods:

- *Water cure:* the mixture is flooded, or mist sprayed continuously.
- *Water retaining methods:* different materials are used to cover the mixture (sand, canvas, etc.) to keep the mixture wet.
- *Plastic film seal:* the mixture is wrapped in a plastic film to keep the mixture wet.
- *Chemical seal:* chemical sealants are applied to keep the mixture wet.

The above information was considered at the time the project proposal was submitted and, thus, dictated the instrumentation used during the initial stage of this project. As described previously, the material temperature during the curing process is a crucial variable and can be used to assess the likelihood of the material cracking during the curing process. For this reason, the team installed several thermocouples in the samples at different locations. Based on similar reasoning embedded strain gauges were installed and acoustic emission (AE) sensors were placed on different locations of each cube. One parameter that was not considered and perhaps could show some evidence of the likelihood of cracking due to curing is the moisture or water content of the material. Unfortunately, this parameter was not considered important during the development of the proposal, and therefore it was not measured.

During the first round of testing, Company 1 recommended that the wooden forms and plastic film covering each sample should be kept in place the entire time, thus protecting the samples from moisture loss. It should be noted that Company 2 does not have any specifications with respect to sample projection with respect to water loss due to the interaction with the environment.

After it was clarified that the objective of the project was to determine whether macro-fractures related to the curing process could be created, Company 1 was willing to allow the team to strip all the wooden forms and the plastic cover from the samples. The change in the environment of the samples (i.e., with and without protection) can be seen clearly in the data collected by the embedded strain gauges in the samples with the standard material proportions for both companies.

In other words, Company 1 recommends a plastic film seal method for curing, while in the case of Company 2 there is no recommended method used to ensure proper curing. During the mine visit described previously, despite the seals being built five (5) years before the visit, the plastic seal film wrapping the mine seals was kept in place.

9.2.1.2 *Heat evolution curve - Portland Cement / Concrete*

The following discussion is extracted from reference [1]. The cement hydration, as in many chemical processes, has reactants and products of the reaction. When the reactants, four clinker minerals, clinker alkali sulfate, and gypsum are mixed with water, one exothermic reaction starts to occur. The heat generally increases to a peak value and then gradually declines with time. The typical shape of such behavior for Portland concrete is presented in Figure 9.1.

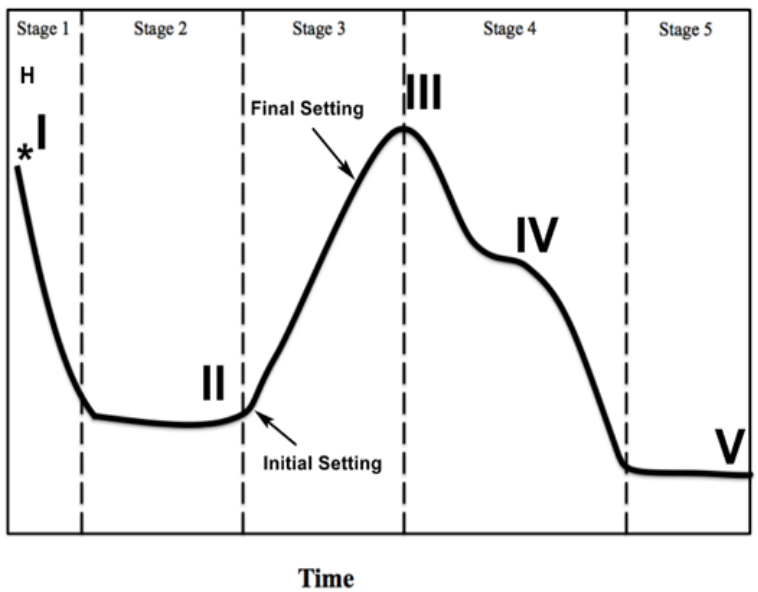

Figure 9.1 Typical heat evolution curve of hydrating Portland cement (Source: Adapted from reference [1])

In Figure 9.1, the vertical axes (H) represent the rate of heat evolution (the velocity at which the heat changes), usually measured in watts per kilogram of cement. The figure does not include the first part of the curve where a fast increase (possibly lasting only a few minutes) in the heat evolution is observed (when water is added) followed by a fast decrease. Only the final stage of this change is represented by Point I. After Point I, there is a dormant or induction period (segment between point I and II). In some cases, this period shows a rapid drop and then a portion of the segment represented by a horizontal line. After this period, the concrete sets and starts to gain strength. When the concrete starts to gain strength, the exothermic reaction takes place, and the heat evolution reaches a peak at point III. After the peak, there are small increases in the heat evolution, reaching point IV. Finally, the heat evolution tails off over the following days and weeks.

In addition to the characteristic points in the curve, the whole hydration process can be divided into five (5) different reaction stages. Table 9.1, adapted from [2], is an oversimplification of the description of each stage in Figure 9.1.

Table 9.1 Typical hydration process of cement. Adapted from [2]

Reaction Stage	Kinetics of Reaction	Chemical Processes
1-Initial hydrolysis	Chemical control; rapid	Dissolution of ions: Concrete in fluid form
2-Induction Period	Nucleation control; slow	Continued dissolution of ions: Concrete start to be in a plastic state
3-Acceleration	Chemical control; rapid	The initial formation of hydration products: Concrete setting begins, and early hardening begins. Concrete strength starts development.
4-Deceleration	Chemical and diffusion control; slow	Continued formation of hydration products: Hardening continues increasing and maximum strength starts to be fully developed.
5-Steady state	Diffusion control; slow	Slow formation of hydration products. The concrete reaches almost its maximum strength and is a totally hard material.

The study of the heat evolution curve and the different stages is essential for concrete technologies, given that the final shape of the curve is dictated by numerous variables such as the amount and concentration of the different minerals in the clinker and the aggregates, the water, the additives, and its thermochemical reactions. This can be seen in Figure 9.2 which was adapted from reference [3].

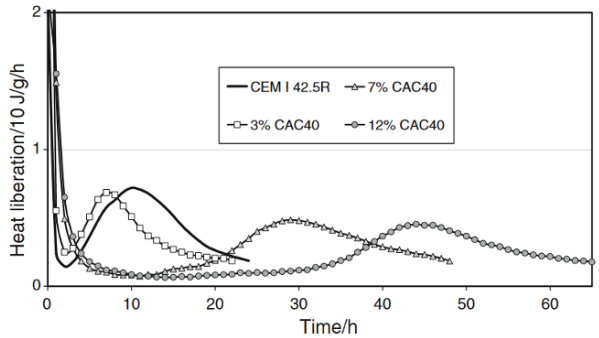

a) Heat evolution of Portland cement with calcium aluminate cement (CAC 40) used as an additive.

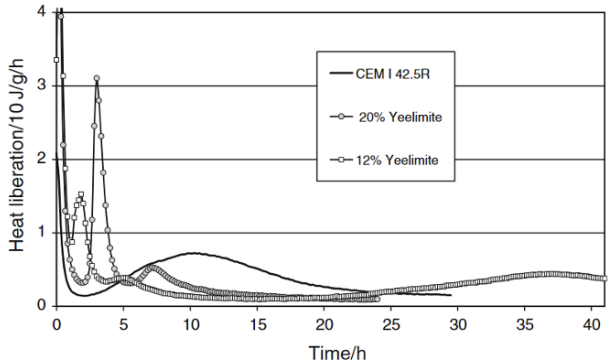

b) Heat evolution of Portland cement with varied amounts expansive additive-calcium sulfoaluminate (yeelimite)

Figure 9.2 Changes in the typical heat evolution curve with different expansive additives (Source: Adapted from reference [3])

Figure 9.2 illustrates the complexity of the problem and how different additives affect the heat evolution curve when compared to concrete using standard Portland cement. It should be noted that every cementitious mixture will have a characteristic heat evolution curve depending on several factors. Below is a list of the main factors influencing the cement hydration process and the heat evolution curve, adapted from [4].

- Chemical composition of cement,
- Sulfate content,
- Fineness (Overall particle size distribution of cement),
- Water/Cement ratio,
- Initial temperature (environmental and mixture),
- Supplemental cementitious materials,

9.3 ***Appendix III:*** *Theoretical concepts – Concrete Cracking Index – Heat evolution & the assessment of the risk of thermal cracking in concrete.*

The study of the heat evolution curve is not only important to understand the different stages of the concrete as it transitions from its liquid state to the phase where it is completely hardened. It is also essential for the analysis of the risk of thermal cracking.

The heating and cooling processes that the concrete experiences generate expansion and contraction of the material. If unrestrained, the material will expand and contract without stresses being induced [6]. However, the concrete is always restrained to some degree. In the study of concrete, there are two types of restrains recognized. Internal and external restrains. Both restrains are interrelated, and they usually exist to some degree in all concrete elements [7]. According to [7], the computation of thermal volume change can be summarized in the following expression:

$$\Delta V = \left[T_f - (T_i + T_{ad}) + T_{env}\right] * CTE \qquad \text{Eq.5}$$

Where:
ΔV =volume change of the concrete,
T_f =final stable temperature of the concrete,
T_i =initial placing temperature of the concrete,
T_{ad} =adiabatic temperature rises of the concrete,
T_{env} =temperature change from the heat added or subtracted from the concrete due to environmental conditions,
CTE =coefficient of thermal expansion

The adiabatic temperature rises of the concrete (T_{ad}) should be measured by performing careful tests using the cement type for the concrete under study and maintaining the conditions that represent those that will occur in the field. Reference [8] includes the details of one of such types of tests (Isothermal calorimeter). Figure 9.3 shows the typical adiabatic temperature rise of the four most common Portland cement used in the concrete industry.

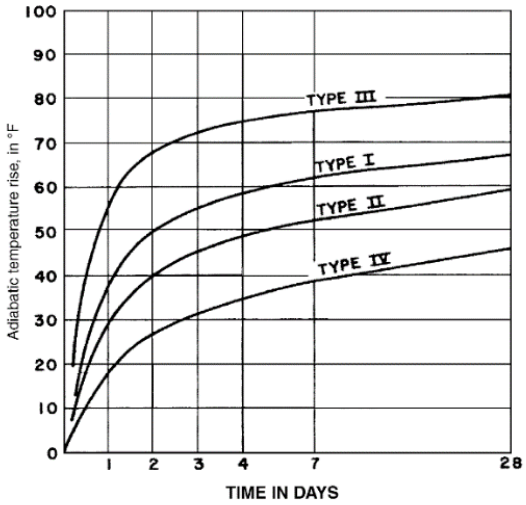

Cement type	Fineness ASTM C 115 cm^2/gm	28-day heat of hydration, Calories per gm
I	1790	87
II	1890	76
III	2030	105
IV	1910	60

Figure 9.3 Typical adiabatic temperature rise, for different Portland cement (Source: Adapted from reference [7])

Unfortunately, those curves are not available for this project given the specialized equipment and tests required [8], so it is not possible to calculate the volume change of the samples in this project.

As mentioned before, the restrain conditions are fundamental for the development of cracks at the early age of the concrete (during curing). Figure 9.4 indicates the most important factors influencing the temperature-induced stresses and cracks.

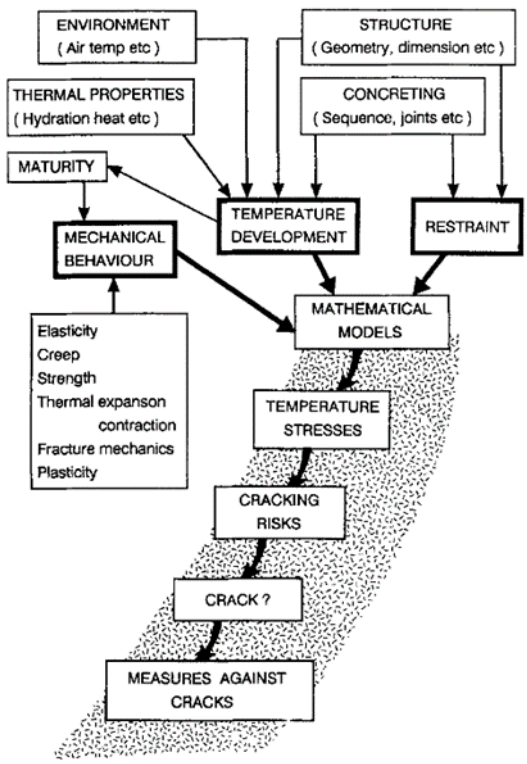

Figure 9.4 Factors influencing a generation of cracks at the early age of the concrete (Source: Adapted from reference [6])

As seen in Figure 9.4, the risk assessment of the cracking of concrete in early ages is complex and involves specific tests, to mathematical models, usually solved, using Finite Element Techniques (FEM or FE).

As mentioned before, to study the problem of cracking related to the restraint of the concrete, it is assumed that the internal restraint is associated with one type of cracking while the external restraint to another. The external restraint exists along the concrete's contact surface and any material against which the concrete has been cast. The degree of restraint depends primarily on the relative dimensions, strength, and modulus of elasticity of the concrete and restraining material [7]. Figure 9.5 shows the concept of external restraint and the formation of cracks due to this type of restraint. In Figure 9.5, the restraint is located in the lower part of the fresh sample of concrete. In the situation when there is no restraint, it is expected that the fresh concrete changes its volume uniformly. On the other hand, if the lower face of the sample is restrained, the changes in temperature will generate changes in volume, and it is expected the generation of fractures in some areas of the sample (lower zone). In this case, the cracking is induced by the difference between the peak temperature and the final temperature in the sample, as indicated in Figure 9.5.

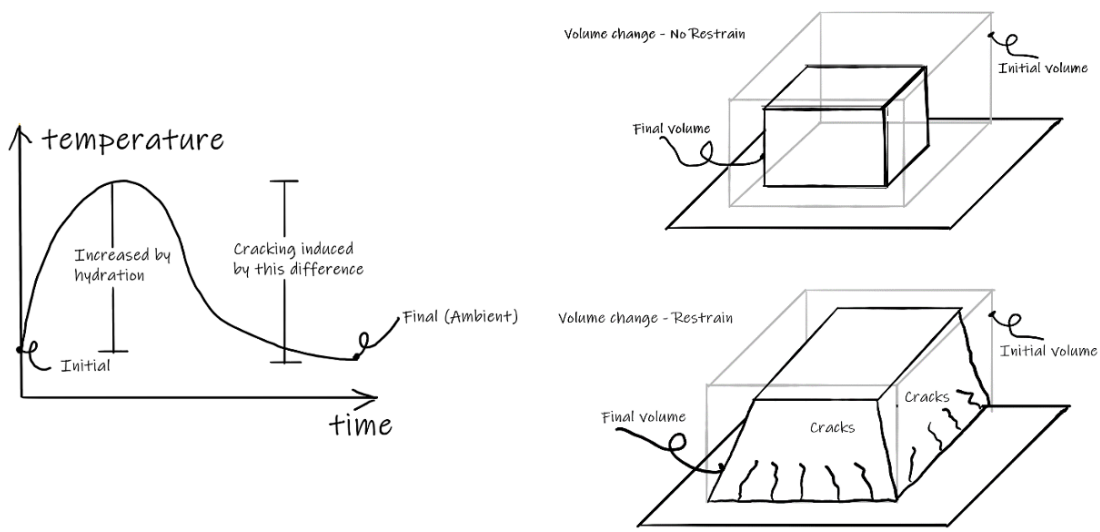

Figure 9.5 Crack formation due to external restrain (Source: Adapted from reference [4])

The internal restraint is produced by the difference in the consistency or behavior of the concrete in different areas of the sample during the curing process. When a cross-section of a concrete sample is analyzed, the center of the sample generally has a higher temperature, and the internal volume tries to expand. On the other hand, it is expected that the surface of the sample experiences a lower temperature, and the concrete tries to contract. This difference, i.e., expansion and contraction, will generate zones in the sample subjected to compression and others to tension. Figure 9.6 shows the concepts related to crack formation due to internal restrain.

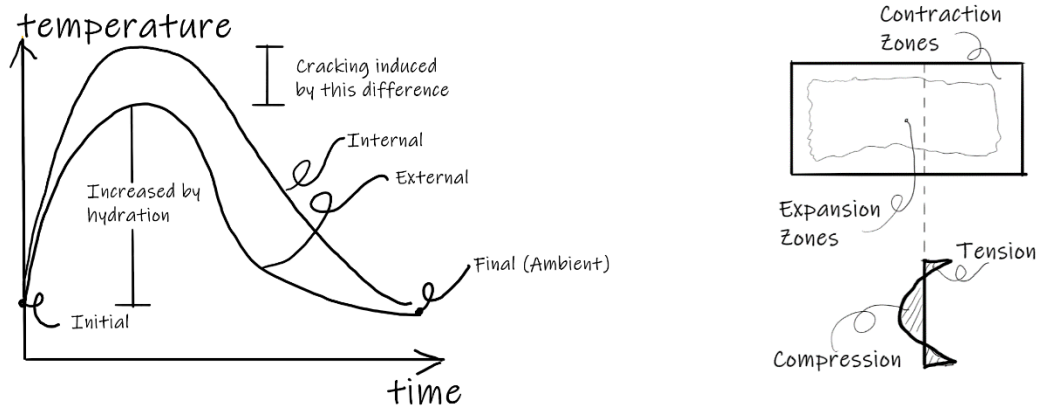

Figure 9.6 Crack formation due to internal restrain (Source: Adapted from reference [4])

In the specific case of mine seals, it is expected that both types of cracking mechanisms occur. The assessment of both types of cracking is complex, and in most cases, the finite element technique is used to determine the thermal distribution and thermal stress in the mass of concrete. References [9] and [10] are two examples of the study of thermal stress due to temperature changes in concrete.

In the U.S., the ACI guides do not have any specific provisions for cracking induced by the heat of hydration except imposing some limits for temperature drop in cold weather concreting [4]. One proposal to assess the likelihood of cracking due to internal restraints is the Korean concrete standard. Such a standard proposes a parameter called the crack index. The crack index is expressed in the following equation [4].

$$I_{cr}(t) = \frac{f_{sp}(t)}{f_t(t)} \qquad \text{Eq. 6}$$

Where:
$I_{cr}(t)$ =Crack index due to internal restraint at time t,
$f_{sp}(t)$ =tensile strength of the concrete at time t
$f_t(t)$ =maximum thermal stress at time t (can be analyzed using FEM or measured as in this case)

The assumption is that the tensile strength also changes with time as the compression strength increases during curing. In theory the tensile strength is proportional to approximately 10% of the uniaxial compressive strength.

Figure 9.7 shows the relationship between the probability of crack growth (occurrence) and the crack index.

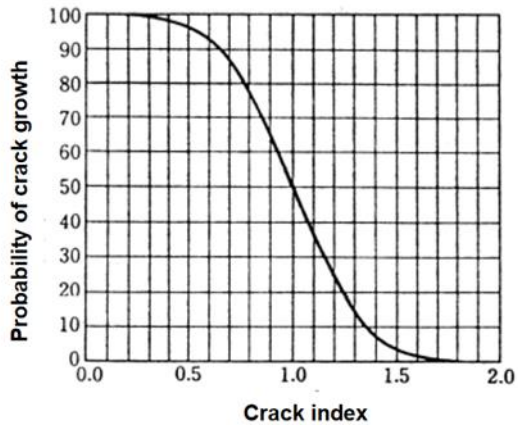

Figure 9.7 Crack index and probability of crack growth (occurrence) (Source: Adapted from reference [11]) Crack index and probability of crack growth (occurrence) (Source: Adapted from reference [11])

Using the crack index, the concrete engineer has a guideline to actions to be taken regarding cracking due to internal restraints. The actions are in the following Table 9.2. If the stress is higher than the strength, possibilities do exist for cracks forming. In theory if strength is higher than stress, no cracks will start to form.

Table 9.2 Thermal (internal restraint) crack criteria. Adapted from [11]

Action	Intervals
Cracks have a low probability of growth (no action)	$I_{cr} \geq 1.5$
Cracks can occur, and actions are required to limit the growth	$1.2 \leq I_{cr} < 1.5$
Cracks most likely will appear and actions are required to avoid harmful cracking	$0.7 \leq I_{cr} < 1.2$

Given that Equation 6 requires the calculation or assessment of the maximum thermal stress with the time (use of FEM), a simplification of equation 6 is included by the Korean Concrete Institute. Equation 7 is a crack index as a function of temperature for the internally restrained condition [12],[13].

$$I_{crs}(i) = \frac{15}{\Delta T_i} \qquad \text{Eq. 7}$$

Where:
ΔT_i= maximum temperature difference across the concrete section in ˚C

The factor in Equation 7 (the value of 15) is related to the type of constitutive relation used for the analysis (elastic, plastic, elasto-plastic, etc.) and the instant where the difference in temperature is measured. A modification to Equation 7 according to reference [13] is included in equations 8 and 9.

$$I_{crs}(i) = \frac{15.4}{\Delta T_{i-peak}} \qquad \text{Eq. 8}$$

ΔT_{i-peak}= peak temperatures and elastic model

$$I_{crs}(i) = \frac{25}{\Delta T_{i-peak}} \qquad \text{Eq. 9}$$

ΔT_{i-peak}= peak temperatures and hypo-elastic model

Equation 9 considers the pattern of development of heat hydration, the member size, curing conditions, the form removal, the hardening properties of concrete etc., and it is considered more realistic for practical applications.

In the use of Equations 7 to 9, the temperature difference across the section of the concrete element is the primary information for the evaluation of the tendency of cracks to form induced by the internal restraint.

9.4 ***Appendix IV*** *- UCS tested samples on different days*

7 DAYS UCS TEST MIXTURE A

7 DAYS UCS TEST MIXTURE B

7 DAYS UCS TEST MIXTURE C

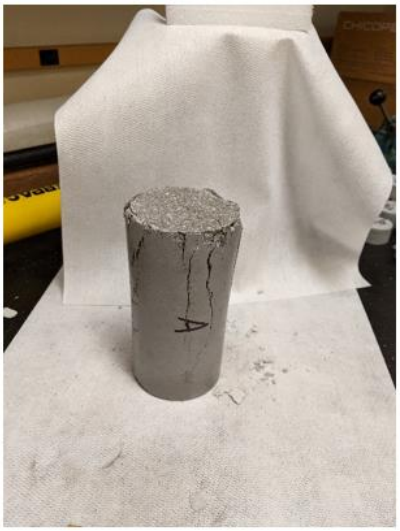

14 DAYS UCS TEST MIXTURE A

14 DAYS UCS TEST MIXTURE B

14 DAYS UCS TEST MIXTURE C

28 DAYS UCS TEST MIXTURE A

28 DAYS UCS TEST MIXTURE B

9.5 ***Appendix V*** *Visual interpretation of changes in the texture of the samples*

Mixture B – Company 1 – Tracer Gas Sample (DSC 2307)

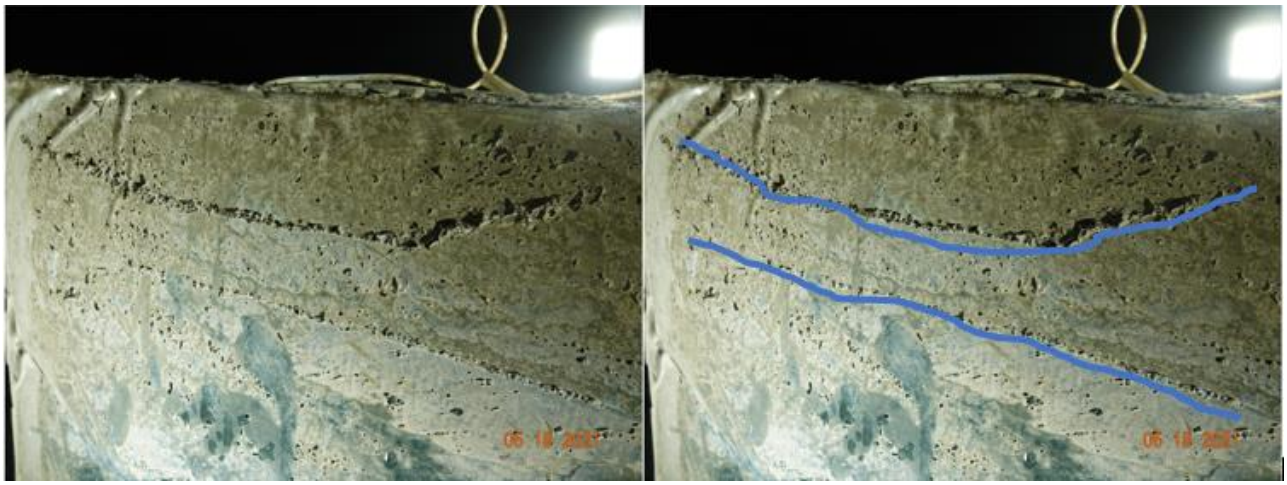

Mixture B – Company 1 - Control Sample (DSC 2327)

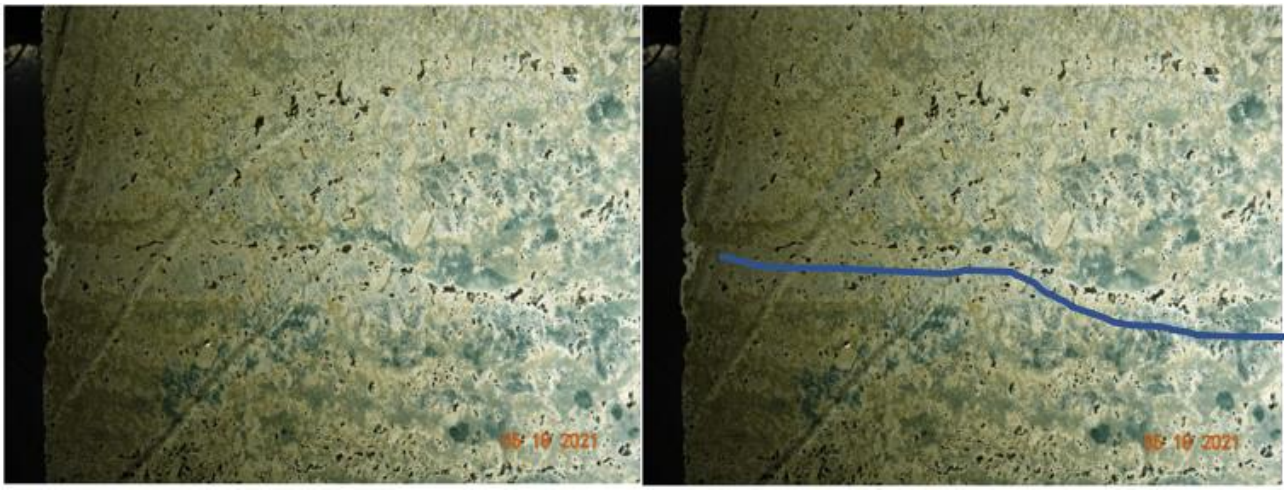

Mixture A – Company 1 – Control Sample (DSC 2329, 2330, 2337, 2338, 2340)

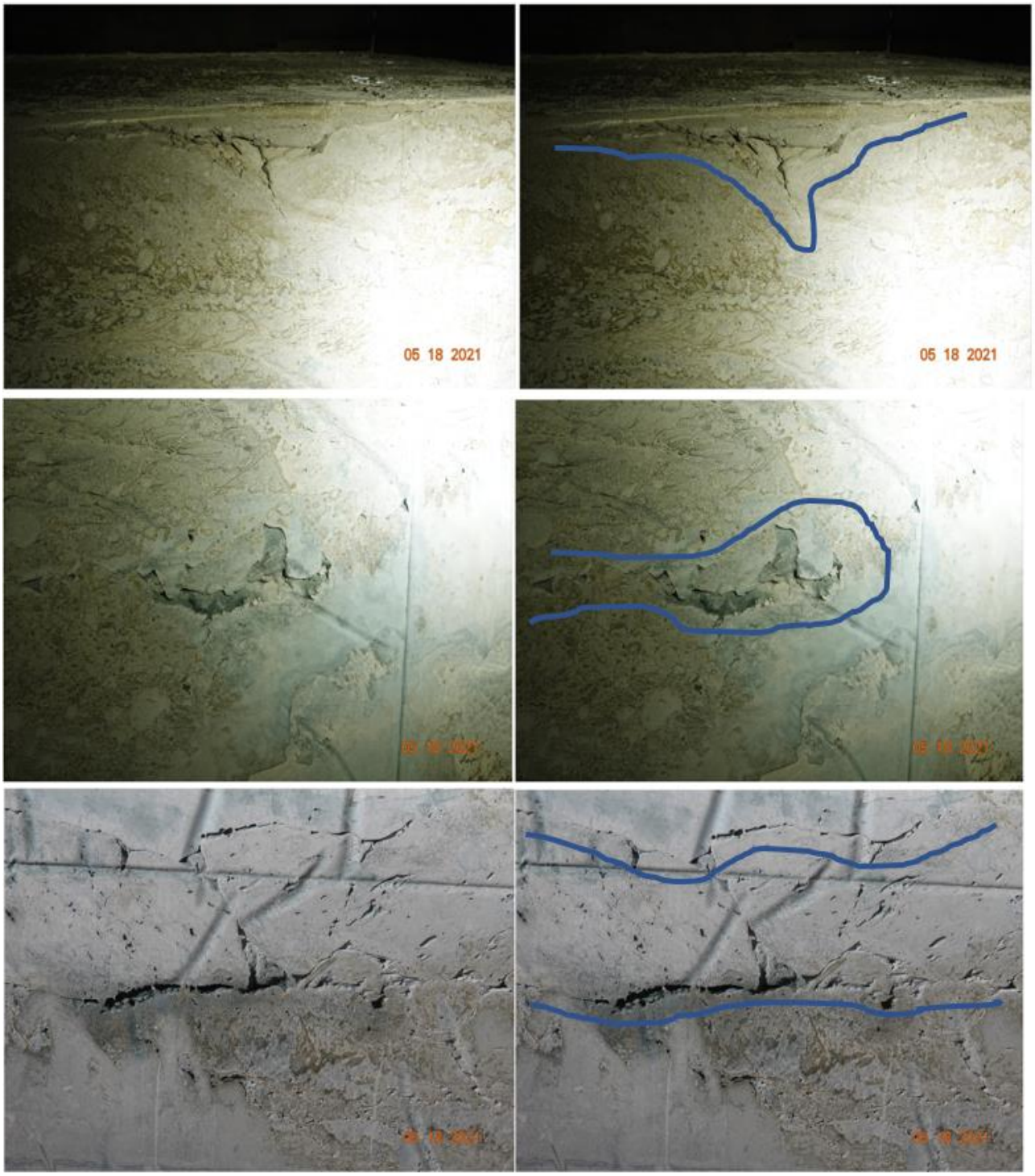

Mixture B – Company 1 – Strain Gauges Sample (DSC 2387, 2393)

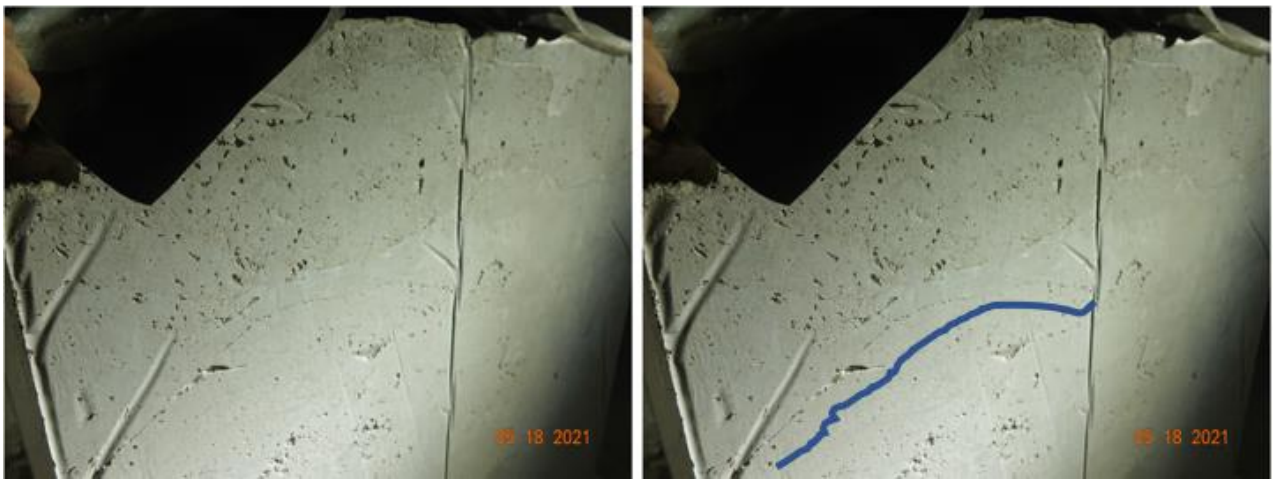

Mixture C – Company 2 – Thermocouple Sample (DSC 2432, 2437)

9.6 ***Appendix VI*** *Tracer Gas – Standard Preparation*

Standard Preparation

Samples for quantitative analysis were supplied in the original TEDLAR® bags collected in the underground test atmosphere without any additional preparation. Standards were prepared using a total of 8 different prescribed standards (Jong).

Calibration Standards

Step 1. Prepare master standard using 10 µL of PMCH diluted in 40mL of Hexane (446.75 ng/µL).

Step 2. Prepare individual liquid standards using 0.5, 2, 14, 30, 50, 100, 200, and 400 µL of the master standard diluted in 8 x 40 mL vials filled with 40 mL of hexane.

Step 3. Inject $10\mu L$ of each liquid standard into separate $40mL$ screw-top, septum-sealed headspace vials to prepare the gaseous standards.

For each standard, 100µL of gas was injected onto the GC/MS in triplicate for preparation of calibration curve.

PMCH Calibration Curve Preparation

Stock Solution (SS) or STD	Weight or Vol. used	Final Vol. Hexane	Std Conc. 2nd Step (SS2)	Vol. SS2 used to prepare final Std	Final Vol. Air	Final Conc., pg/mL
SS 1- PMCH	10 µL	40 mL	446.75 ng/µL			
STD1 – MCPH SS2	0.5µL of SS 1	40 mL	5.58 ng/mL	10 µL	40 mL	1.40
STD2 – MCPH SS2	2µL of SS 1	40 mL	22.33 ng/mL	10 µL	40 mL	5.58
STD3 – MCPH SS2	14µL of SS 1	40 mL	156.28 ng/mL	10 µL	40 mL	39.09
STD4 – MCPH SS2	30µL of SS 1	40 mL	334.75ng/mL	10 µL	40 mL	83.77
STD5 – MCPH SS2	50µL of SS 1	40 mL	557.63 ng/mL	10 µL	40 mL	139.61

STD6 – MCPH SS2	100µL of SS 1	40 mL	1,113.87ng/mL	10 µL	40 mL	279.22
STD7 – MCPH SS2	200µL of SS 1	40 mL	2,222.21 ng/mL	10 µL	40 mL	558.44
STD8 – MCPH SS2	400µL of SS 1	40 mL	4,422.41 ng/mL	10 µL	40 mL	1,116.88

*9.7 **Appendix VII** Tracer Gas – GC/MS individual sample analysis in triplicate.*

GC/MS analysis of Sample 1

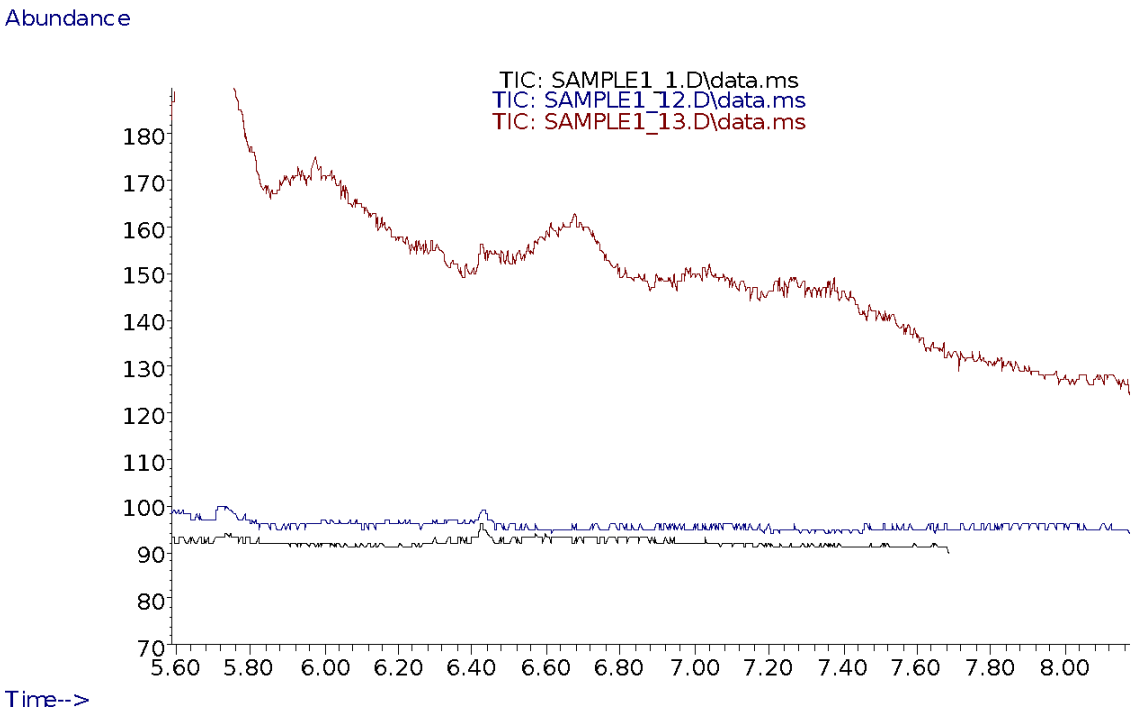

GC/MS analysis of Sample 2

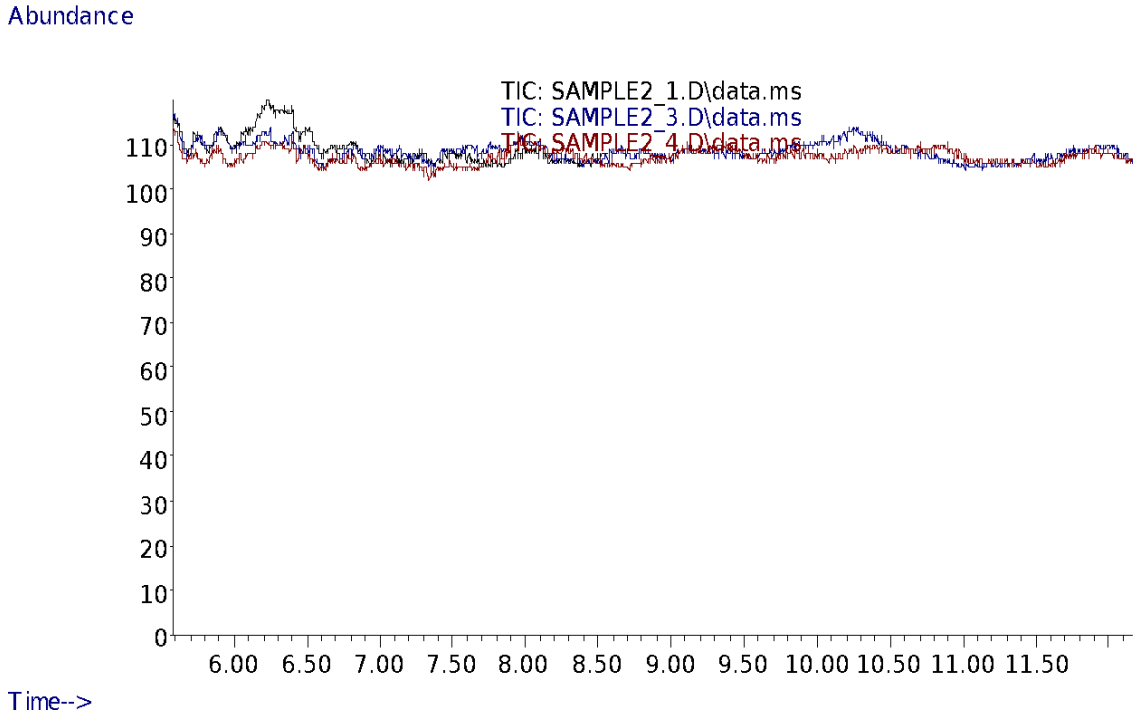

GC/MS analysis of Sample 3

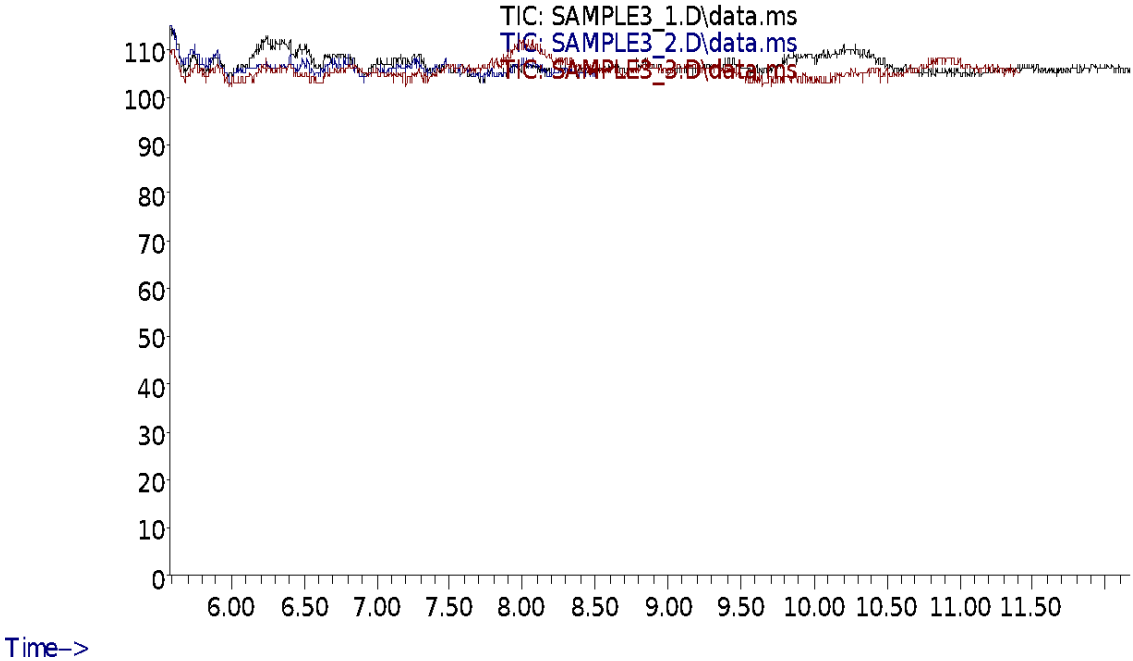

GC/MS analysis of Sample 4

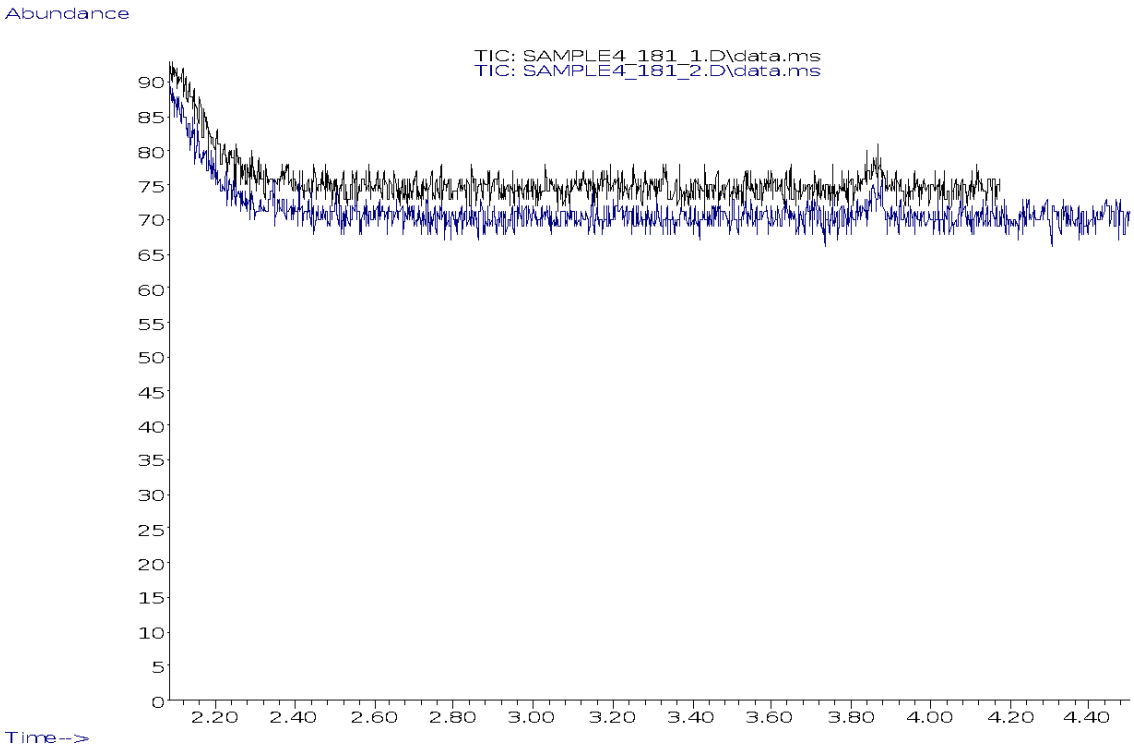

GC/MS analysis of Sample 5

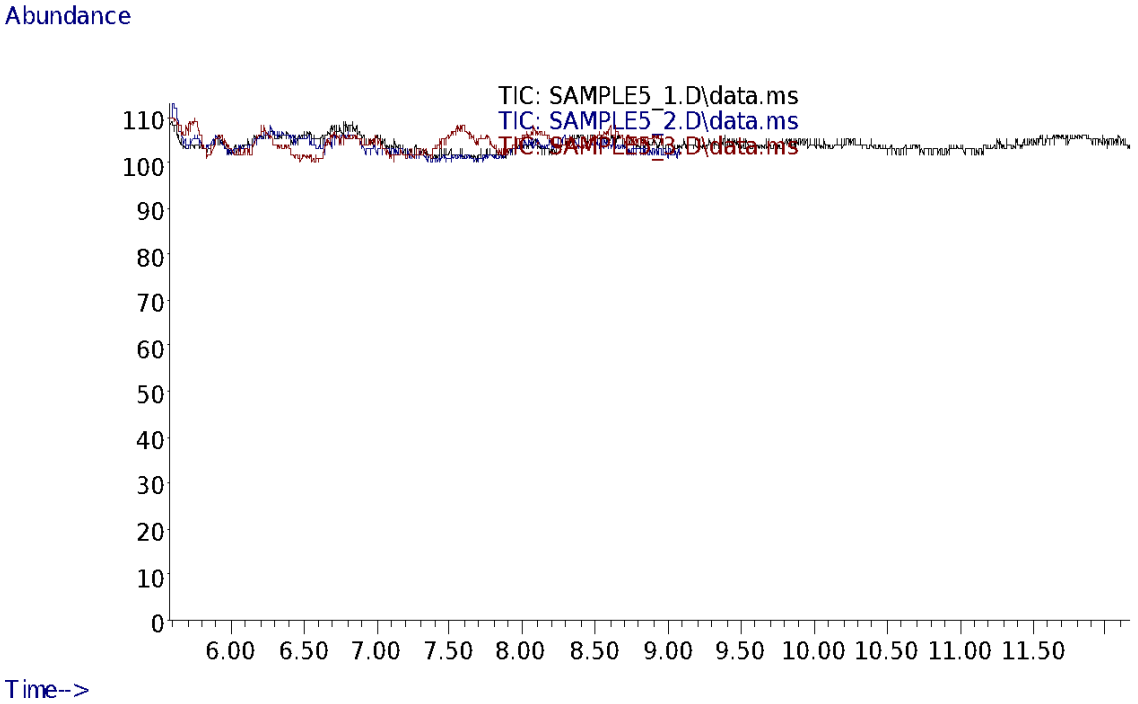

GC/MS analysis of Sample 6

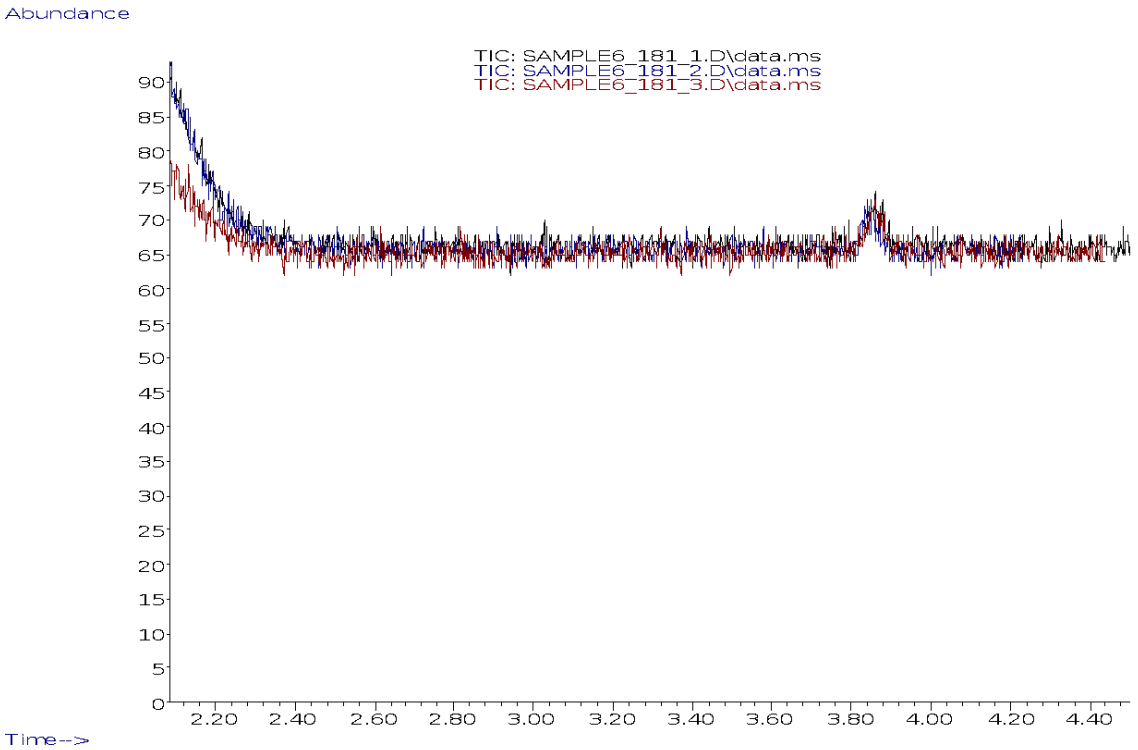

GC/MS analysis of Sample 7

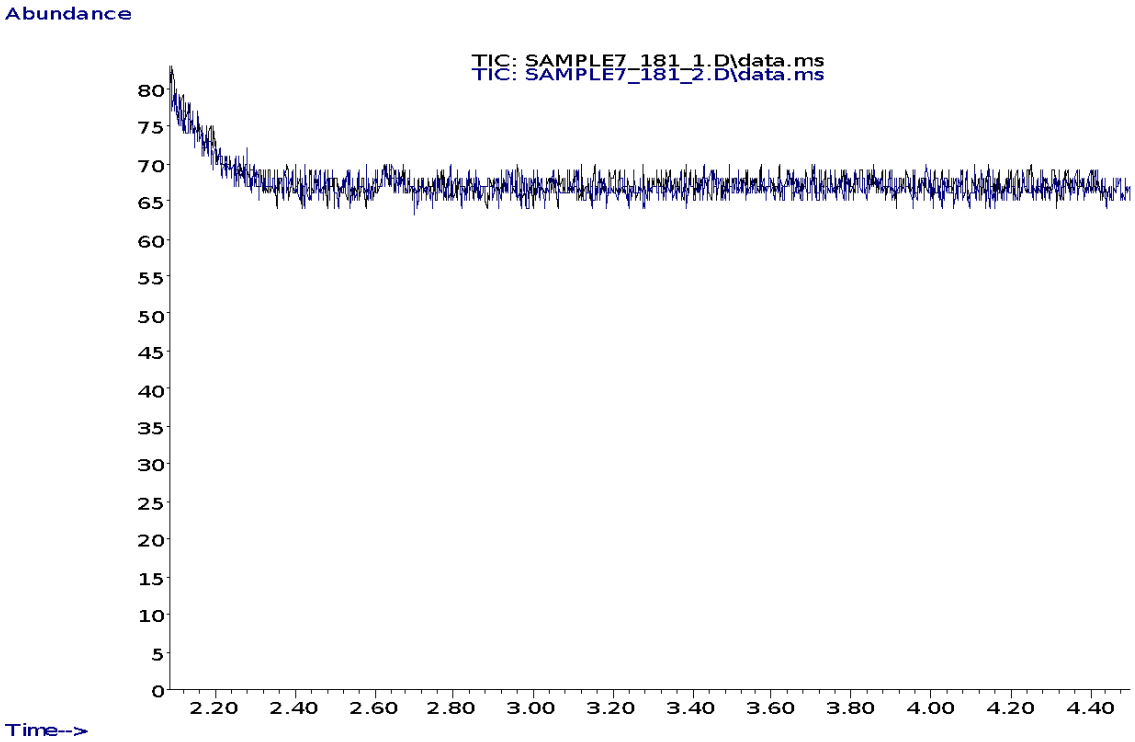

GC/MS analysis of sample 8

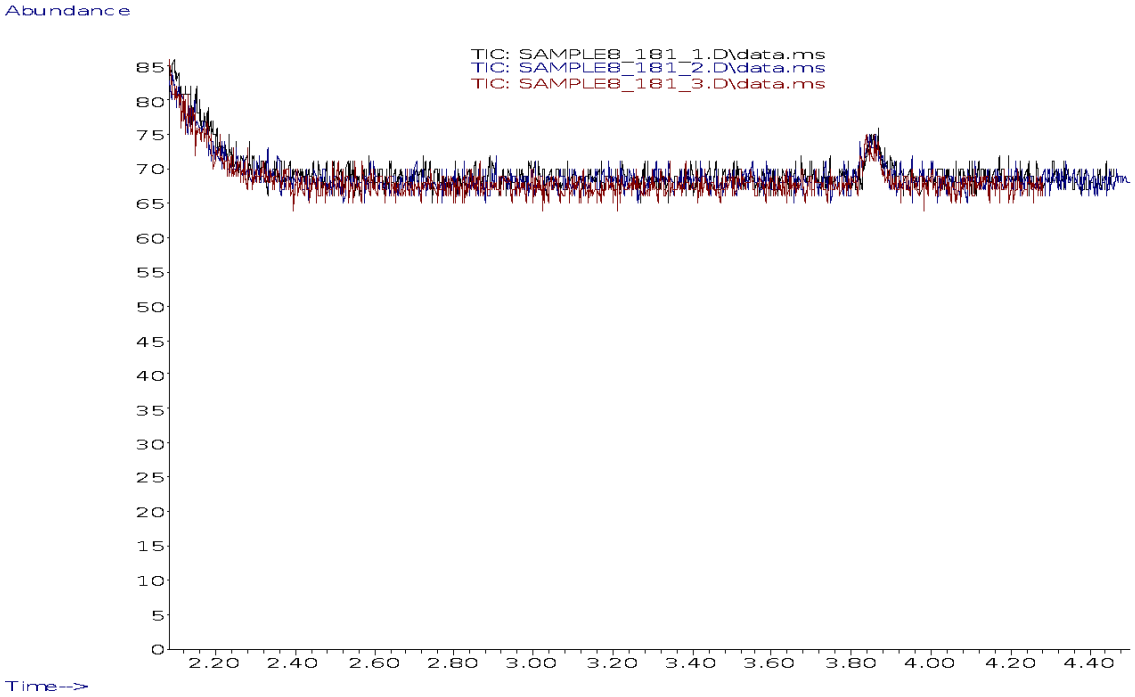

GC/MS analysis of Sample 9

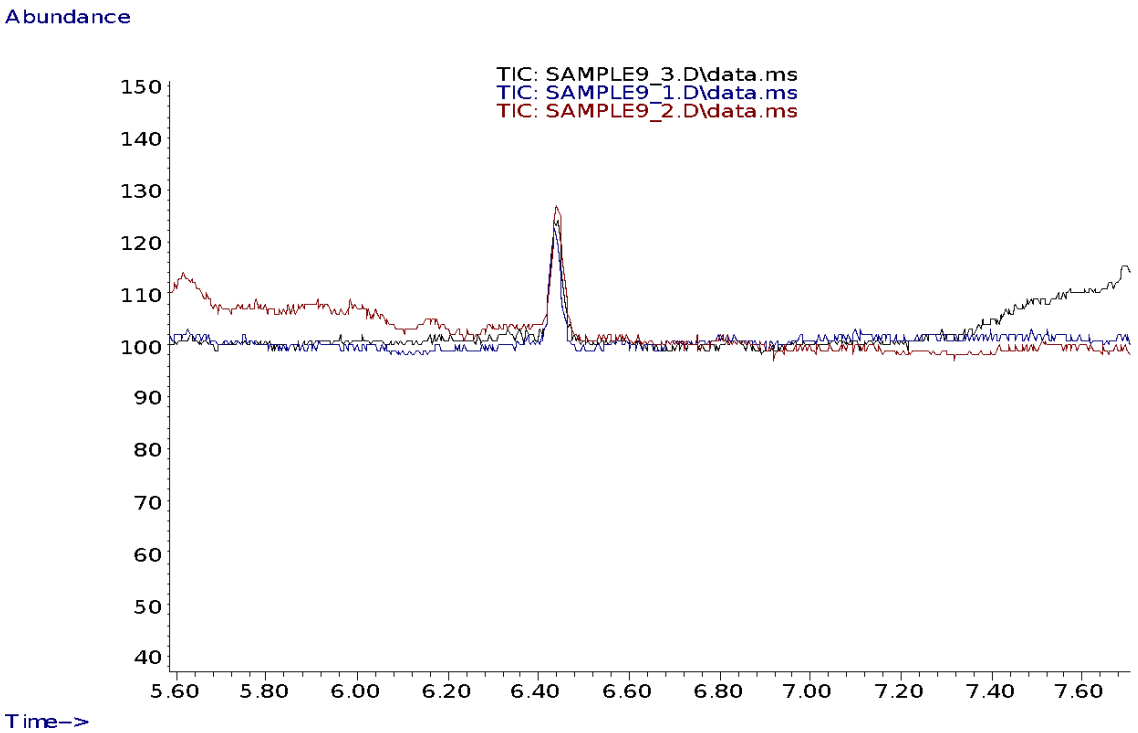

GC/MS analysis of Sample 10

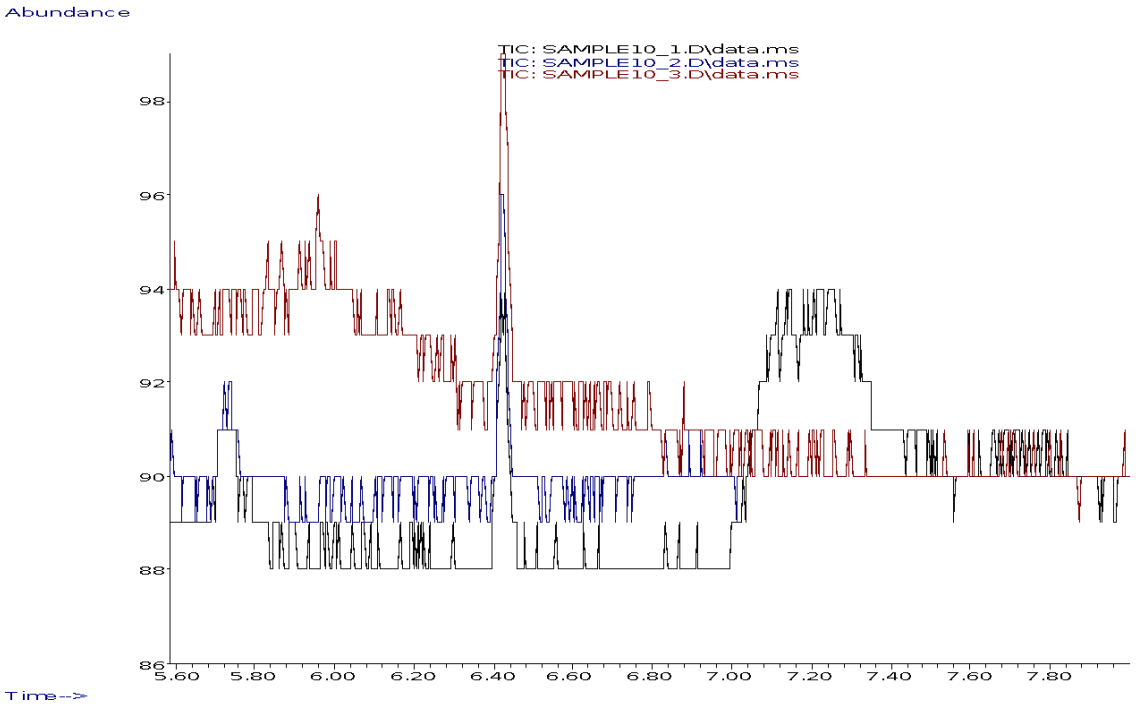

GC/MS analysis of Sample 11

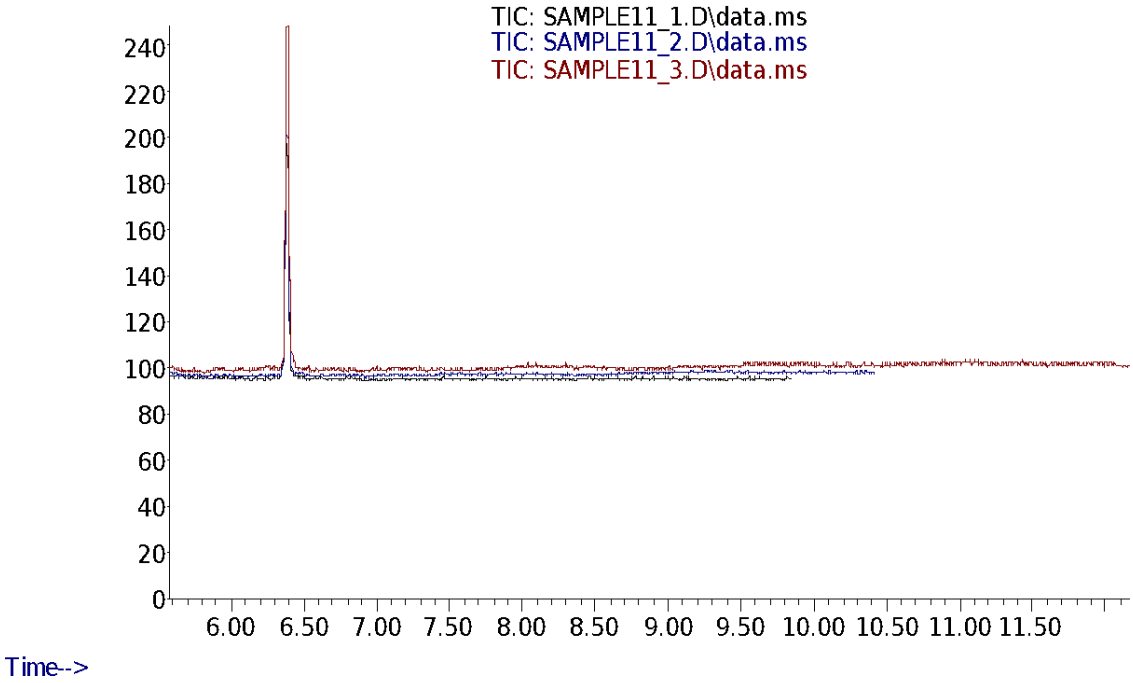

GC/MS analysis of Sample 12

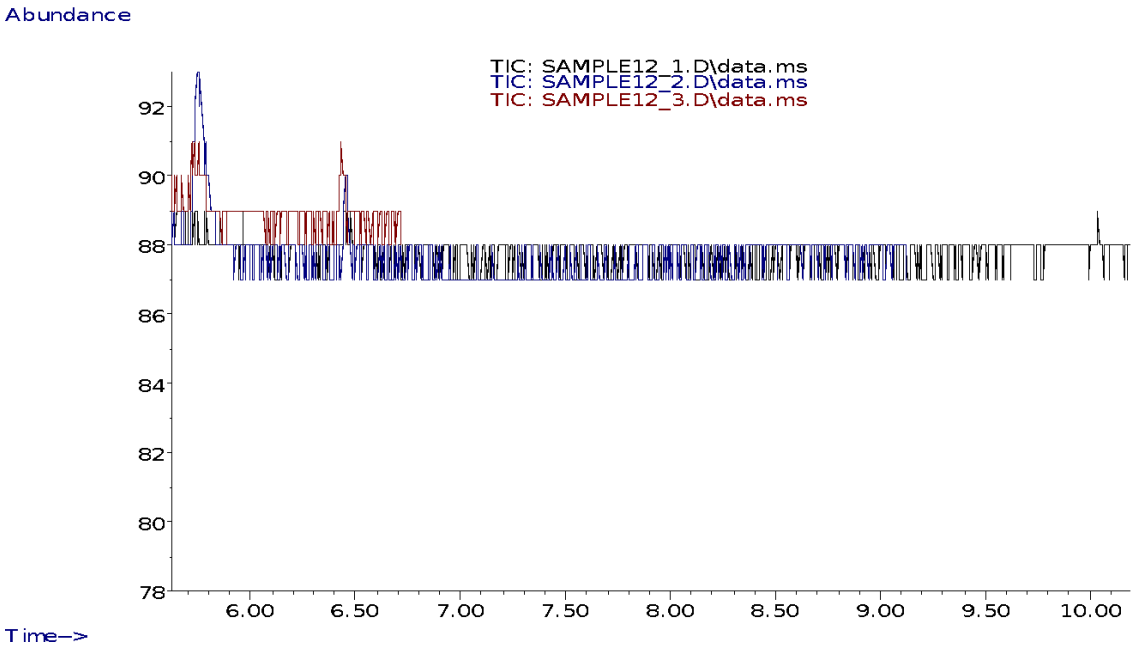

GC/MS analysis of Sample 13

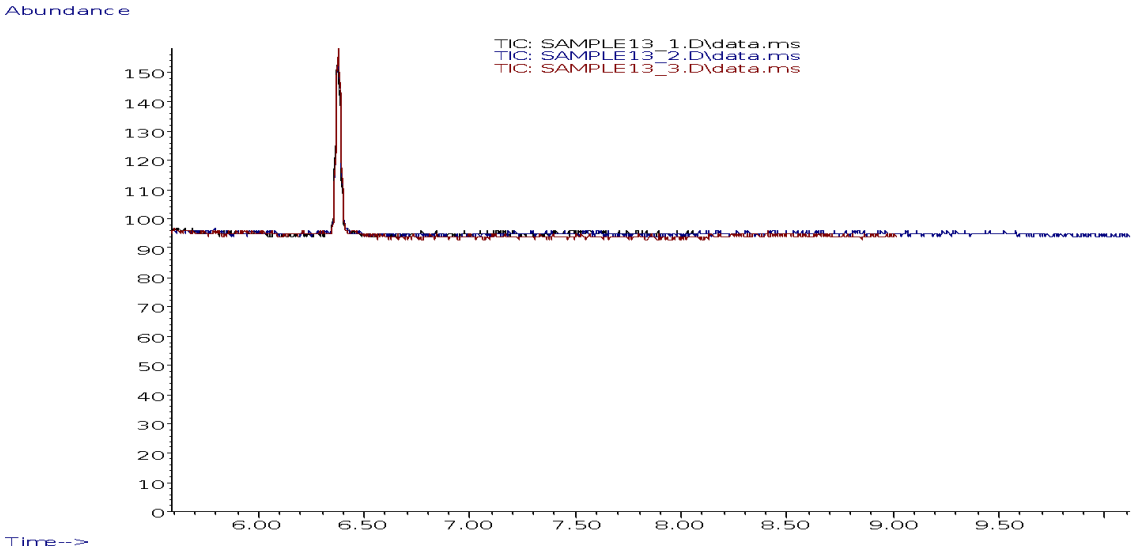

GC/MS analysis of Sample 14

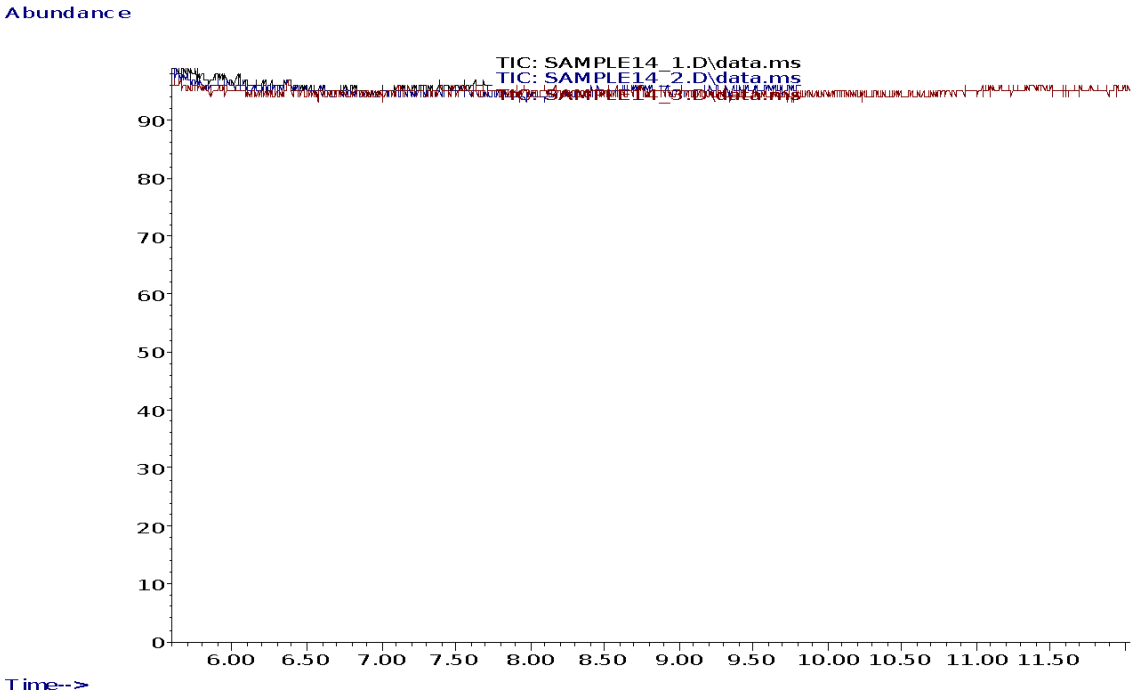

GC/MS analysis of sample 15

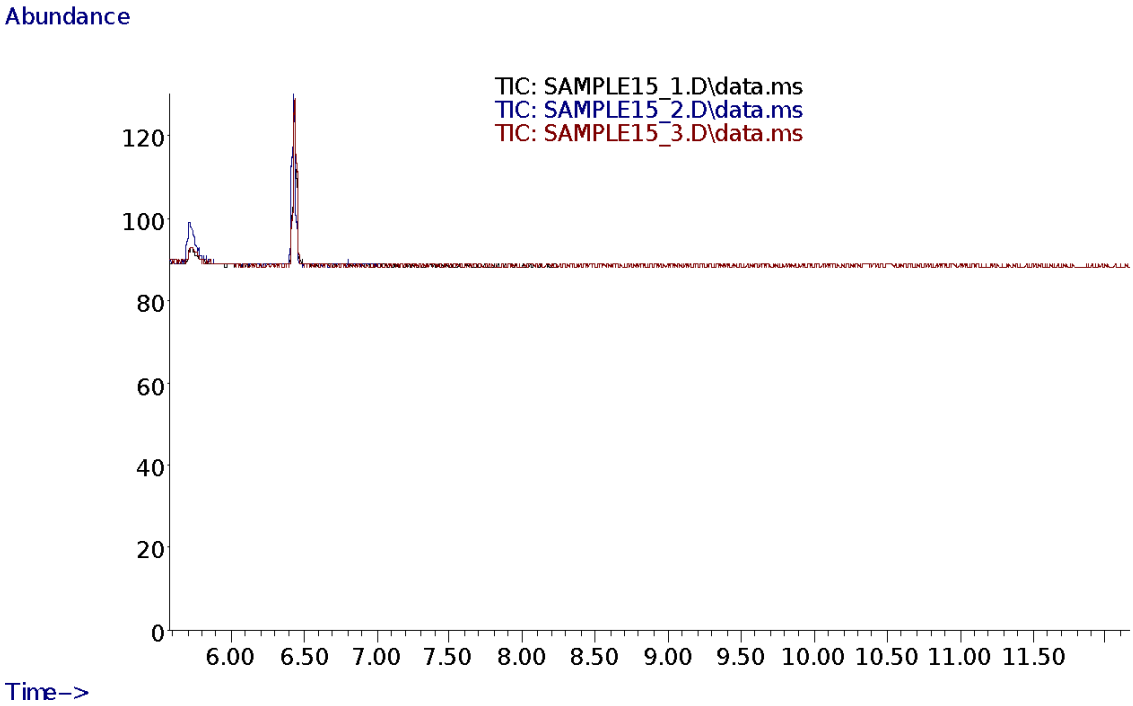

GC/MS analysis of Sample 16

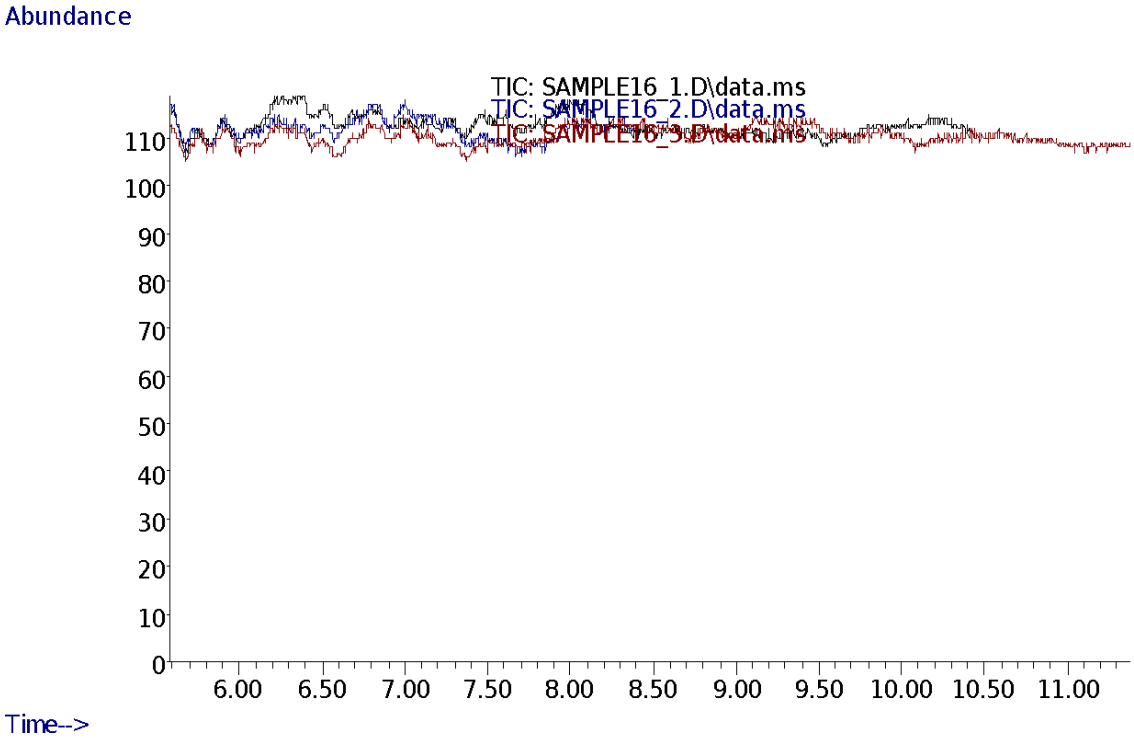

GC/MS analysis of Sample 17

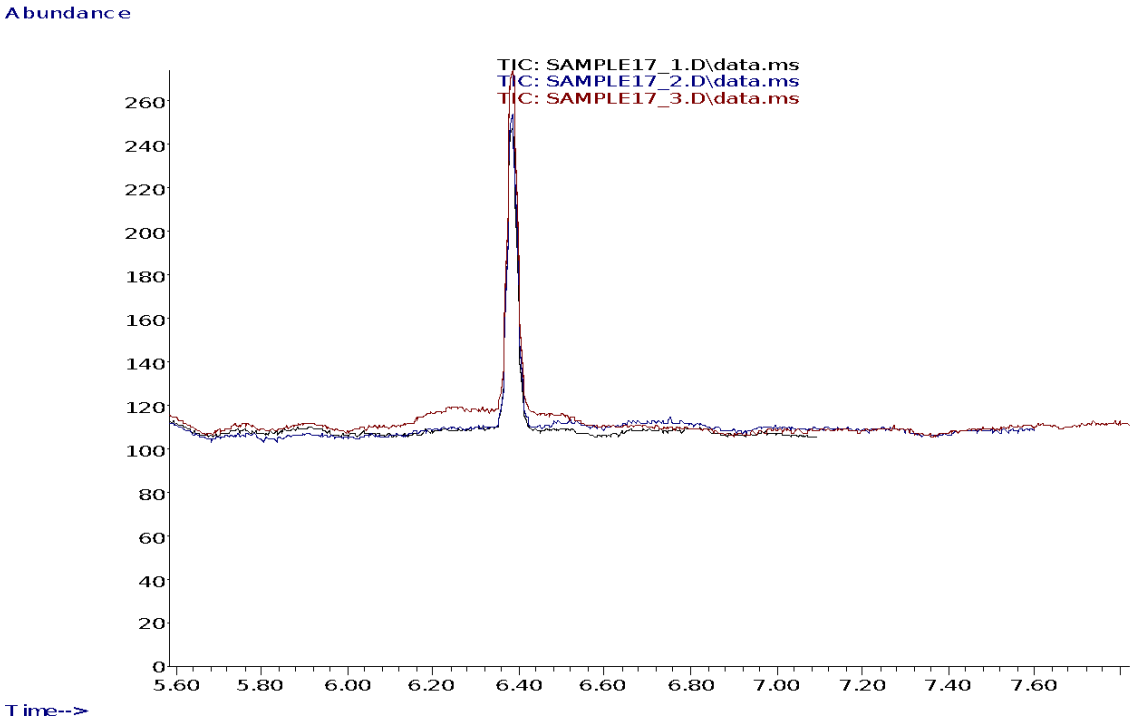

GC/MS analysis of Sample 18

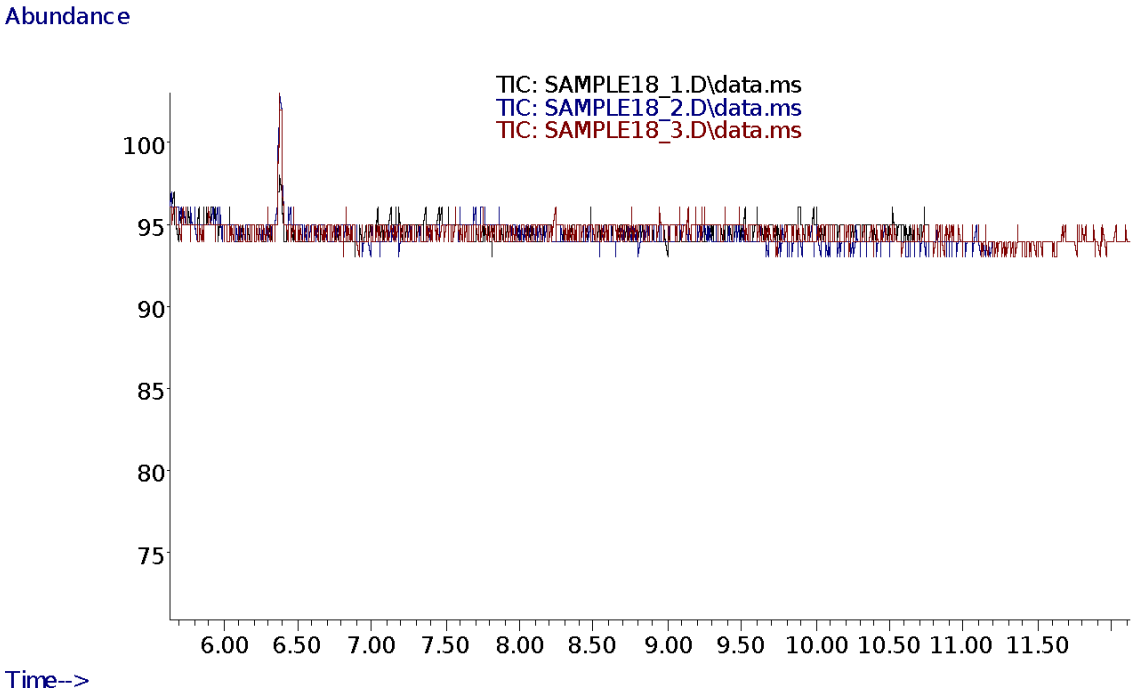

GC/MS analysis of Sample 19

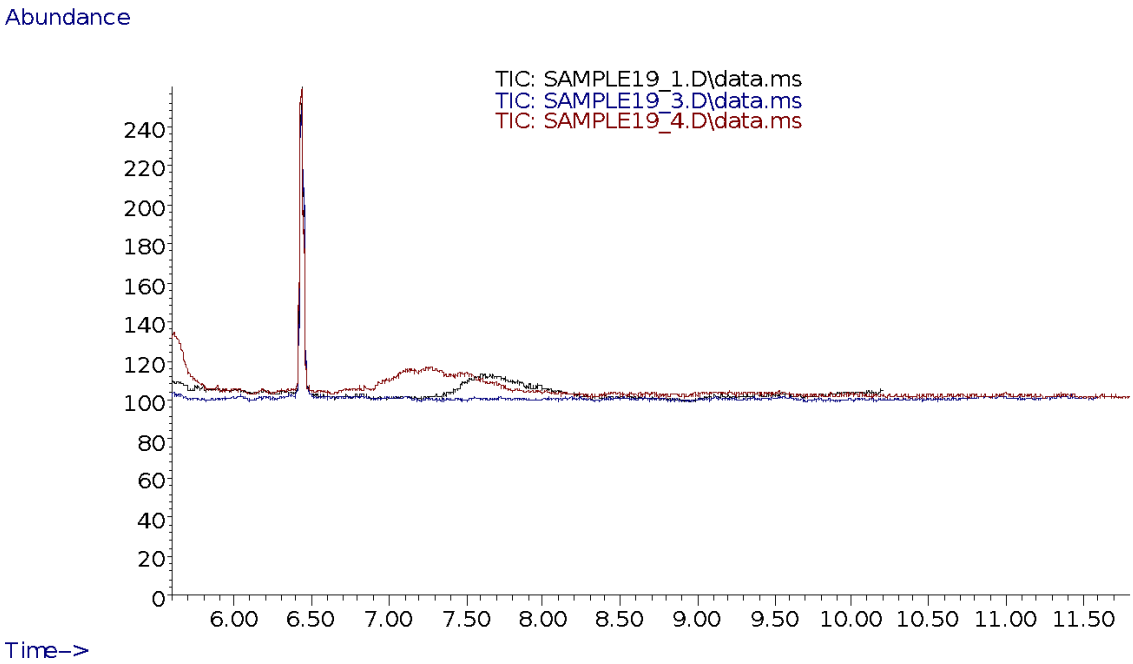

GC/MS analysis of Sample 20

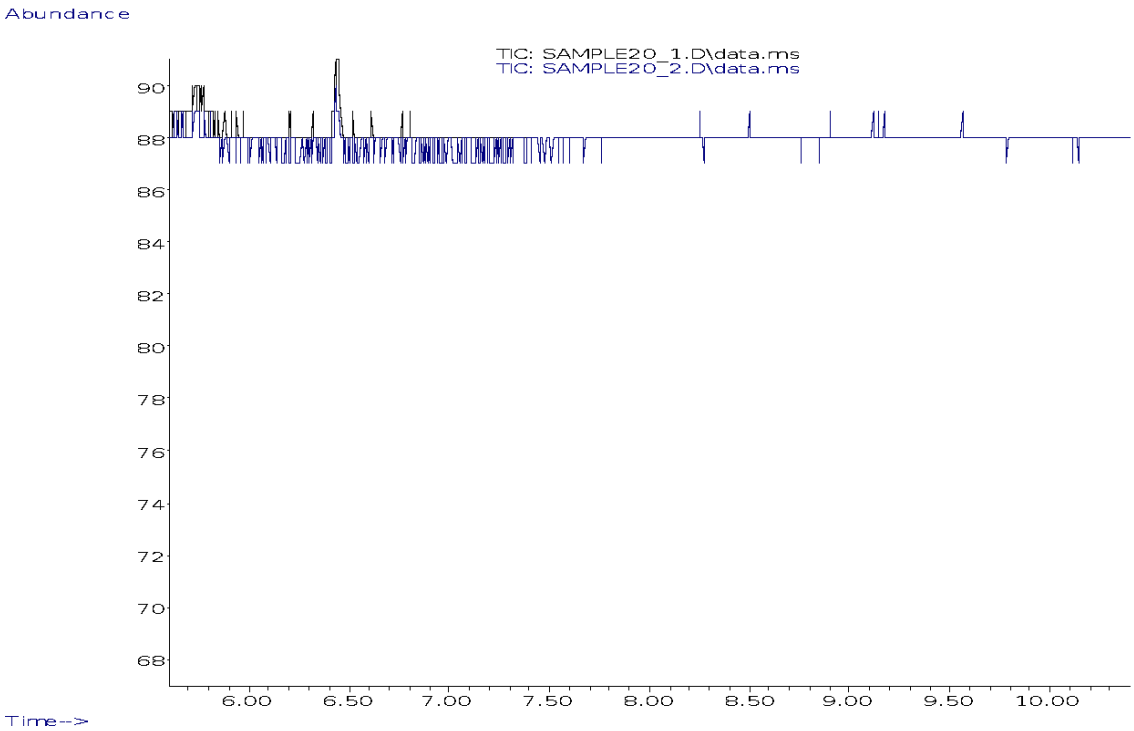

GC/MS analysis of Sample 21

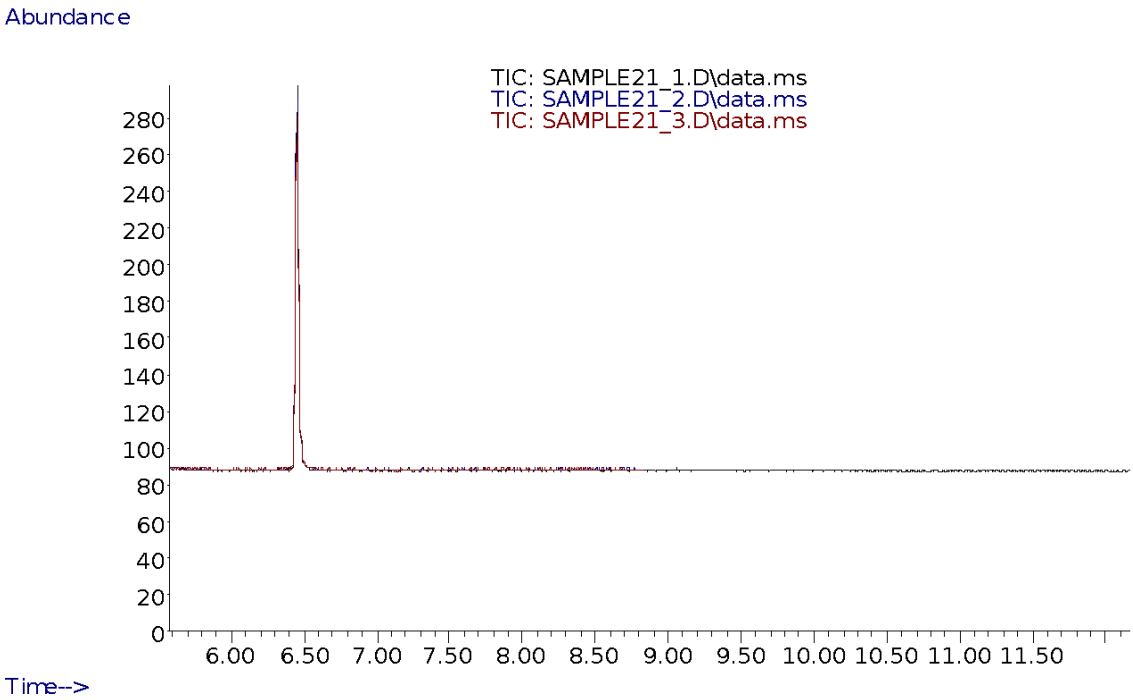

GC/MS analysis of Sample 22

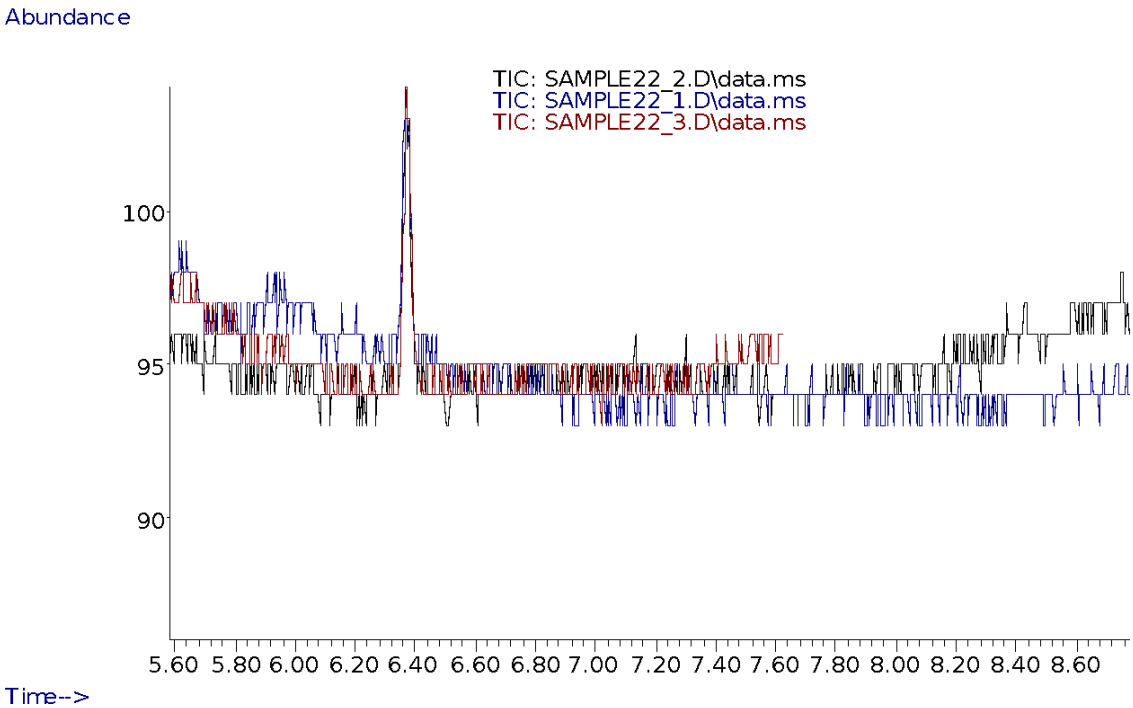

GC/MS analysis of sample 23

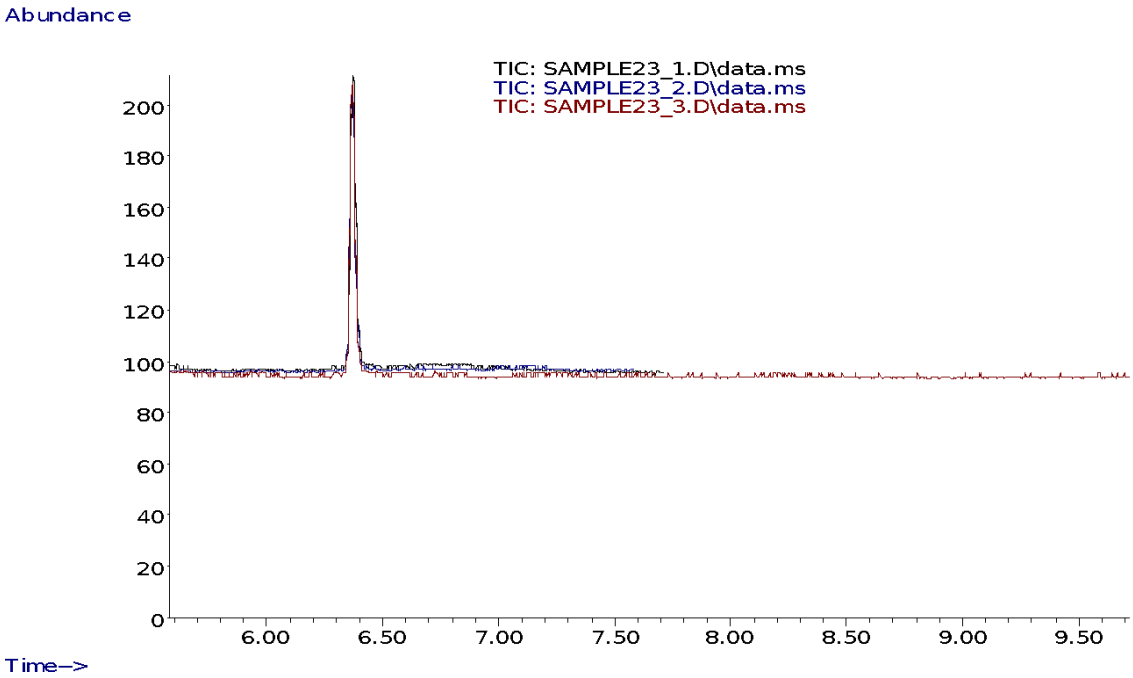

GC/MS analysis of Sample 24

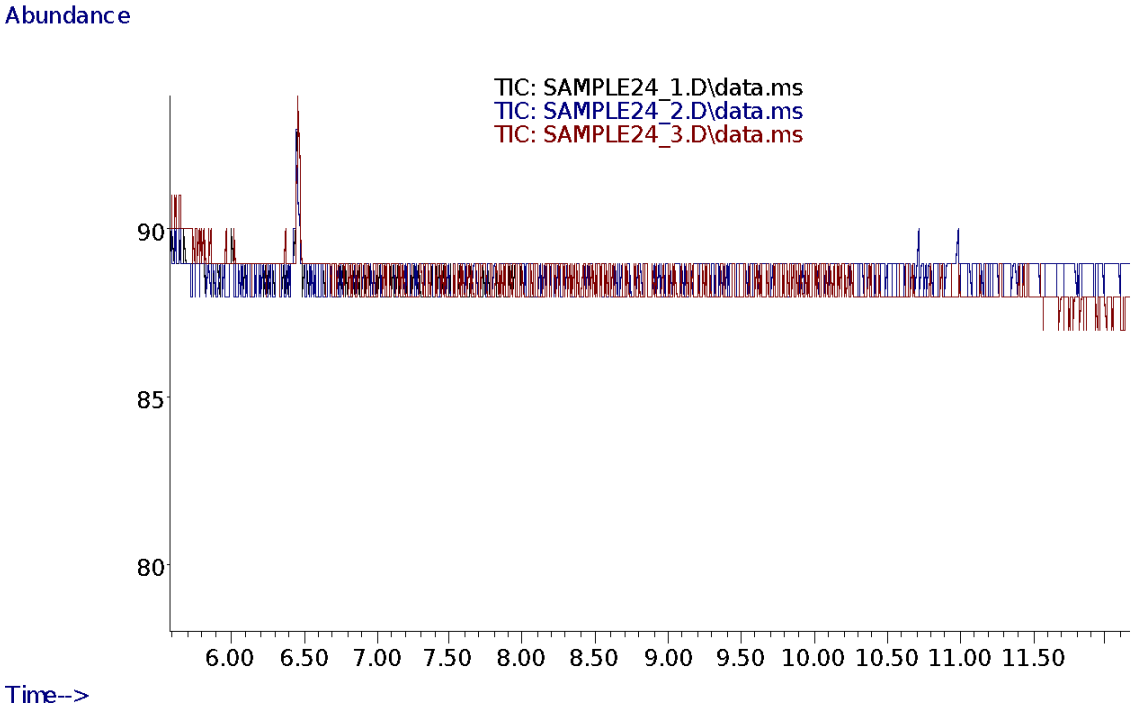

GC/MS analysis of Sample 25

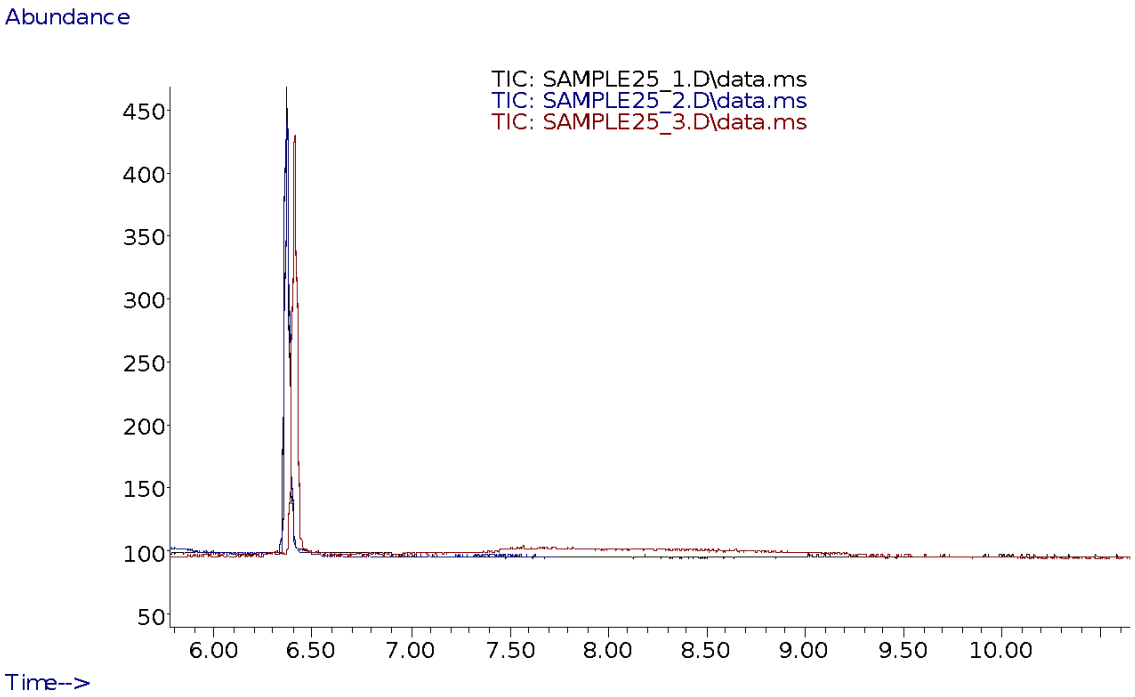

GC/MS analysis of Sample 26

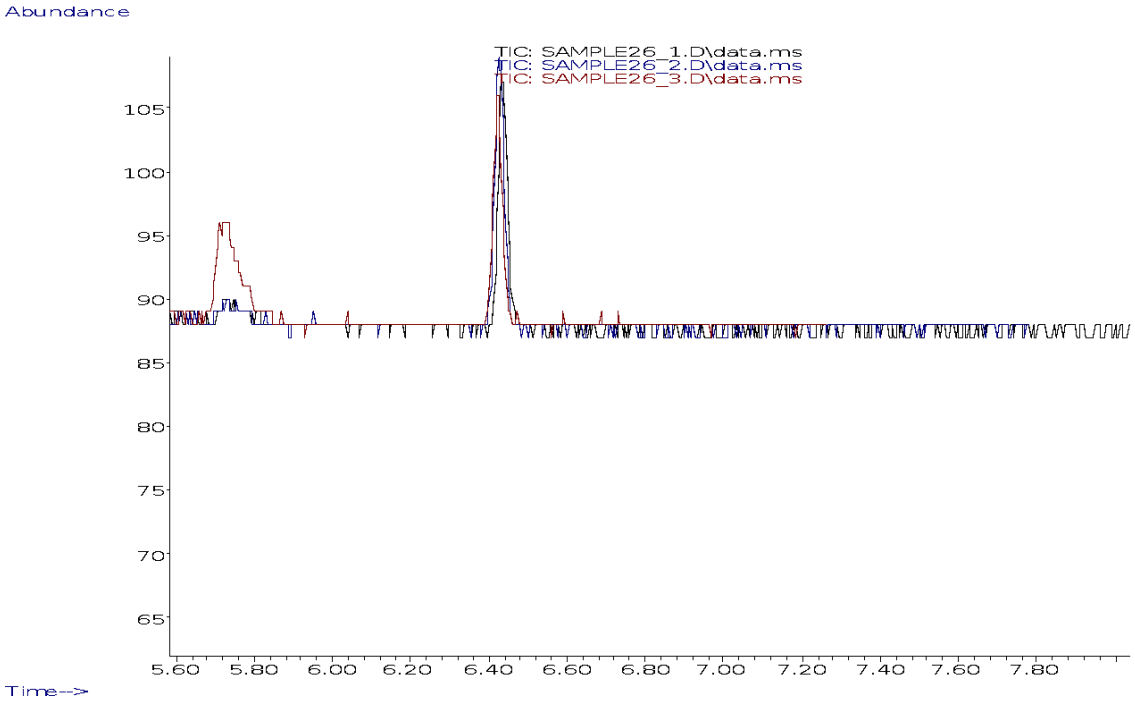

GC/MS analysis of Sample 27

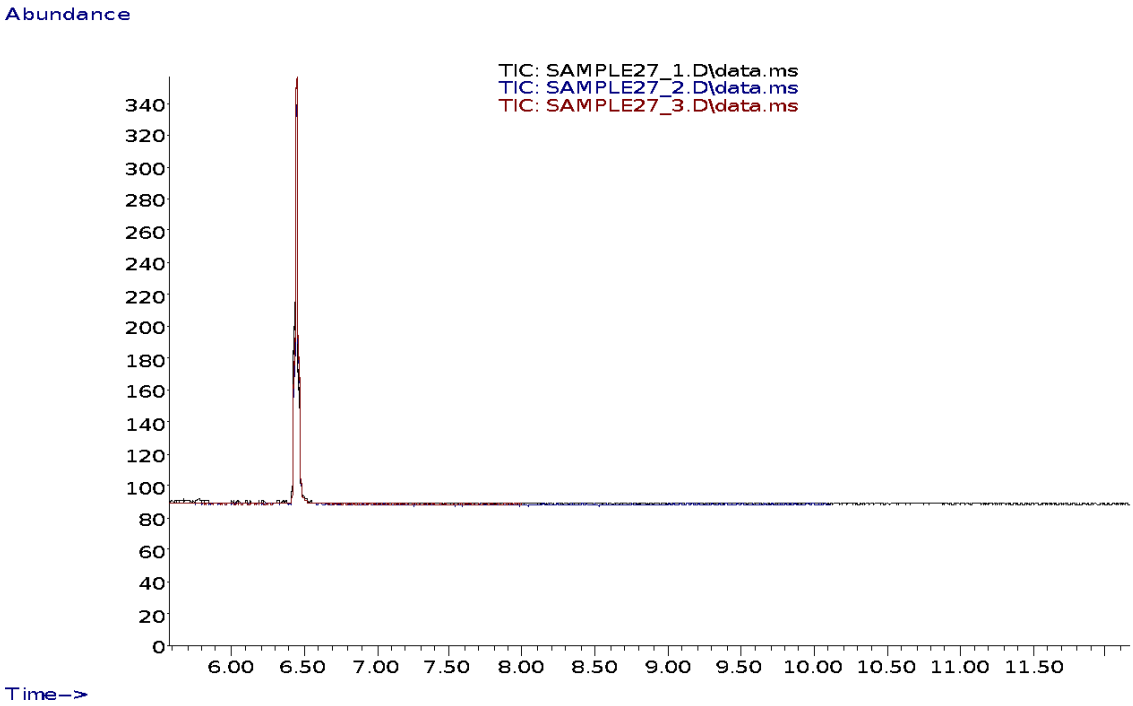

GC/MS analysis of Sample 28

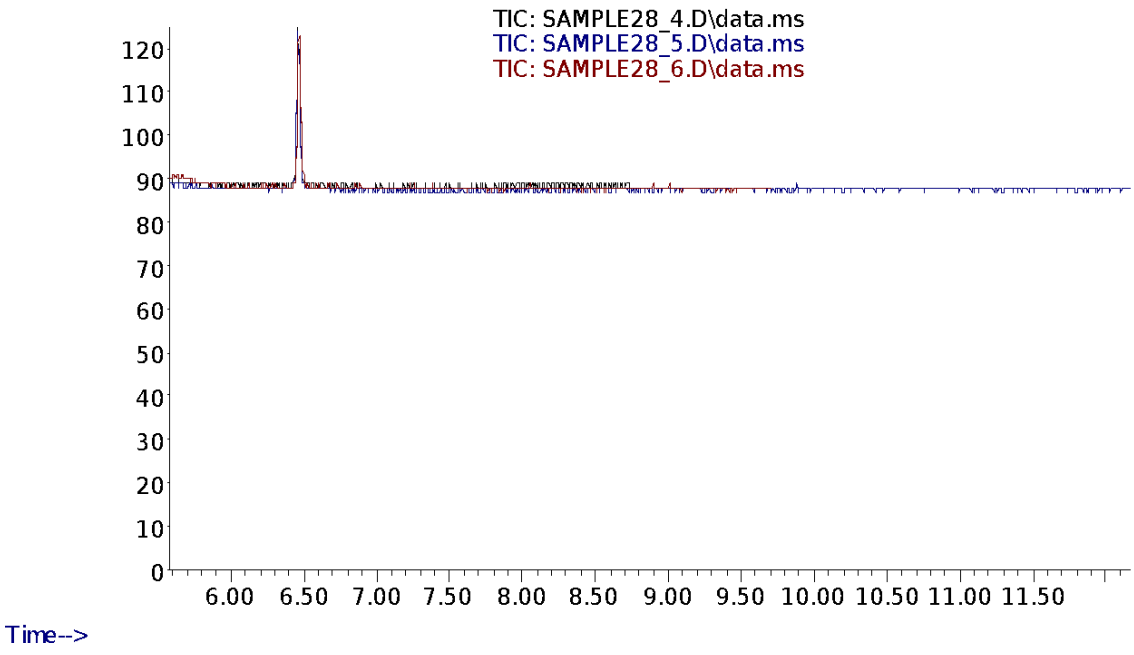

GC/MS analysis of Sample 29

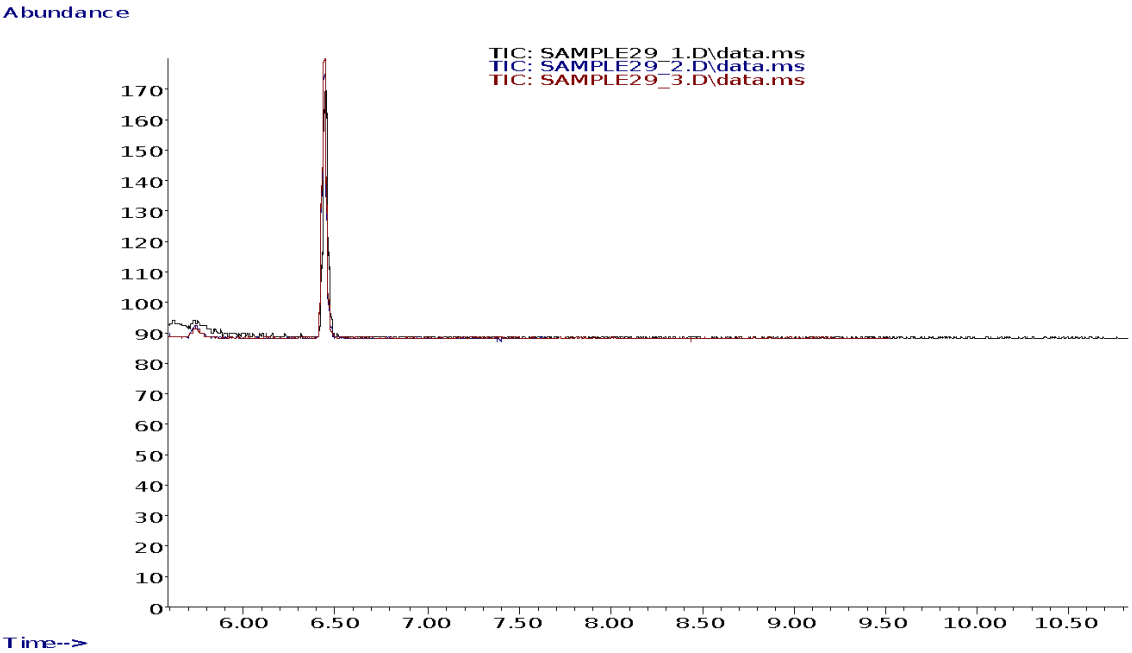

GC/MS analysis of Sample 30

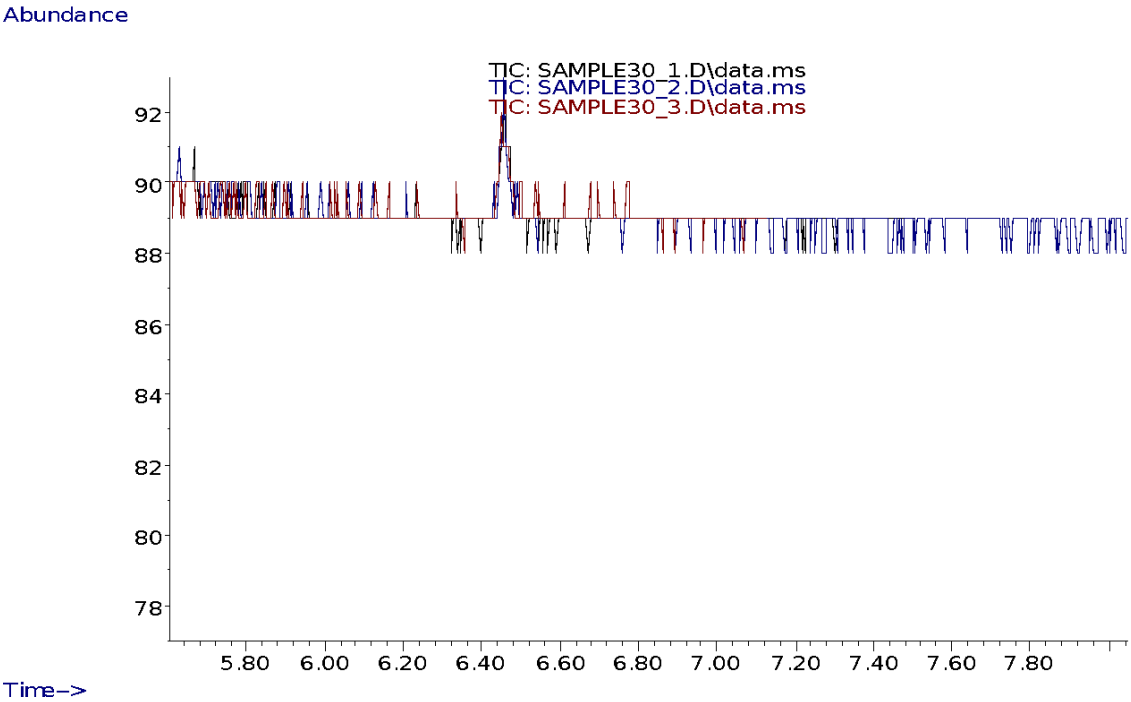

GC/MS analysis of Sample 31

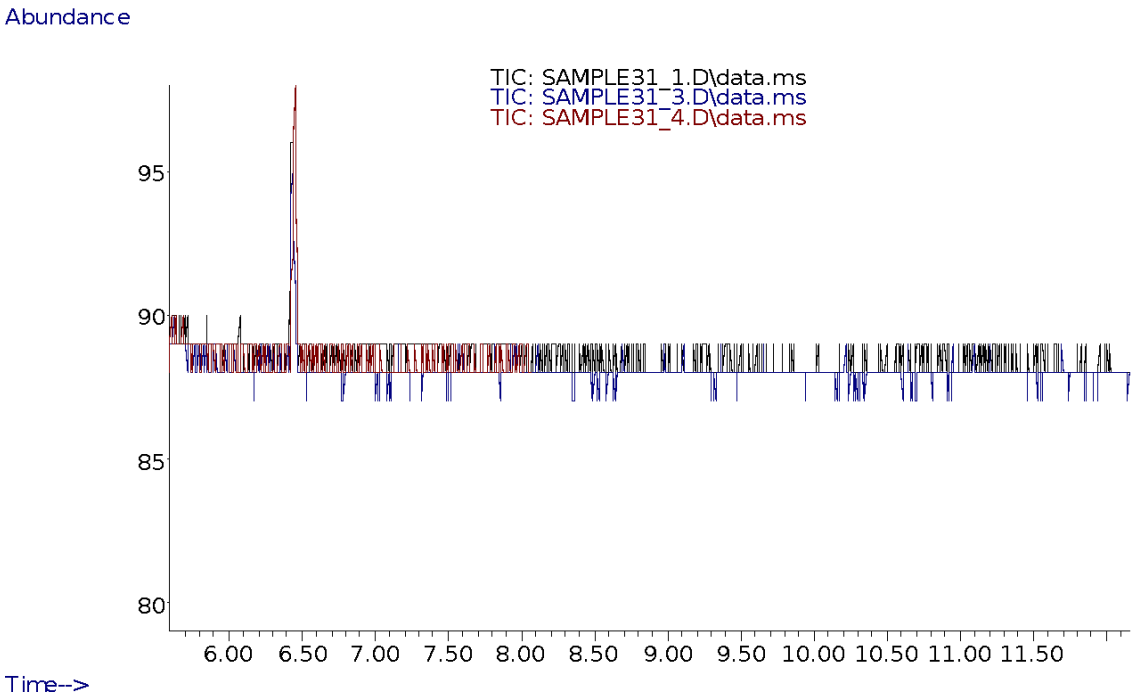

GC/MS analysis of Sample 32

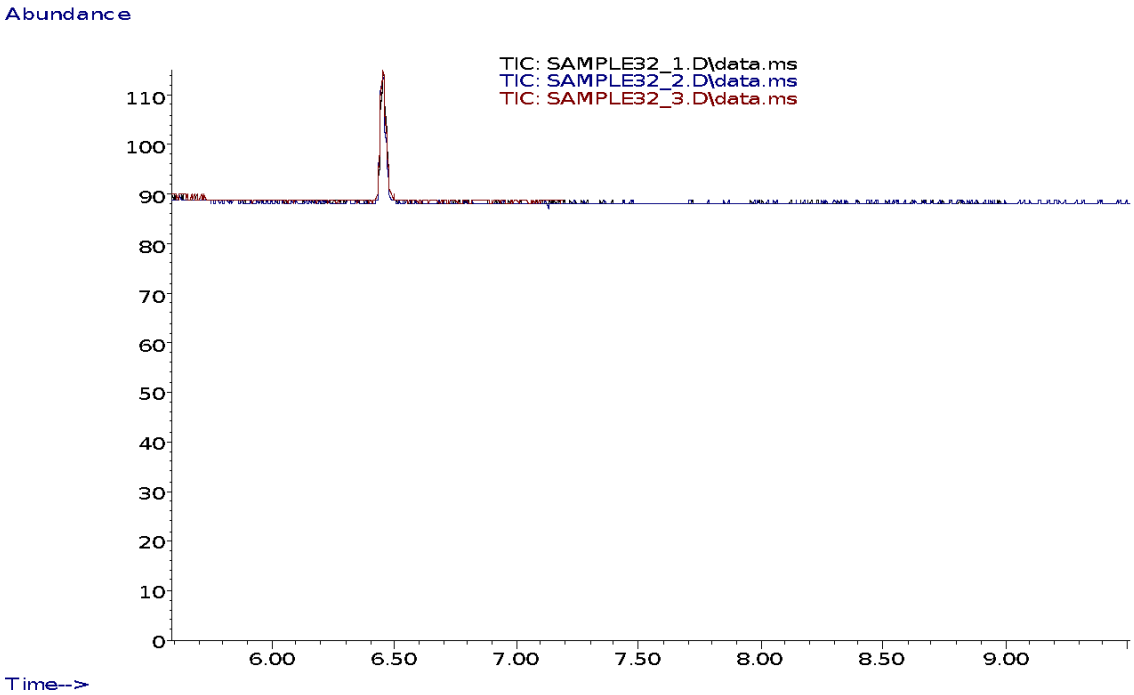

GC/MS analysis of Sample 33

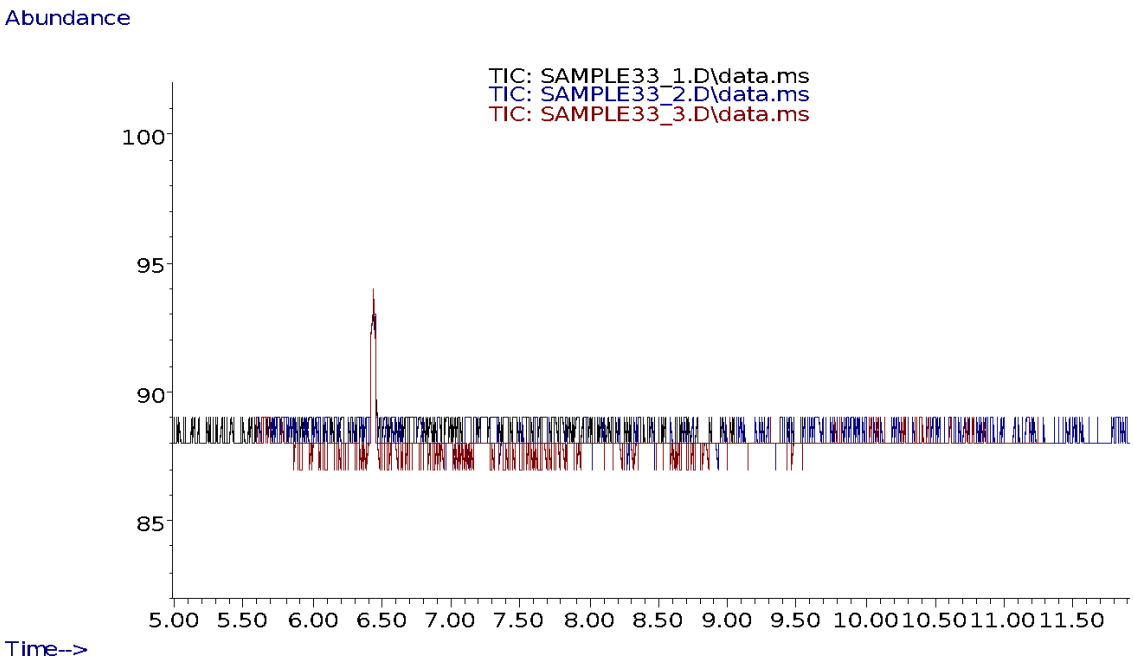

GC/MS analysis of Sample 34

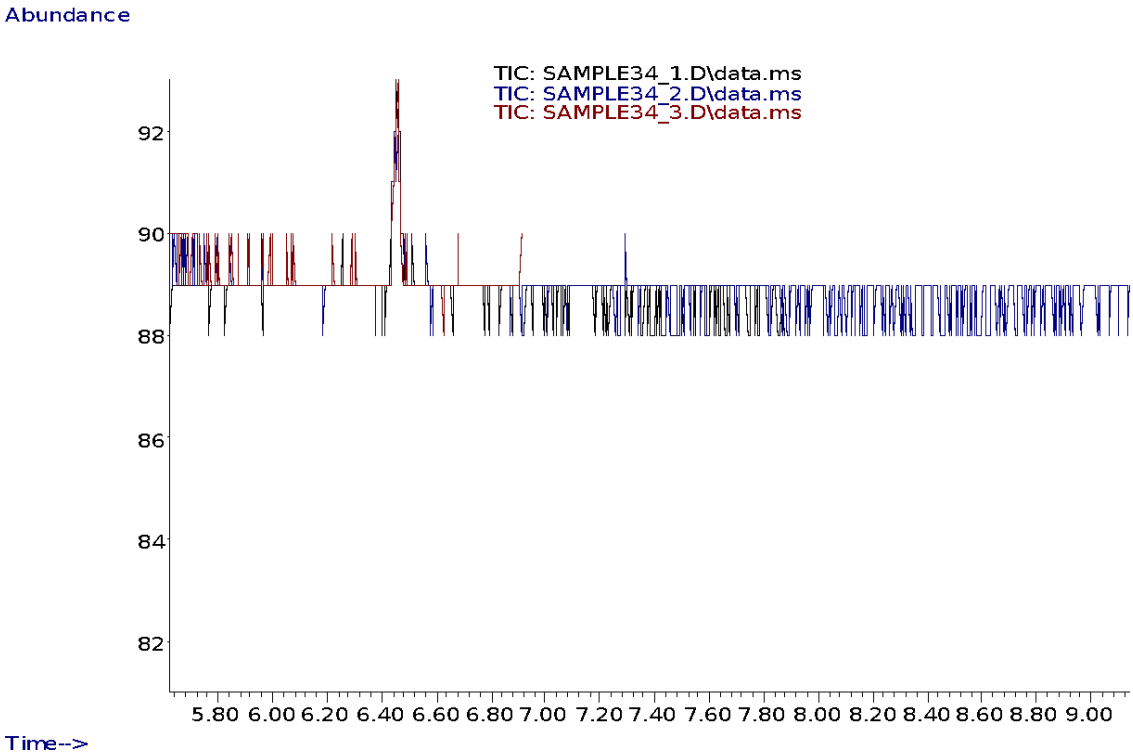

GC/MS analysis of Sample 35

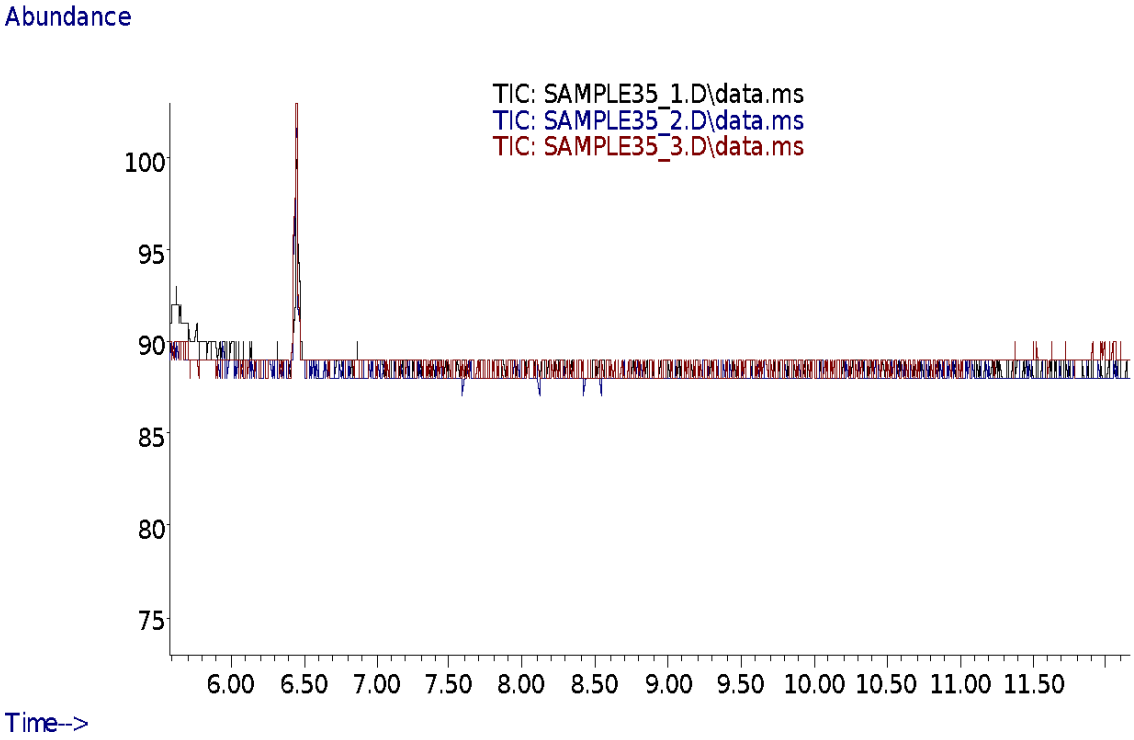

GC/MS analysis of sample 36

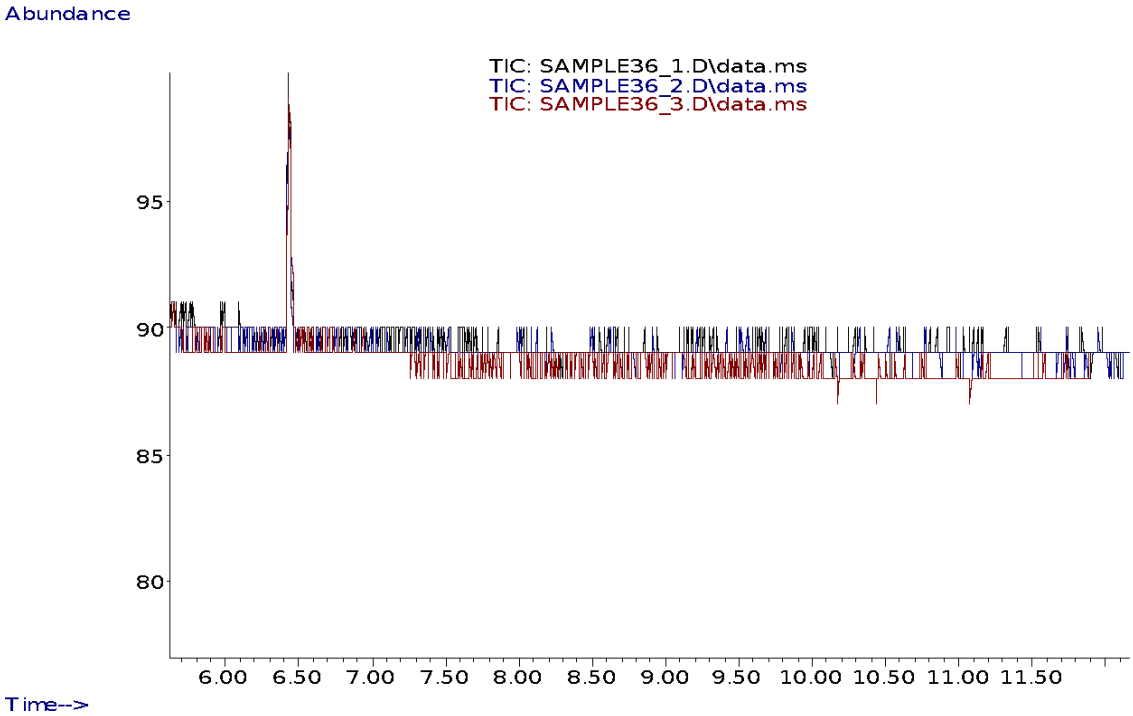

GC/MS analysis of Sample 37

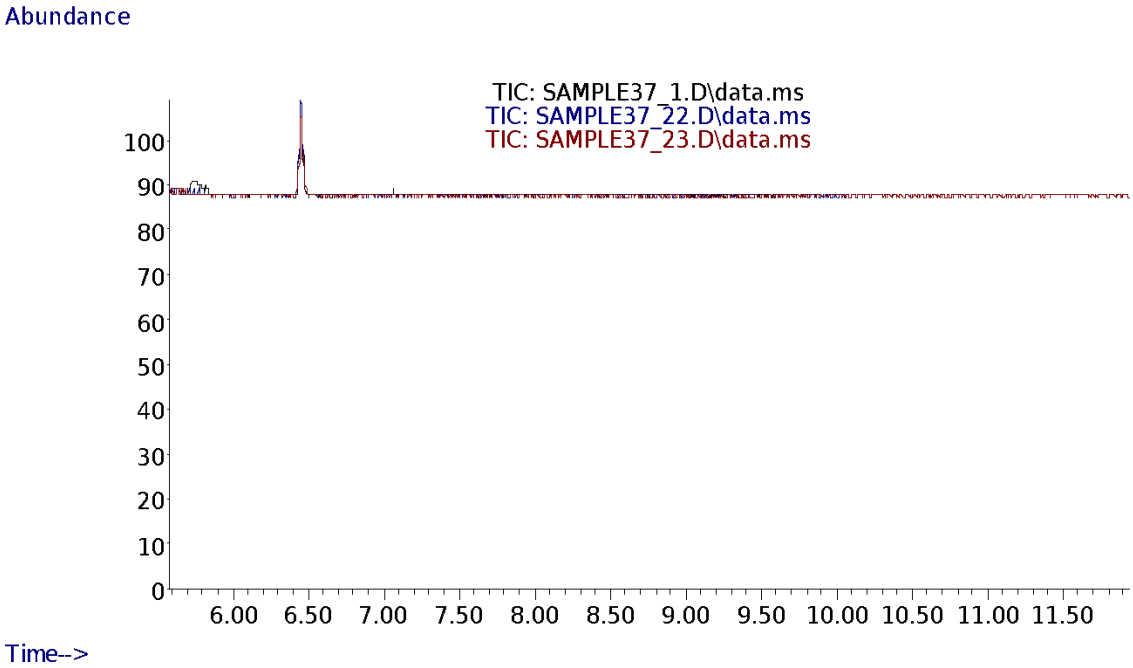

GC/MS analysis of Sample 38

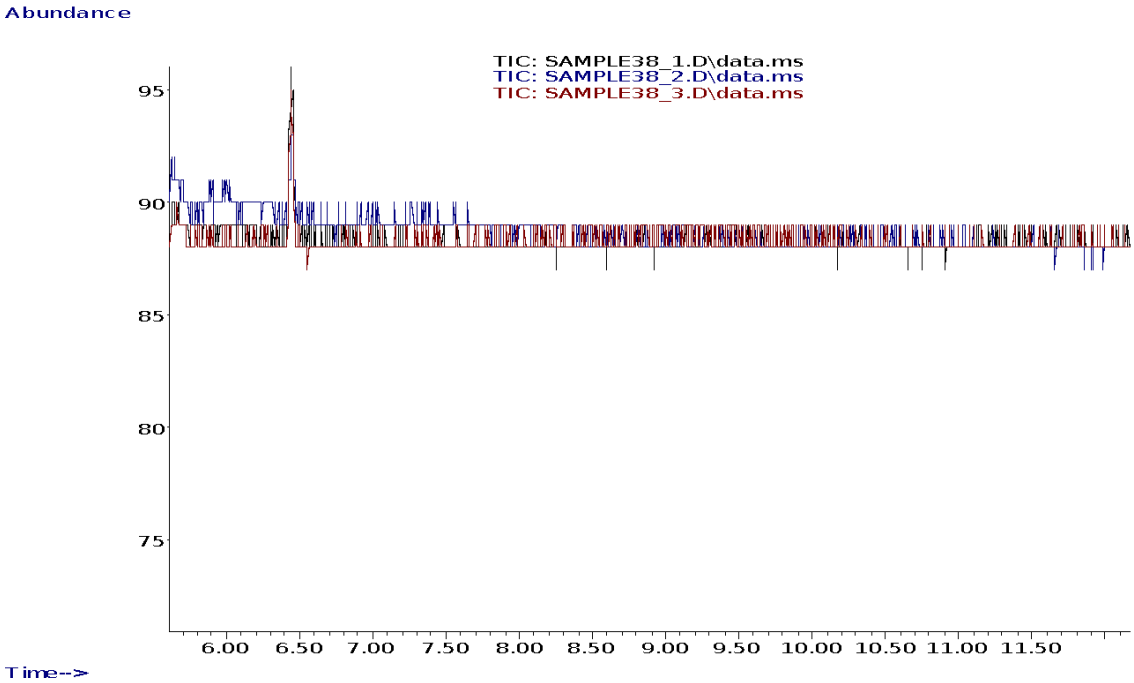

GC/MS analysis of Sample 39

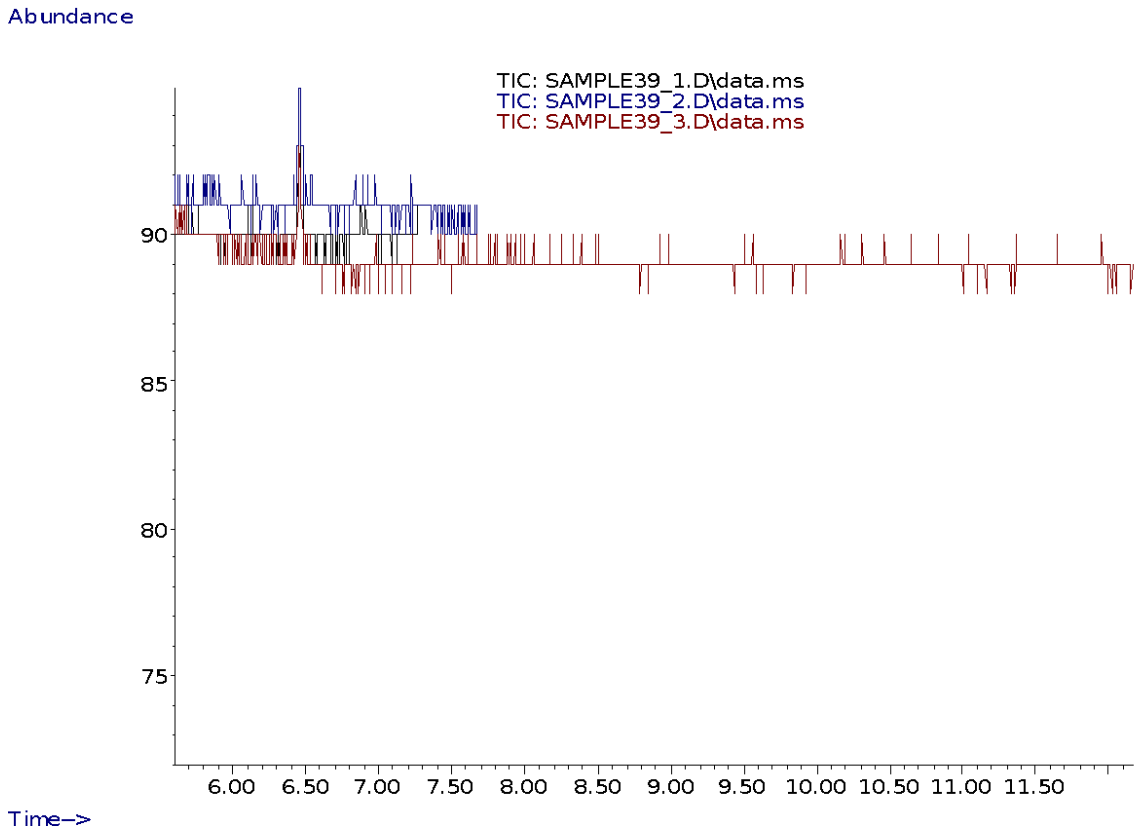

9.8 ***Appendix VIII*** *Full GPR Report*